2020

THE PHENOTYPIC FLEXIBILITY OF THERMOGENIC CAPACITY: FROM PHYSIOLOGICAL MECHANISM TO EVOLUTIONARY IMPLICATIONS

Maria Stager

THE PHENOTYPIC FLEXIBILITY OF THERMOGENIC CAPACITY: FROM PHYSIOLOGICAL MECHANISM TO EVOLUTIONARY IMPLICATIONS

By

MARIA STAGER

B.S. Natural Resources, Cornell University, Ithaca, New York, 2008
M.S. Ecology, Ethology & Evolution, University of Illinois, Urbana, IL, 2014

Dissertation

presented in partial fulfillment of the requirements
for the degree of

Doctor of Philosophy
in Organismal Biology, Ecology, and Evolution

The University of Montana
Missoula, MT

August 2020

Approved by:

Scott Whittenburg, Dean of The Graduate School
Graduate School

Dr. Zachary A. Cheviron, Chair
Division of Biological Sciences

Dr. Creagh W. Breuner
Division of Biological Sciences

Dr. Lila Fishman
Division of Biological Sciences

Dr. Tom E. Martin
W. A. Franke College of Forestry and Conservation

Dr. Bret W. Tobalske
Division of Biological Sciences

Stager, Maria, PhD, Summer 2020 Organismal Biology, Ecology, and Evolution

The phenotypic flexibility of thermogenic capacity: from physiological mechanism to evolutionary implications

Chairperson: Dr. Zachary A. Cheviron

Abstract

Individuals face many selection pressures that change throughout their lives. Phenotypic flexibility, the ability to flexibly and reversibly modify a trait value, is one way an individual can optimally match its phenotype to the prevailing environmental conditions. In this dissertation, I used juncos as a lens to understand the causes of variation in flexibility within physiological systems and among individuals. In my first chapter, I investigated how Dark-eyed Juncos (*Junco hyemalis*) alter mechanisms of heat production and heat conservation to cope with variation in ambient conditions. My results demonstrate the ability of birds to adjust thermoregulatory strategies in response to thermal cues and reveal that birds may combine multiple responses to meet the specific demands of their environment. To further explore the thermoregulatory strategies available to juncos, in my second chapter, I assess their potential use of non-shivering thermogenesis. My results indicate that muscular non-shivering thermogenesis is not an important mechanism of avian thermoregulation, potentially as a consequence of a tradeoff between the many demands placed on avian muscles. In my third chapter, I measured 20 additional physiological traits to explore the mechanistic basis of flexibility in complex phenotypes. I show that the relationships among traits contributing to whole-organism performance varied with the environmental context. Moreover, whole-organism flexibility in thermogenic performance was correlated with only a handful of subordinate phenotypes. In my fourth chapter, I identified drivers of variation in flexibility among juncos. To do this, I integrated measures of population genetic variation with assays of thermogenic performance and indices of environmental heterogeneity for individuals across the genus *Junco*. I find that native temperature heterogeneity correlates both with population genetic variation and the degree of thermogenic flexibility exhibited by an individual. In my fifth chapter, I present a review that considers the evolutionary implications of phenotypic flexibility and contrast those with developmental plasticity. I hypothesize that because these two processes experience selection distinctly, confer stability to populations differentially, and will likely evolve at different rates. Collectively, this work helps us understand the role of flexibility in adaptation and species' resilience to environmental change.

Table of Contents

Acknowledgments

I am exceedingly grateful for generous funding to support this research from the American Museum of Natural History, the American Philosophical Society, the American Ornithological Society [née Union], the Explorer's Club, the Illinois Ornithological Society, the Montana Institute on Ecosystems, the National Science Foundation, the Nuttall-Blake Ornithological Society, P.E.O., Sigma Xi, the Society for Integrative and Comparative Biology, the Society for the Study of Evolution, the Society of Systematic Biologists, the University of Illinois, the University of Montana, and the Wilson Ornithological Society.

We have a really good thing going in (OB)EE at the University of Montana and I feel so privileged to have been a graduate student here. Thank you to (OB)EE faculty and to my committee members, Creagh Breuner, Lila Fishman, and Tom Martin for your guidance and support, and especially Bret Tobalske for your overwhelming altruism with your time, resources, and expertise. Thank you also to my master's committee member, Dave Swanson, for your continued generosity.

I am wholly indebted to my advisor, Zac Cheviron, for taking me on as a master's student when I had zero relevant experience — and then signing on again for my PhD. Thank you for your support these last eight years; the amount that I have learned from you is incalculable. Thank you also to Christy, Finn, and Noa Cheviron for welcoming me into your home and for sharing Zac with us: it's been so fun to watch your family grow.

One of the biggest lessons that Zac imparted to me is the value of creating a great community. In that vein, I cannot imagine a better place to do my PhD. Thank you to Cheviron lab members past and present: Phred Benham, Shane Campbell-Staton, Keely Corder, Ryan Mahar, Henry Pollock, Rena Schweizer, Nick Sly, Jon Velotta, Kate Wilsterman, and Cole Wolf. There's no one I would have rather spent grad school with. Thank you to the old guard, for setting high standards and continuously pushing me, and especially to Cole and Jon, for always being there to talk science, lend a hand, vent over beers, wipe tears, or share laughs. You've been my second family and I appreciate you more than I can say.

Thank you to Brett Addis, whose encouragement and laughter kept me sane this past year, and who ensured that I did not survive on chips and salsa alone. I would have become a malnourished hermit without you.

Thank you to Oliver for patiently accompanying me during late nights at the Fort and my solo collecting trip to South Dakota, reminding me to take breaks and go for walks, and being an infinite source of hilarity.

To my parents, thank you for your endless encouragement and assistance, and for things too numerous to list here (including designing and building RFID feeders that didn't even make it into my dissertation).

Finally, to Nathan, whose role in this dissertation is immeasurable. Thank you for: moving to Missoula for my PhD; traveling all over the West catching juncos; putting up with me before sunrise; driving through the night with a car full of birds *on three separate occasions*; spending evenings at the Fort; making sure that I eat; late night conversations about my science when you should be asleep; reading to me when I can't otherwise turn my brain off; line-editing my grants and every word in this dissertation, while knowing that I am going to reject many (most?) of your edits; talking through every idea, every analysis, every result — even when I get annoyed at you for sharing your opinion after I expressly asked for it; poking fun at me when I'm being ridiculous; picking me up when I crumble; and celebrating my successes, no matter how small. In short, thank you for being supportive in every way possible. I don't know how people complete PhDs without Nathan Senner in their life.

Preface

Physiology is the means by which organisms balance the competing demands of their life cycle and environment. Variation in physiological responses can therefore have dramatic fitness consequences and, as a result, understanding physiological adaptation is critical for understanding large-scale evolutionary processes. In this dissertation, I seek to expand our recognition of the processes underlying physiological adaptation by exploring phenotypic flexibility – the ability to reversibly modify a trait value to match fluctuating environmental conditions within an individual's lifetime – in physiological systems. Specifically, I characterize both the mechanisms that enable organisms to mount flexible responses to changing environmental conditions and the environmental drivers of inter-individual variation in physiological flexibility.

At its basis, this dissertation is focused on flexibility in a complex physiological trait, thermogenic capacity (the ability to produce heat). Maintaining a relatively stable body temperature is key to endothermic homeostasis and survival. Seasonal climates therefore necessitate changes in endogenous heat production (and/or heat dissipation) by small endotherms in order to mediate fluctuations in their thermal environment. As a result, songbirds that reside at temperate latitudes increase their thermogenic capacity in winter (Swanson 2010) and this enhances their overwinter survival (Petit et al. 2017). Characterizing the mechanisms that underlie this flexible response and what drives variation in flexibility among individuals is important for understanding both large-scale physiological patterns and potential responses to future environmental change. For instance, thermal tolerance varies across latitudes for both ectotherms and endotherms with temperate zone organisms exhibiting broader thermal tolerances than their tropical counterparts (*e.g.*, Ghalambor et al. 2006; Sunday et al. 2011; Naya et al. 2012; Pollock et al. 2019) and this general pattern has been used to assess comparative risk under projected global-change related warming scenarios. However, studies of this kind usually rely on a single metric of thermal tolerance as a canalized trait across a species' range. This fails to account for the fact that many physiological traits are flexible, and incorporating this flexibility could improve both our understanding of biogeographic patterns and the predictive capacity of adaptive response models. In this dissertation, I thus ask: (1) How do birds maintain normothermia in the cold? (2) Are there potential tradeoffs between mechanisms for heat production? (3) How do they coordinate changes in traits within physiological systems? And (4) How do populations potentially differ in their ability to flexibly respond to their environment? The answers to these questions will shed light on endothermic physiological adaptation and be instructive for parameterizing and improving species distribution models and assessment of vulnerability to global change.

In the first half of this dissertation, I present a large acclimation study using Dark-eyed Juncos (*Junco hyemalis*). I exposed 106 juncos to chronic cold in the laboratory for varying durations and explore their physiological responses in three sequential chapters. In Chapter 1*, I use these individuals as a case study to understand the contribution of two processes underlying endothermic body temperature maintenance: heat generation and heat conservation. I assayed summit metabolic rate (a proxy for shivering capacity), thermal conductance of the skin and plumage (i.e., heat loss to the environment), and ability to maintain normothermia in acute cold trials. My findings both demonstrate the ability of birds to adjust their thermoregulatory

strategies in response to thermal cues and reveal that birds may combine multiple responses to meet the specific demands of their environments.

Nonetheless, neither index of heat generation nor conservation fully explained variation in junco body temperature maintenance. Consequently, in Chapter 2*, I investigate the potential role of a second mechanism of heat generation – non-shivering thermogenesis – in avian body temperature regulation. Although non-shivering thermogenesis is well documented in mammals, its importance to birds is, as of yet, unclear due in large part to the absence of brown adipose tissue (the principal non-shivering thermogenic organ in many mammals). Recent work in mammals has also pointed to a prominent role for the sarco/endoplasmic reticulum calcium ATPase (SERCA) in muscular non-shivering thermogenesis (Rowland et al. 2015). However, SERCA's involvement in both shivering and non-shivering thermogenesis posits a tradeoff between these two heat-generating mechanisms. To explore this potential tradeoff, I assayed pectoralis gene expression for the same individuals that I had exposed to temperature acclimations. My results suggest that non-shivering thermogenesis is not an important mechanism of avian thermoregulation in the cold. In culmination with those from my first chapter, these findings also indicate that cold-acclimated juncos may have achieved improvements in body temperature maintenance by increasing the efficiency of cellular processes, like calcium transport, that are essential to shivering thermogenesis.

As these first two chapters begin to suggest, many flexible phenotypes, like thermogenic capacity, are complex whole-organism responses that are underlain by many lower-level, subordinate traits (Schulte et al. 2011). A system's capacity for flexibility may therefore be determined by its underlying trait architecture, and these relationships can have important implications for both organismal adaptation and the evolvability of acclimatization responses. To explore the mechanistic basis of phenotypic flexibility in complex traits, in Chapter 3, I provide 20 additional physiological traits for these same acclimated individuals from my first two chapters. I assessed how relationships among traits vary as the environmental context changes, as well as the number of trait modifications that contribute to changes in whole-organism performance. My results suggest that simple and reversible modifications can significantly impact whole-organism performance, and thus that the evolution of phenotypic flexibility in a single component part could impart flexibility for the entire system.

This first work was all performed on individuals from a single population, thus I assumed that flexible responses among these individuals were similar. To understand what drives variation in physiological flexibility *among* individuals, I needed to take a broader approach. Theory predicts that the relative degree of flexibility exhibited by a population will positively correlate with the environmental heterogeneity they experience (Moran 1992; Sultan and Spencer 2002; Ernande and Dieckmann 2004), yet there are few empirical examples to support this. Thus, in Chapter 4, I integrate assays of population genetic variation with whole-organism measures of thermogenic performance and indices of environmental heterogeneity for individuals across the *Junco* distribution. I combined measures of thermogenic capacity for close to 300 individuals collected throughout the United States, more than 28,000 single nucleotide polymorphisms genotyped for 192 individuals, and laboratory acclimation experiments replicated on five *Junco* populations. Together, the results from these efforts suggest that thermogenic flexibility may play a key role in local adaptation in this broadly distributed lineage.

Zooming out, in Chapter 5, I review the eco-evolutionary importance of phenotypic flexibility. Specifically, I address the following questions: (1) What are the environmental conditions under which flexibility evolves? (2) What kinds of traits are likely to be flexible? (3) How does selection act on flexible traits? And (4) how might flexibility confer stability on populations in the future? This synthesis helps put the results of my first four chapters into a broader context by suggesting how flexibility in a single, complex trait, like thermogenic capacity, may have evolved and how it may be important for *Junco* populations in this era of climatic change.

Ultimately, my dissertation reveals the strength of taking a multi-pronged approach. By integrating mechanistic physiological studies with broad-scale indices of population divergence and environmental variation, we can gain a better understanding of flexibility's role in adaptation and species' resilience to environmental change.

REFERENCES

Ernande, B., and U. Dieckmann. 2004. The evolution of phenotypic plasticity in spatially structured environments: implications of intraspecific competition, plasticity costs and environmental characteristics. Journal of Evolutionary Biology 17:613–628.

Ghalambor, C. K., R. B. Huey, P. R. Martin, J. J. Tewksbury, and G. Wang. 2006. Are mountain passes higher in the tropics? janzen's hypothesis revisited. Integrative and Comparative Biology 46:5–17.

Moran, N. A. 1992. The Evolutionary maintenance of alternative phenotypes. The American Naturalist 139:971–989.

Naya, D. E., L. Spangenberg, H. Naya, and F. Bozinovic. 2012. Latitudinal patterns in rodent metabolic flexibility. The American Naturalist 179:E172–E179.

Petit, M., S. Clavijo-Baquet, and F. Vézina. 2017. Increasing winter maximal metabolic rate improves intrawinter survival in small birds. Physiological and Biochemical Zoology 90:166–177.

Pollock, H. S., J. D. Brawn, T. J. Agin, and Z. A. Cheviron. 2019. Differences between temperate and tropical birds in seasonal acclimatization of thermoregulatory traits. Journal of Avian Biology 50.

Rowland, L. A., N. C. Bal, and M. Periasamy. 2015. The role of skeletal-muscle-based thermogenic mechanisms in vertebrate endothermy: Non-shivering thermogenic mechanisms in evolution. Biological Reviews 90:1279–1297.

Schulte, P. M., T. M. Healy, and N. A. Fangue. 2011. Thermal performance curves, phenotypic plasticity, and the time scales of temperature exposure. Integrative and Comparative Biology 51:691–702.

Stager, M., H. S. Pollock, P. M. Benham, N. D. Sly, J. D. Brawn, and Z. A. Cheviron. 2016. Disentangling environmental drivers of metabolic flexibility in birds: the importance of temperature extremes versus temperature variability. Ecography 39:787–795.

Sultan, S. E., and H. G. Spencer. 2002. Metapopulation structure favors plasticity over local adaptation. The American Naturalist 160:271–283.

Sunday, J. M., A. E. Bates, and N. K. Dulvy. 2011. Global analysis of thermal tolerance and latitude in ectotherms. Proceedings of the Royal Society B: Biological Sciences 278:1823–1830.

Swanson, D. L. 2010. Seasonal metabolic variation in birds: functional and mechanistic correlates. Pages 75–129 *in* C. F. Thompson, ed. Current Ornithology Volume 17. Springer New York, New York, NY.

[*] Chapters 1 and 2 are reproduced here with permission from the Company of Biologists and Royal Society Publishing, respectively.

© 2020. Published by The Company of Biologists Ltd | Journal of Experimental Biology (2020) 223, jeb221853. doi:10.1242/jeb.221853

RESEARCH ARTICLE

Body temperature maintenance acclimates in a winter-tenacious songbird

Maria Stager[1,*], Nathan R. Senner[2], Bret W. Tobalske[1] and Zachary A. Cheviron[1]

ABSTRACT

Flexibility in heat generation and dissipation mechanisms provides endotherms the ability to match their thermoregulatory strategy with external demands. However, the degree to which these two mechanisms account for seasonal changes in body temperature regulation is little explored. Here, we present novel data on the regulation of avian body temperature to investigate how birds alter mechanisms of heat production and heat conservation to deal with variation in ambient conditions. We subjected dark-eyed juncos (*Junco hyemalis*) to chronic cold acclimations of varying duration and subsequently quantified their metabolic rates, thermal conductance and ability to maintain normothermia. Cold-acclimated birds adjusted traits related to both heat generation (increased summit metabolic rate) and heat conservation (decreased conductance) to improve their body temperature regulation. Increases in summit metabolic rate occurred rapidly, but plateaued after 1 week of cold exposure. In contrast, changes to conductance occurred only after 9 weeks of cold exposure. Thus, the ability to maintain body temperature continued to improve throughout the experiment, but the mechanisms underlying this improvement changed through time. Our results demonstrate the ability of birds to adjust thermoregulatory strategies in response to thermal cues and reveal that birds may combine multiple responses to meet the specific demands of their environments.

KEY WORDS: Thermoregulation, Summit metabolic rate, Thermal conductance, Seasonality, Dark-eyed junco

INTRODUCTION

Body temperature (T_b) influences all aspects of animal function, from the rate of chemical reactions to metabolism, growth and locomotion. Endogenous heat generation allows homeothermic endotherms to maintain a relatively constant T_b across a broad range of environmental temperatures, thereby providing physiological advantages (Bennett and Ruben, 1979; Crompton et al., 1978) that have enabled them to occupy a wide variety of habitats and climates. To maintain this high internal temperature, homeothermic endotherms coordinate changes occurring at multiple hierarchical levels of biological organization to respond to fluctuations in their environment.

The demands of T_b regulation are especially pronounced in temperate biomes, where climates are often cooler than thermoneutrality. Winter, in particular, can impose large temperature differentials for resident endotherms, and this thermoregulatory challenge is layered on top of other stresses, including reduced food availability, decreased daylight for foraging, and long nights of fasting (Marsh and Dawson, 1989). Unlike mammals that hibernate, a wide variety of birds remain active in temperate biomes all winter (Swanson, 2010). Some birds make use of heat-conservation mechanisms to cope with these conditions, such as huddling and utilizing microclimatic refugia, or employ facultative hypothermia, thereby decreasing their temperature differential with the environment and reducing energy consumption (Douglas et al., 2017; Korhonen, 1981; Mckechnie and Lovegrove, 2002). In spite of the benefits of these mechanisms, birds still need to eat, and they can frequently be seen foraging on even the most blustery days.

To remain active throughout the temperate winter, birds employ two primary physiological strategies to achieve normothermia: first, they can increase heat production and, second, they can decrease thermal conductance. In general, avian thermogenesis results from shivering (Marsh and Dawson, 1989) or as a by-product of metabolism and activity (Dawson and O'Connor, 1996), although the role of non-shivering thermogenesis in adult birds is not well characterized (Hohtola, 2002). Peak oxygen consumption under cold exposure (summit metabolic rate; M_{sum}) is often used as a proxy for thermogenic capacity, and many birds have been shown to increase M_{sum} by 10–50% in winter (Swanson, 2010). These seasonal changes have been credited with higher heat production and increased cold tolerance (O'Connor, 1995; Swanson, 1990a). At the same time, fueling an elevated metabolic rate requires increased foraging – and thus concomitantly escalates exposure to predators (Lima, 1985) – in addition to the potential energetic cost of restructuring internal physiology to meet these heightened aerobic demands (Liknes and Swanson, 2011). Few studies, however, have fully explored these potential trade-offs in natural systems (but see Petit et al., 2017), and shivering thermogenesis is frequently thought to represent the major mechanism by which birds maintain normothermia in winter (Swanson, 2010). Nonetheless, improved cold tolerance can occur independent of increases in M_{sum} (Dawson and Smith, 1986; Saarela et al., 1989), indicating additional strategies may be employed.

For small passerines that have high surface to volume ratios, seasonal decreases in thermal conductance (i.e. the transport of energy across a temperature gradient) may also be favored by natural selection. Direct measures of heat transfer are scarce (Wolf and Walsberg, 2000), but indirect measures indicate that thermal conductance decreases with decreasing ambient temperature in interspecific comparisons (Londoño et al., 2017), which may be associated with increases in plumage density (Osváth et al., 2018). However, the role of seasonal adjustments to thermal conductance in birds is not well understood. Although some birds increase plumage mass in winter (Møller, 2015), it is unclear how this is achieved: most passerines molt only once per year, and their winter feathers are thus also their eventual summer feathers. Birds could

[1]Division of Biological Sciences, University of Montana, Missoula, MT 59812, USA. [2]Department of Biological Sciences, University of South Carolina, Columbia, SC 29208, USA.

*Author for correspondence (maria.stager@umontana.edu)

M.S., 0000-0002-5635-580X; N.R.S., 0000-0003-2236-2697

Received 16 January 2020; Accepted 4 May 2020

also make behavioral adjustments in the cold, including postural changes to reduce surface area – especially of unfeathered areas, such as the head and feet (Ferretti et al., 2019) – or erecting feathers to trap air around the body (Morris, 1956). Given these knowledge gaps, the question remains: what are the relative contributions of heat conservation and heat generation processes to avian body temperature regulation in the cold?

Such questions are particularly important in this era of rapid climatic change. Although ambient conditions can vary predictably, recent increases in climatic variability (e.g. Kolstad et al., 2010) highlight the need for animals to respond rapidly to changing conditions. Each of the aforementioned potential physiological responses is likely tied to different environmental cues – primarily photoperiod and temperature (Swanson and Vézina, 2015). However, we do not understand how birds respond to environmental stimuli to balance heat loss and heat production, which is vital to projections of endothermic distributions under predicted future climate change scenarios (Buckley et al., 2018).

To understand how birds modify their thermoregulatory ability in the cold, we performed an acclimation experiment using dark-eyed juncos [*Junco hyemalis* (Linnaeus 1758)]. Juncos are small songbirds that overwinter across much of North America and are not known to huddle or use torpor (Nolan et al., 2002). We exposed juncos sampled from a single population to one of 10 experimental treatments that varied in temperature and the duration of cold exposure. Following acclimation to these experimental treatments, we quantified metabolic rates, heat loss across the skin and plumage, and T_b maintenance within the same individuals. Our results shed light on the ability of birds to respond to thermal cues and elucidate the mechanisms underlying their physiological responses to cold temperatures.

MATERIALS AND METHODS

Acclimation experiments

We captured adult juncos breeding in Missoula County, Montana, USA (~47.0°N, −113.4°W), from 12 to 19 July 2016 (n=56) using mist nets. To increase sample sizes, we captured additional individuals between 27 July and 3 August 2017 (n=52) and repeated all procedures. We immediately transferred birds to husbandry facilities at the University of Montana and housed them individually under common conditions for 42 days (18°C, 10 h:14 h light:dark). After this 6-week adjustment period, we assayed metabolic rates (see below). Following metabolic trials, we allowed birds to recover for ~24 h before we randomly assigned individuals to acclimation groups and subjected them to one of two temperature treatments, cold (−8°C) or control (18°C), lasting 7 days (week 1), 14 days (week 2), 21 days (week 3), 42 days (week 6) or 63 days (week 9) in duration. We chose to acclimate birds to −8°C, which is a temperature that juncos experience in the northern parts of their winter range for weeks at a time (Fig. S1) and which could elicit more dramatic physiological responses than previous experiments with juncos performed at 3°C (Swanson et al., 2014). Photoperiod was maintained at a constant 10 h:14 h light:dark in both treatments (the photoperiod in Missoula County in November and February), and food and water were supplied *ad libitum* for the duration of the experiment. Birds were fed white millet and black oil sunflower seeds at a 2:1 ratio by mass, supplemented with ground dog food, live mealworms and vitamin drops (Wild Harvest D13123 Multi Drops) in their water. We did not repeat the week 9 treatment in 2017. Also, one individual died 12 days into the cold treatment in 2016 and another died during the adjustment period in 2017 (causes unknown), resulting in a total sample size of 106 individuals (n=12 per treatment, except $n_{control\_1}$=11, $n_{control\_9}$=6, n_{cold_9}=5).

As an index of body size, we measured the tarsus lengths (mm) of both legs and calculated the average measure for each individual. We quantified this feature only once (after the bird was euthanized) assuming that tarsus length did not change over the duration of the acclimation because all individuals were adults. The sample is heavily male-biased (90.5%) but includes 10 females (9.5%) across the 2 years. These females were randomly distributed across most treatment groups. Brood patches and cloacal protuberances were not present after the 6-week adjustment period. Sex was confirmed post-acclimation by identification of the gonads during dissection. For five additional males captured at the same time but not included in the study, we confirmed by dissection that testes had regressed before the acclimations began.

Ethics

All procedures were approved by the University of Montana Animal Care Committee (protocol 010-16ZCDBS-020916). Birds were collected with permission from Montana Fish Wildlife & Parks (permits 2016-013 and 2017-067-W, issued to M.S.) and the US Fish & Wildlife Service (permit MB84376B-1 to M.S.).

Metabolic assays

We measured resting metabolic rate (RMR) and M_{sum} in a temperature-controlled cabinet using open-flow respirometry before and after acclimation treatments. RMR trials were conducted in the evening during the birds' dark cycle (start time mean=19:11 h; range=18:00–23:20 h). M_{sum} trials were conducted the following day largely within the birds' light cycle (start time mean=13:30 h; range=09:00–20:42 h). Birds were not fasted before either measurement so as not to limit aerobic performance and to ease comparison between measures. For RMR trials, birds were placed in a modified 1 liter Nalgene container and measured in a dark, quiet temperature cabinet (Sable Systems Pelt Cabinet with Pelt-5 Temperature Controller) at 27°C, which is within the thermoneutral zone of juncos (Swanson, 1991). Three individuals were assayed simultaneously with an empty, identical chamber serving as the baseline. We cycled through individuals at 15-min intervals alternated with 5-min baseline measures, such that each individual was measured for at least 30 min over the course of 2 h. We subjected an individual to additional rounds of measurement if the O_2 trace suggested that it was active. Ambient air was first dried (using Drierite™) and then pumped through the animal chamber at 500 ml min^{-1}, and excurrent air was subsampled manually from one chamber at a time at 100–150 ml min^{-1} through barrel syringes. We dried excurrent air again, then CO_2 was scrubbed with ascarite, and the outflow dried again before passing through a FoxBox (Sable Systems) to quantify O_2. All chambers – animal and baseline – were plumbed into the same system. We spanned the FoxBox using baseline air at 20.95% O_2 before each trial began. Flow was controlled using a mass flow meter (Sable Systems). From these measures, we quantified oxygen consumption according to Lighton (2008). We first corrected for any fluctuations in baseline concentrations using a linear correction and then calculated RMR as the lowest oxygen consumption (ml O_2 min^{-1}) averaged over a 10-min period using custom scripts in the R programming environment (https://www.r-project.org/).

M_{sum} trials were conducted using a similar setup with static cold exposure. Trials were conducted in a heliox environment (21% helium, 79% oxygen) with flow rates of 750 ml min^{-1}. The high thermal conductance of heliox facilitates heat loss at higher temperatures than is necessary in air to avoid injury to experimental subjects (Rosenmann and Morrison, 1974). Heliox

Journal of Experimental Biology (2020) 223, jeb221853. doi:10.1242/jeb.221853

flow rates were measured using a mass flow meter (Alicat M-series) programmed for the specific gas mixture. Pre-acclimation M_{sum} trials were conducted using the above temperature cabinet set to −5°C. Trials ended when a bird's CO_2 production plateaued or after 1 h, whichever came first. Immediately upon removing birds from the temperature cabinet, we measured body temperature using a thermistor probe inserted into the cloaca. We considered birds hypothermic if their body temperature was ≤37°C (per Swanson et al., 2014). One individual that was not hypothermic at the end of the M_{sum} trial was removed from further analysis. We corrected for drift then calculated M_{sum} as the highest oxygen consumption (ml O_2 min^{-1}) averaged over a 5-min period using custom scripts in R. As a measure of thermogenic endurance, we calculated the number of minutes that an individual maintained 90% or more of their M_{sum} (Cheviron et al., 2013).

Because we expected acclimated birds to differ in their cold tolerance, we performed post-acclimation M_{sum} trials at lower temperatures for cold-acclimated birds (mean±s.d. starting cabinet temperature=−24.47±2.87°C) than control-acclimated birds (mean±s.d.=−15.94±5.98°C) using a laboratory freezer (Accucold VLT650). These temperatures, concurrent with a heliox atmosphere, represent rather severe conditions that juncos are unlikely to encounter in the wild, but were chosen because previous work has demonstrated that cold exposure in excess of −9°C in heliox is necessary to induce hypothermia within 90 min in winter-acclimatized juncos (Swanson, 1990a). Although we aimed for static cold exposure, logistical constraints did not allow for precise temperature control. We thus recorded temperature inside the cabinet for the duration of the trial to account for variation within and among trials. Post-acclimation trials ended after an extended period of declining CO_2 production coincident with the bird's body temperature dropping below 30°C (see below).

We used multiple respirometry setups in order to complete all pre-acclimation measurements precisely 42 days after the day of capture (three units in 2016, four in 2017). *Post hoc* tests revealed significant differences in the metabolic measurements made by each respirometry unit. Because systems were regularly checked for leaks, we think these differences likely derived from calibration differences among units. To control for these effects, we regressed each metabolic trait (RMR or M_{sum}) on respirometry unit for each year and then subtracted the resulting beta coefficient (slope) from the metabolic rate (Table S1). Although all post-acclimation measures were conducted using a single respirometer, we used the same correction factor to make the before and after measures comparable. In a few instances, this resulted in negative M_{sum} values that were removed from further analysis (n=3 pre-acclimation measures, n=1 post-acclimation). Metabolic trials for cold individuals were conducted earlier in the day than those of control individuals because the temperature cabinet tended to increase in temperature each time it was opened. For this reason, we tested for, but did not find, a significant interaction between trial start time and temperature treatment on post-acclimation M_{sum} (P=0.21).

We measured body mass (M_b; in g) immediately before each metabolic assay. Birds were banded with a unique combination of two or three plastic leg bands; the mass of these bands has been removed from all reported M_b. Directly following the post-acclimation M_{sum} trial, we euthanized individuals using cervical dislocation, removed organs and tissues within the body cavity, filled the body cavity with a wet paper towel to preserve moisture, and froze carcasses at −20°C until thermal conductance assays were performed in May and June 2019. To quantify the change in each trait value with acclimation, we subtracted an individual's pre-acclimation trait value from their post-acclimation value (ΔM_b, ΔRMR and ΔM_{sum}). We did not compare endurance measures pre- and post-acclimation because trial conditions varied before and after acclimation.

Body temperature maintenance

To quantify the ability to maintain normothermia during acute cold exposure, we measured T_b continuously for the duration of the post-acclimation M_{sum} acute cold trial. Immediately prior to this trial, we inserted a temperature-sensitive passive integrated transponder (PIT) tag (12 mm, Biomark) into the cloaca of the bird. PIT tags were inserted at room temperature; thus, even cold-acclimated birds were exposed to warmer conditions for a few minutes preceding the M_{sum} trial. To secure the tag, we glued the feathers surrounding the cloaca together using cyanoacrylate adhesive (super glue). We quantified M_b before the addition of the PIT tag. An antenna was placed inside the temperature cabinet next to the animal chamber and connected to an external reader that recorded T_b eight times per second (Biomark HPR Plus Reader). We averaged the T_b measurements over each 1-min interval of the trial and coded each 1-min interval as hypothermic or normothermic. We deemed birds hypothermic once they lost 10% of their initial T_b and maintained T_b below this level. Because birds differed in their initial T_b (36–42°C), we repeated all analyses using the commonly accepted threshold of 37.0°C to define the hypothermic state, but this did not change our overall results (Table S2). In some cases, super glue did not hold the cloaca closed, and birds ejected their PIT tags during the trial. We removed from the sample six individuals for which PIT tag ejection occurred before hypothermia could be assessed. We also removed eight individuals for which gaps longer than 1 min existed (due to the position of the bird relative to the antenna) at critical periods that prevented precise detection of their hypothermic state, resulting in a total sample size of n=92. We used different respirometry chambers (either a custom-made plexiglass box or modified Nalgene) for the post-acclimation M_{sum} trials between years. Because these chambers had different thermal properties that may have contributed to differences in the way the individuals experienced temperature in the cold trials, we also tested for an effect of year on risk of hypothermia (see below).

Thermal conductance assays

We measured the conductive properties of the skin and plumage by quantifying the amount of power input (mW) required to maintain a constant internal temperature of 39°C with the ambient temperature providing a gradient. To do this, we first thawed carcasses at room temperature and dried the feathers. We removed any adipose or muscle tissue remaining in the body cavity, then inserted an epoxy mold (~35 mm long×16 mm in diameter; PC-Marine Epoxy Putty) into the coelom that we designed to fill the coelom without significant stretching of the superficial thoracic and abdominal regions. Within this mold, we embedded a centrally placed thermocouple and a length of nichrome wire for heating. These were connected to a custom-made board containing a voltage logger (Omega OM-CP-Quadvolt), an amperage logger (Omega OM-CP-Process 101A-3A) and a temperature controller (Omega CNI1622-C24-DC). Power was supplied to the circuit using a 12 V DC battery. We sewed the body cavity together using sewing thread, leaving a small hole near the cloaca for the wires to exit. We suspended the carcass from a single thread through the nares, supported by the wires from below, such that birds were in an upright position with legs hanging freely. We cleaned the feathers with cornmeal to remove oils and combed the feathers into place.

Journal of Experimental Biology (2020) 223, jeb221853. doi:10.1242/jeb.221853

Wings were positioned at the sides, tucked in as best as possible. We removed six carcasses damaged beyond repair in post-processing.

Conductance trials were conducted in a small, closed room without airflow and at ambient (laboratory) temperature (mean±s.d.=23.4±0.61°C). The mold was first brought to 39°C and power was supplied whenever the temperature dropped below 38°C. We recorded the amperage, voltage and temperature of the thermocouple for each second of an 18 min trial. We calculated the average power input (conductance, mW) as the mean volts×amps over a 10 min period. We excluded two individuals for which temperatures did not stay within the specified range, resulting in a total sample size of n=98. All assays were performed by a single individual (M.S.) and were done blind to the birds' treatment assignments. We did not find a significant effect of the minor variation in ambient temperature that occurred on average power input using a linear regression (P=0.19). Trials were performed across multiple days, but we did not find an effect of measurement day (Table S3) or freeze duration on average power input (P=0.95).

Statistical analyses

We performed all analyses in R. We first quantified the effects of acclimation temperature and duration on mass, tarsus length and conductance using multiple regressions for pre-acclimation, post-acclimation and ΔM_b values. We similarly used multiple regressions to quantify the effects of acclimation temperature and duration on RMR, M_{sum} and endurance with M_b as a covariate, as well as on ΔRMR and ΔM_{sum} with ΔM_b as a covariate. For all models, we also tested for an effect of a temperature×duration interaction but this term was generally not significant (Table S4). Additionally, we tested for associations among the phenotypic traits using Pearson correlation tests. We report means±s.d. in the text.

To assess T_b maintenance, we used T_b interval data to fit Cox proportional hazards regression models using the survival package in R (https://CRAN.R-project.org/package=survival). These standard time to event models analyse non-linear processes without assuming any one shape of response, allowing us to control for differences in temperature stimulus among individuals. We created survival objects with interval data and hypothermic status, then fit regressions using the function coxph to quantify the effects of cabinet temperature, temperature treatment, duration and year with all terms clustered by individual on the risk of hypothermia. We first standardized all variables using the arm package (Gelman, 2008).

We used the same approach to assess the effect of phenotypic traits (M_b, tarsus, RMR, M_{sum}, endurance and conductance) on the risk of hypothermia using a subset of individuals for which we had complete measurements (n=84). Because of the large number of phenotypic variables potentially influencing T_b maintenance, we used a model selection process whereby we tested all possible combinations (including two-way interactions) of the predictor variables. We evaluated all models using Akaike information criterion scores corrected for small sample sizes (AIC_c), where the model with the lowest AIC_c score was considered the most well-supported model. Because there was no single most well-supported model (e.g. w_i>0.90; Grueber et al., 2011), we used model averaging to identify which predictor variables had significant effects on T_b maintenance.

RESULTS

Prior to acclimation, treatment groups did not differ significantly in body size or metabolic traits (Table 1). Acclimation temperature and duration did not influence M_b (mean=22.30±1.79 g) or RMR (mean=1.38±0.29 ml O_2 min^{-1}; Table 1, Fig. 1A). RMR was correlated with M_b both before and after acclimation (Table 1).

In contrast, cold-acclimated birds exhibited a 20% elevation in M_{sum} compared with control birds (Table 1, Fig. 1B). The duration of cold exposure did not influence M_{sum} and M_{sum} was not correlated with M_b before or after acclimation (Table 1). Similarly, M_{sum} did not correlate with RMR at either time point (r_{pre}=−0.01, P_{pre}=0.85; r_{post}=0.15, P_{post}=0.13). Thermogenic endurance did not vary with temperature treatment or duration (Table 1), nor did it correlate with M_{sum} (r=−0.16, P=0.11).

Conductance properties of the skin were largely unchanged across acclimation treatments (Table 1). However, there was an interaction between treatment and duration (β=−8.52±2.56, P=0.0013). To investigate this relationship, we reran our regression model with duration as a categorical rather than continuous variable (Table 2). This revealed that the skin and plumage of cold-acclimated week 9 birds exhibited a reduction in heat transfer compared with other treatment groups (Fig. 2). The average power input required to maintain core temperature at 39°C was not correlated with M_b (r=−0.14, P=0.16), tarsus length

Table 1. Linear effects of cold treatment and treatment duration on phenotypic traits before and after acclimation

			Intercept		M_b			Cold treatment			Duration			
	Phenotype	n	β	s.e.	β	s.e.	P	β	s.e.	P	β	s.e.	P	Adjusted R^2
Pre	M_b	106	22.34	0.31				0.02	0.31	0.94	−0.05	0.06	0.41	−0.01
	Tarsus	106	19.91	0.11				0.10	0.11	0.33	0.04	0.02	0.07	0.02
	RMR	106	0.28	0.31	**0.05**	**0.01**	**8.9×10^{-4}**	−0.01	0.04	0.82	−0.01	0.01	0.13	0.10
	M_{sum}	102	4.90	0.79	0.06	0.04	0.07	0.10	0.12	0.40	−0.01	0.02	0.52	0.02
	Endurance	103	37.56	18.20	−0.48	0.81	0.55	1.52	2.76	0.58	0.05	0.55	0.93	−0.02
Post	M_b	106	22.83	0.33				0.47	0.32	0.14	−0.13	0.06	0.04	0.04
	RMR	105	0.30	0.43	**0.05**	**0.02**	**2.3×10^{-3}**	−0.04	0.05	0.51	−0.02	0.01	0.13	0.10
	M_{sum}	105	5.12	1.71	0.07	0.07	0.31	**1.31**	**0.25**	**8.1×10^{-7}**	−0.10	0.05	0.07	0.23
	Endurance	105	17.88	21.85	0.15	0.93	0.87	−6.04	3.19	0.42	1.24	0.65	0.06	0.04
	Conductance	98	323.63	6.89				−0.50	6.89	0.94	−1.07	1.35	0.43	−0.01
Δ	M_b	106	0.49	0.37				0.45	0.37	0.22	−0.08	0.07	0.28	0.01
	RMR	106	0.10	0.06	**0.05**	**0.02**	**2.2×10^{-3}**	−0.02	0.06	0.71	0.00	0.00	0.82	0.06
	M_{sum}	102	0.57	0.26	−0.10	0.06	0.12	**1.14**	**0.24**	**1.2×10^{-5}**	−0.09	0.05	0.06	0.19

Mass (M_b) is included as a covariate for metabolic traits. Delta (Δ) represents change over acclimation period (post- minus pre-acclimation) for traits that were measured at both time points. Bold indicates significant effects after Bonferroni correction for multiple models (P<0.004). RMR, resting metabolic rate; M_{sum}, summit metabolic rate.

Journal of Experimental Biology (2020) 223, jeb221853. doi:10.1242/jeb.221853

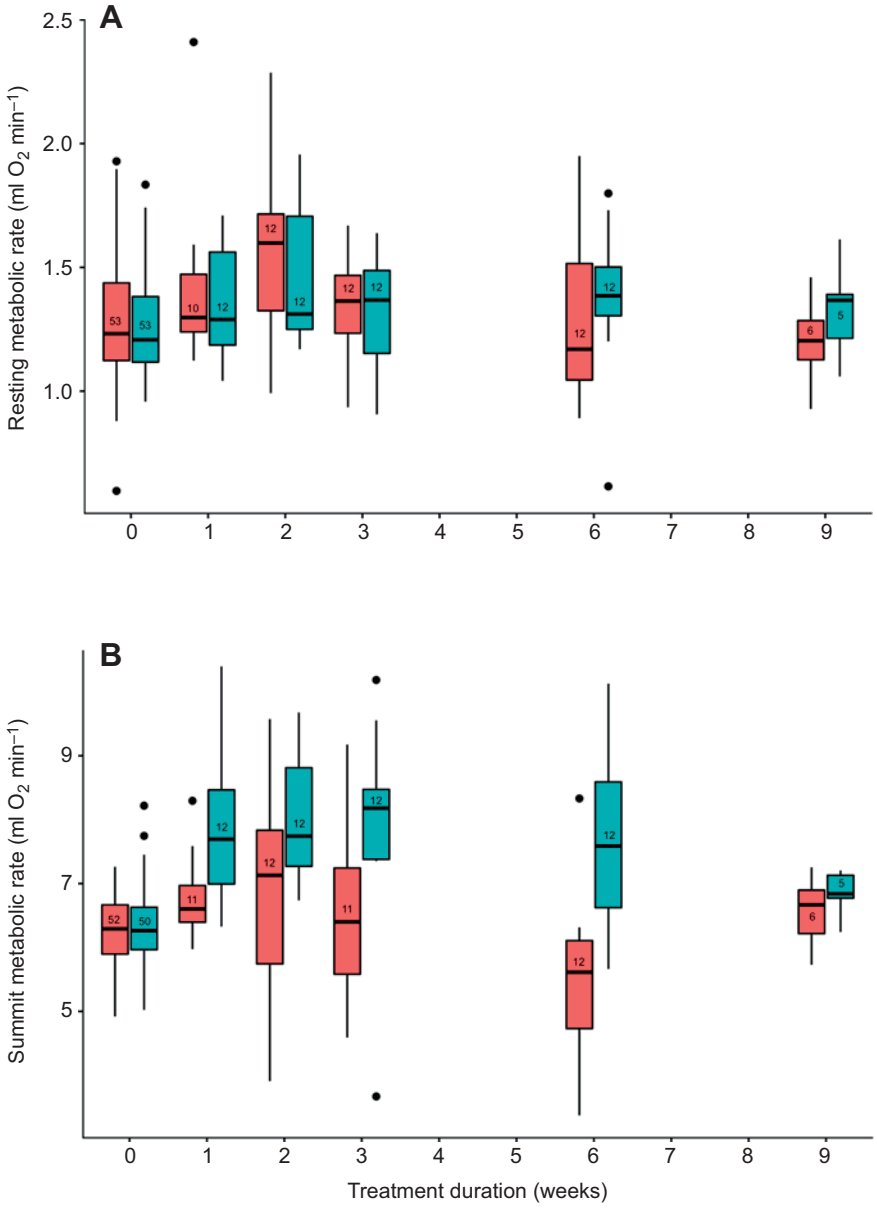

Fig. 1. Metabolic rate of juncos across treatments. (A) Resting metabolic rate. (B) Summit metabolic rate. Pre-acclimation measures for all individuals shown at week 0. Numbers in boxes indicate sample sizes for each group. Red, control treatment; blue, cold treatment. Boxplots show the median values (horizontal line in the box), the 25th and 75th percentiles (lower and upper margins of the box) together with the minimum and maximum values ≤1.5×IQR from the box margin (whiskers), and outlying points (circles).

(r=−0.11, P=0.29), RMR (r=−0.14, P=0.16) or M_{sum} (r=0.03, P=0.77).

Body temperature trajectories varied among individuals in acute cold trials. Some juncos showed a steady decline in T_b over time, while others exhibited an oscillating T_b (Fig. 3). Thirteen individuals, distributed across treatment groups, demonstrated the ability to increase T_b above normothermia after sustaining substantial losses in T_b. Birds did not differ in T_b among temperature acclimation groups at the start of the trial (t-test: t_{94}=0.45, P=0.65).

Higher cabinet temperatures elicited a reduced risk of hypothermia with a 17% reduction in per-minute hazard for every 1°C increase in cabinet temperature (Table 3). For this reason, we included cabinet temperature as a covariate in all subsequent models. Cold-acclimated birds exhibited an 87% reduction in the per-minute risk of hypothermia in acute cold trials (Fig. 4A). Every week of acclimation duration was associated with a 15% reduction in the per-minute risk of hypothermia. This was true for both the cold and the control treatments, so to further investigate this relationship, we tested for the effect of duration as a categorical, rather than a continuous, variable. Within the control treatment, only week 9 individuals showed a reduction in hypothermia risk compared with week 1 birds (Table 4). However, within the cold-acclimated birds, weeks 2, 6 and 9 all showed a reduced risk of hypothermia compared with week 1 (Table 4, Fig. 4B). Year did not influence the risk of hypothermia (Table 3).

There was no single model best predicting risk of hypothermia using phenotypic traits (Table 5). However, model averaging identified M_{sum}, endurance and their interaction as significant predictor variables (Table 6). The interaction term indicates that birds with both higher M_{sum} and endurance were better able to maintain their T_b. In comparison, M_b, tarsus length, RMR and conductance were not correlated with time to hypothermia (Table 6).

DISCUSSION

To support their energetic lifestyle, homeothermic endotherms maintain a relatively high and constant T_b despite changes in the

Journal of Experimental Biology (2020) 223, jeb221853. doi:10.1242/jeb.221853

Table 2. Linear effects of treatment temperature, duration (as categorical variable) and their interaction on conductance properties of the skin and plumage

Variable	β	s.e.	*P*
Intercept	316.88	10.06	$<2.0\times10^{-16}$
Cold treatment	16.37	13.91	0.24
Week 2	−15.51	13.62	0.26
Week 3	12.15	13.63	0.37
Week 6	6.31	14.62	0.67
Week 9	20.55	16.44	0.21
Cold treatment×Week 2	−4.38	19.23	0.82
Cold treatment×Week 3	−9.65	19.03	0.61
Cold treatment×Week 6	−28.78	20.18	0.16
Cold treatment×Week 9	−74.36	23.77	2.4×10^{-3}

Control week 1 is reference.

environment. Regulating T_b within this narrow window necessitates responding to changes in their environment that may arise both predictably and stochastically. Here, we show that the capacity for T_b maintenance is a flexible avian phenotype that can acclimate to changes in the thermal environment. The ability to maintain normothermia during acute cold exposure improved with cold acclimation, as well as the duration of the acclimation treatment. Modifications to thermoregulatory ability occurred on relatively short time scales (within 1 week) and without changes in photoperiod, suggesting that juncos can match their thermoregulatory physiology to current thermal conditions independent of broad-scale seasonal cues. At the same time, further enhancements to the ability to maintain T_b were made over successive time steps, indicating a lag in the induction of some physiological modifications. These results emphasize the potential for temporal constraints on individual flexibility.

Correlates of improved T_b maintenance ability

Summit metabolic rate has previously been implicated as the main factor governing avian cold tolerance in studies of seasonal flexibility (Swanson, 2010). We found that M_{sum} increased with cold acclimation within one week of cold exposure, but that further enhancements to this trait did not occur with longer acclimation durations. In this respect, our study is unique in that it shows responses in M_{sum} occurring on the order of days rather than weeks or months. Furthermore, our results indicate that the magnitude of the change in M_{sum} over this short timescale is on the order of seasonal increases in M_{sum} exhibited in wild juncos between summer and winter (28%; Swanson, 1990a), as well as that previously shown for juncos exposed to laboratory acclimations under more moderate conditions (16–19% at 3°C for 6 weeks; Swanson et al., 2014). The comparable magnitude of response to these two different temperature treatments contrasts with previous work showing that wild juncos and other birds modulate M_{sum} with environmental temperature across the winter (Swanson and Olmstead, 1999). Taken together, these findings suggest that M_{sum} might be coarsely adjusted, rather than fine-tuned, to environmental temperature, and that there may be limits to their flexibility in response to temperature variation (Petit and Vézina, 2014). Dissecting the relative contribution of subordinate phenotypic traits to M_{sum} – e.g. pectoralis muscle size, hematocrit or cellular metabolic intensity (Liknes and Swanson, 2011; Swanson, 1990b; Swanson et al., 2014) – will illustrate how birds build this phenotype and which traits (if any) may be limiting its flexibility.

Individuals characterized by both elevated M_{sum} and the ability to sustain heightened M_{sum} (endurance) were also capable of maintaining normothermia longer, indicating an additive effect of enhancing these two phenotypes. Nonetheless, we saw no effect of acclimation treatment or duration on endurance, and individuals continued to enhance their ability to maintain normothermia in successive weeks long after M_{sum} plateaued. These results suggest that either these indices are insufficient indicators of total thermogenic capacity or that individuals reduced their thermal conductance at these later time points.

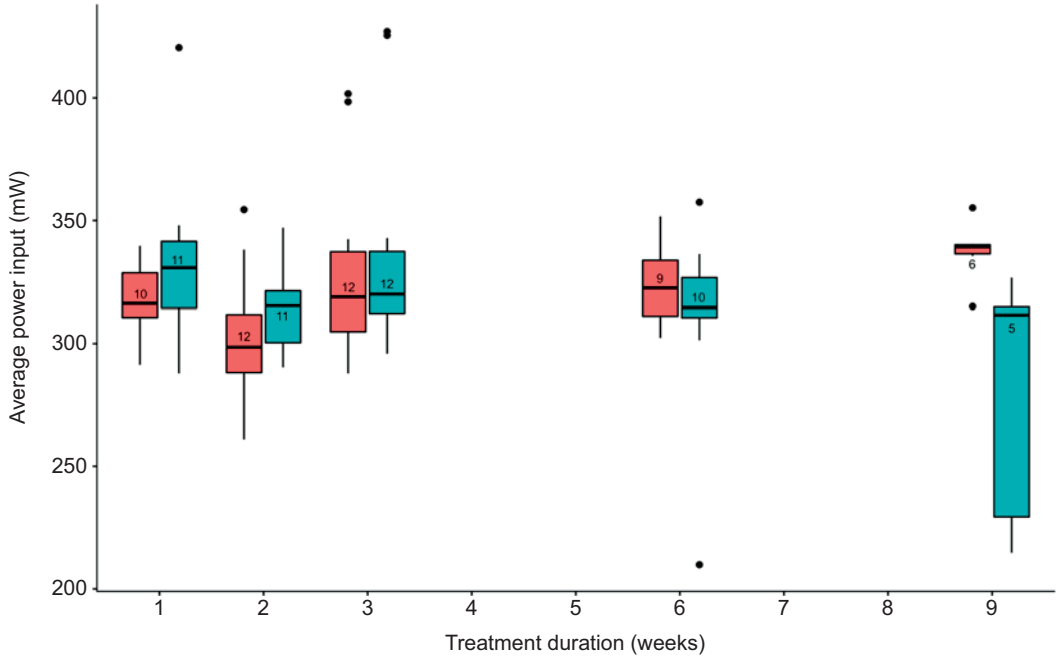

Fig. 2. Heat loss properties of junco skins across treatment groups expressed as the power (mW) required to maintain core body temperature at 39°C with ambient temperature at 24°C. Numbers in boxes indicate sample sizes for each group. Red, control treatment; blue, cold treatment. For boxplot conventions, see legend to Fig. 1.

Journal of Experimental Biology (2020) 223, jeb221853. doi:10.1242/jeb.221853

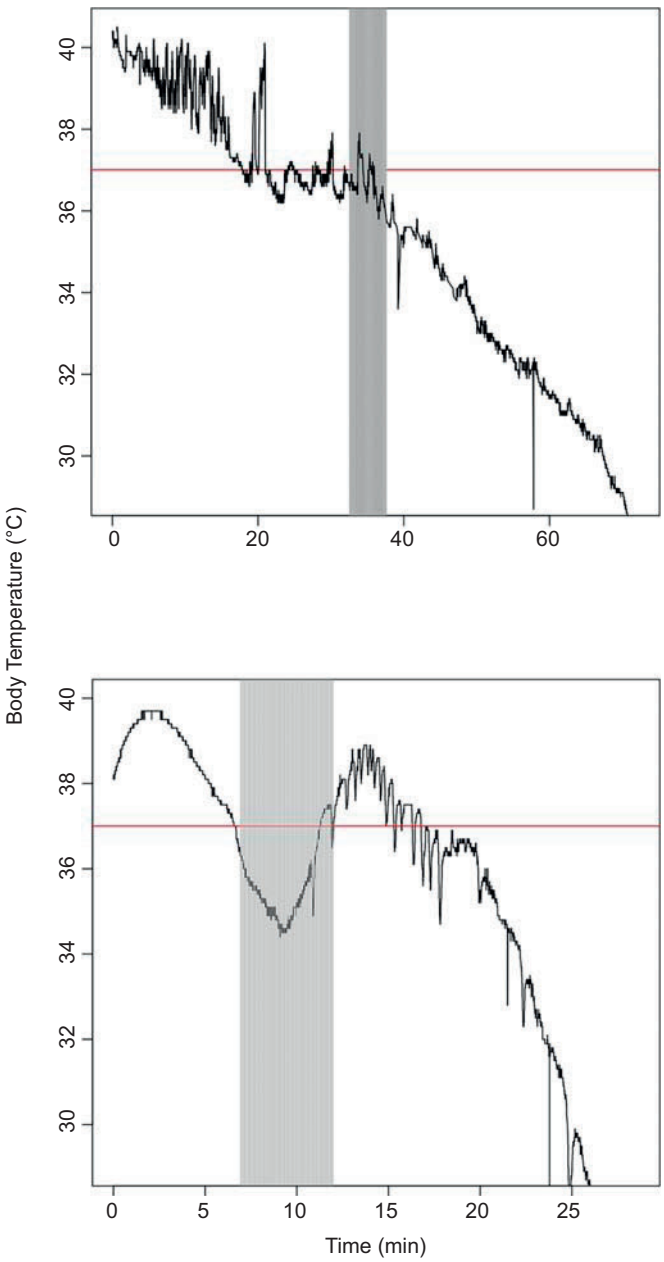

Fig. 3. Example trajectories of body temperature loss during acute cold trials. An individual that exhibits (A) mostly continual loss and (B) one that regains normothermia. Black line, body temperature; red line, 37°C; gray box is the 5-min period corresponding to M_{sum}.

In support of this latter possibility, we found that conductance of the skin and plumage decreased in response to our temperature stimulus. This finding prompts questions about the exact mechanism underlying such a modification. Although we cannot distinguish between potential adjustments made to the properties of the skin or the plumage, the fact that heat loss was only reduced at the last sampling point (week 9) suggests that alterations to thermal conductance may require significant time to implement. We did not see evidence that birds were molting large amounts of feathers during the acclimation, as was obvious when birds first entered captivity (M. Stager, personal observation). Moreover, avian molt is closely tied to photoperiod (Danner et al., 2015), yet conductance changed in the absence of variation in photoperiod. Instead, it seems plausible that birds may have added body feathers to their existing

Table 3. Cox proportional hazards model output for body temperature (T_b) maintenance as a function of cabinet temperature, acclimation temperature treatment, treatment duration and year

Variable	β	s.e.	HR	95% CI	*P*
Cabinet temperature	–3.87	0.55	0.02	–5.17, –2.58	4.8×10^{-9}
Temperature treatment	–2.06	0.48	0.13	–3.22, –0.90	4.9×10^{-4}
Duration	–0.95	0.26	0.39	–1.65, –0.26	7.4×10^{-3}
Year	0.53	0.25	1.70	–0.22, 1.28	0.17

Negative β coefficients represent reduced risk of hypothermia. Hazards ratio (HR) is the exponent of the β coefficient (i.e. a reduction in the hazard by this factor). Control treatment is reference for temperature effect. All continuous variables were standardized; bold indicates predictor variables with statistically significant effects on T_b maintenance.

plumage. Previous work has shown that juncos increase plumage mass in winter compared with summer (Swanson, 1991), as do American goldfinches (*Carduelis tristis*), which additionally have been shown to possess a greater percentage of plumulaceous barbules, as well as more barbules per barb, in winter than in summer (Middleton, 1986). However, goldfinches undergo an alternate molt in the spring, in addition to the basic molt in autumn, whereas juncos exhibit just the single autumn molt (Pyle, 1997). Thus if juncos did selectively add feathers to reduce conductance in the cold, it would suggest that they concomitantly lose select feathers before the subsequent summer to enable increased heat loss when they need it most. Alternatively, it is possible that changes were made to the heat transfer properties of the skin itself. For example, avian skin composition can be flexibly remodeled on the time scales of our experiments in response to humidity (Muñoz-Garcia et al., 2008). It should be noted that although the week 9 treatment was our smallest sample size, our results are statistically robust. Future studies would therefore profitably combine our methodology here with data on the time course of plumage quality and mass to further elucidate the role that heat-saving mechanisms might play in avian T_b maintenance.

Although reduced thermal conductance may explain the final boost in ability to maintain normothermia seen at week 9, variation in neither M_{sum} nor conductance explain the increase in T_b maintenance at weeks 2 and 6. One potential reason for this disparity is that we were unable to quantify total heat loss in live birds and thus may have overlooked additional factors that contribute to minimum conductance – such as vasoconstriction (Irving and Krog, 1955), posture (Pavlovic et al., 2019) and ptiloerection (Hohtola, Rintamäki, and Hissa, 1980) – that may have varied across treatments. To this point, we can anecdotally report from observations made during cold exposure trials that juncos sat on their feet, puffed up their feathers, but did not tuck their heads under their wings; however, we did not quantify these postures. A second potential explanation is that assaying total oxygen consumption could mask potential changes to thermogenic efficiency. For example, juncos may achieve higher metabolic efficiency by increasing fiber size within their muscle, thereby allowing for greater contraction force while simultaneously reducing basal metabolic cost because larger muscle fibers require less energy by Na^+/K^+ ATPase to maintain sarcolemmal membrane potential (Jimenez et al., 2013). Such changes have been documented in black-capped chickadees (*Poecile atricapillus*), which exhibit seasonal decreases in muscle fiber diameter from spring to summer (Jimenez et al., 2019), as well as increases with cold acclimation (Vezina et al., 2020). Additionally, if adult birds are employing non-shivering thermogenesis, the relative proportion

Journal of Experimental Biology (2020) 223, jeb221853. doi:10.1242/jeb.221853

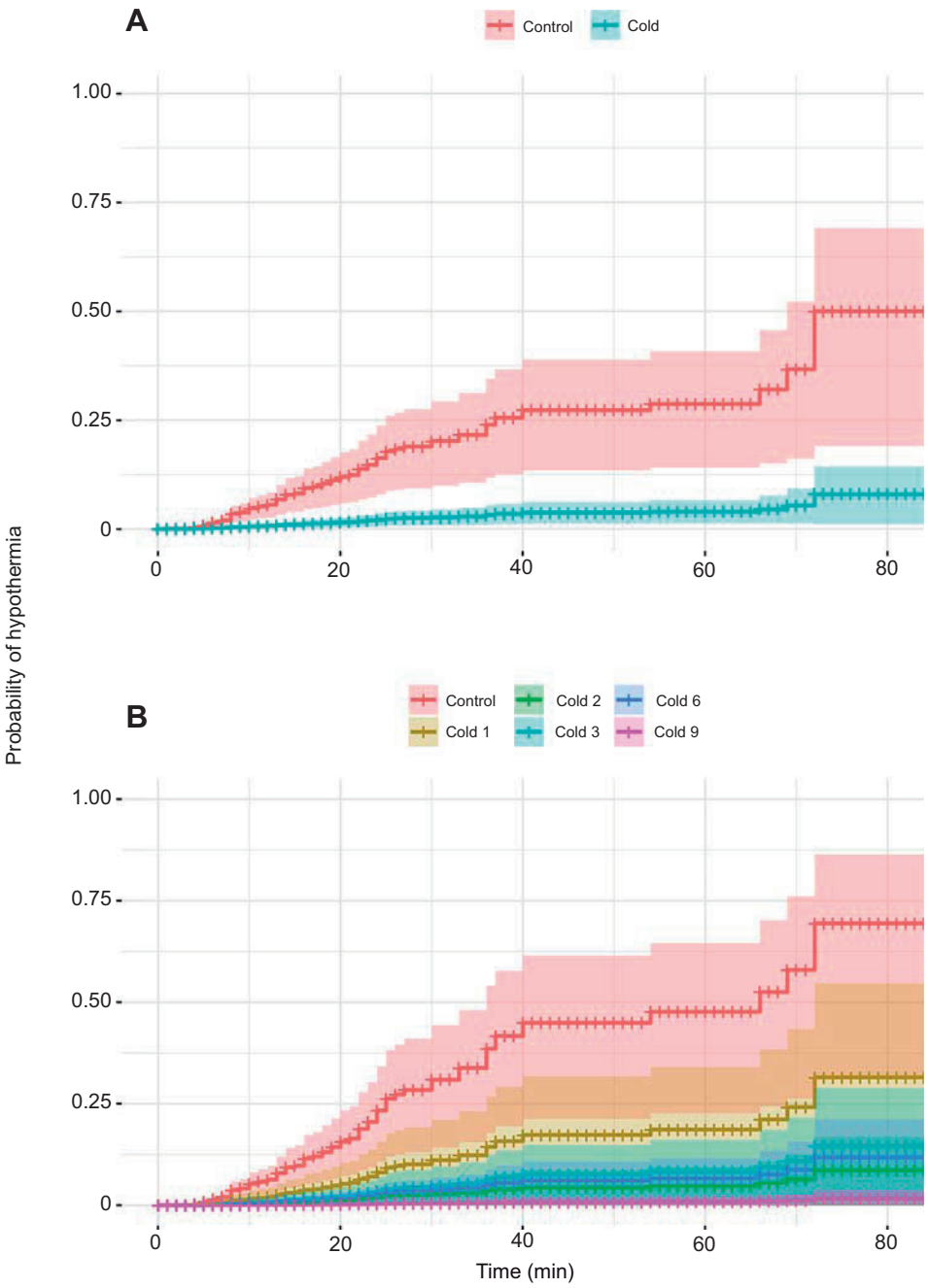

Fig. 4. Survival curves depicting time to hypothermia in acute cold trials while controlling for cabinet temperature. (A) Temperature (n=92) and (B) duration treatments (n=86). Control treatments (excluding week 9) combined in B. Regression lines shown with shaded areas representing 95% confidence intervals.

of shivering to non-shivering processes could be altered seasonally. Direct measures of shivering and/or non-shivering thermogenesis, however, are needed to test for these potential changes. Our results thus point to exciting directions for further exploration regarding the mechanisms governing seasonal acclimatization in avian T_b maintenance.

Thermoregulation and broad-scale ecogeographic patterns

Spatial variation in basal metabolic rate (BMR) is often interpreted as a thermal adaptation to cold conditions, whereby colder climates are correlated with higher endothermic BMR (Lovegrove, 2003; Wiersma et al., 2007). Changes in BMR have also been implicated as a mechanism and/or by-product of avian thermal acclimation across seasons (Dutenhoffer and Swanson, 1996). Here, we did not find increases in RMR associated with cold acclimation. We quantified RMR rather than BMR, meaning that birds were not fasted before measurements. Nonetheless, RMR post-acclimation was similar to previously published BMR values for wild juncos (Swanson et al., 2012). We found that RMR was not correlated with other performance phenotypes (M_{sum}, conductance or T_b maintenance), implying that it is not a good indicator of avian cold tolerance. This result also agrees with previous work showing that M_{sum} and RMR can be uncoupled (Petit et al., 2013; Swanson et al., 2012). Finally, it indicates that the energetic costs associated with enhancing thermoregulatory ability – such as building the metabolic machinery associated with increased M_{sum} – do not necessarily manifest as higher resting energetic use.

M_{sum} is commonly used as a proxy for cold tolerance in macrophysiological studies (e.g. Stager et al., 2016). However, our results highlight a disconnect between these two measures.

Journal of Experimental Biology (2020) 223, jeb221853. doi:10.1242/jeb.221853

Table 4. Survival model output for hypothermic state as a function of treatment duration for control birds only and cold birds only

Variable	β	s.e.	HR	*P*
Control birds				
Cabinet temperature	−0.15	0.06	0.86	0.05
Week 2	−0.98	0.51	0.38	0.36
Week 3	−1.27	0.50	0.28	0.14
Week 6	0.14	0.50	1.15	0.84
Week 9	−2.23	0.59	0.11	1.8×10^{-4}
Cold birds				
Cabinet temperature	−0.50	0.08	0.61	2.5×10^{-7}
Week 2	−1.82	0.52	0.16	1.1×10^{-3}
Week 3	−1.01	0.51	0.36	0.11
Week 6	−1.23	0.49	0.29	0.01
Week 9	−4.44	0.84	0.01	6.1×10^{-4}

Week 1 as reference. Negative β coefficients represent reduced risk of hypothermia. Hazards ratio (HR) is the exponent of the β coefficient (i.e. a reduction in the hazard by this factor). Bold indicates predictor variables with statistically significant effects on T_b maintenance.

Table 6. Model-averaged coefficients for phenotypic variables affecting the maintenance of T_b assessed using Cox proportional hazards models

Variable	β	s.e.	HR	95% CI	*P*
Cabinet temperature	−0.93	0.49	0.39	−1.90, 0.02	0.06
Endurance	**−2.02**	**0.61**	**0.13**	**−3.22, −0.81**	**0.001**
RMR	0.47	0.41	1.60	−0.26, 1.31	0.26
M_{sum}	**−1.04**	**0.45**	**0.35**	**−1.93, −0.15**	**0.02**
Endurance×M_{sum}	**−2.14**	**0.95**	**0.12**	**−4.00, −0.29**	**0.02**
Conductance	0.09	0.24	1.09	−0.41, 0.98	0.70
Tarsus	−0.06	0.19	1.06	−0.85, 0.37	0.75
M_b	0.06	0.23	1.06	−0.57, 1.02	0.80

Negative β coefficients represent reduced risk of hypothermia. Hazards ratio (HR) is the exponent of the β coefficient (i.e. a reduction in the hazard by this factor). All continuous variables were standardized; bold indicates predictor variables with statistically significant effects on T_b maintenance.

Although junco M_{sum} was correlated with T_b maintenance in the cold, it was not as strong a predictor of T_b maintenance as was endurance, and it was the interaction between M_{sum} and endurance that had the largest effect on T_b maintenance. Furthermore, the amount of variation in T_b maintenance explained by M_{sum} alone was relatively small. These results echo those of a previous study in which variation in M_{sum} did not match variation in cold tolerance in two other, disparate junco populations (Swanson, 1993). M_{sum} may, therefore, not be as strong a proxy of cold tolerance as frequently thought. Nonetheless, to discern whether this pattern can be generalized to other taxa, we encourage the collection of T_b data to assess normothermic ability as we have done here. Such data are increasingly easy to obtain using PIT tags and other next-generation tracking technologies (e.g. Parr et al., 2019).

Responding to fluctuating environmental conditions

Nicknamed 'snowbirds' for their winter tenacity, juncos are not unique in their cold hardiness. Their close relative, the white-throated sparrow (*Zonotrichia albicolli*), has been acclimated to even colder conditions than those employed here (3 weeks at −20°C) (McWilliams and Karasov, 2014), and other small songbirds have survived short periods in the laboratory at −60°C (Dawson and Carey, 1976). Given that the climatic conditions juncos experience vary across their broad geographic distribution, junco populations may also differ in their thermoregulatory abilities and the underlying physiological responses they use to moderate T_b. Acclimatizing to these cold temperatures in the wild likely comes with trade-offs, such as increased exposure to predators as a consequence of increased time spent foraging (Lima, 1985). Moreover, as our results demonstrate, the duration of the cold period may dictate which physiological strategies are utilized. For instance, we found that juncos are capable of responding to thermal cues with large changes in M_{sum} occurring within 1 week. However, rapid changes likely require energetic input to fuel this physiological remodeling, in addition to those required to elevate aerobically powered shivering thermogenesis.

Another short-term strategy that birds use to cope with cold temperatures is facultative hypothermia (Mckechnie and Lovegrove, 2002). We witnessed similar patterns of oscillating T_b in some juncos, whereby they raised T_b to normothermic levels following a period of hypothermia. Counter to previous findings (Swanson, 1991), this suggests that juncos may employ facultative hypothermia as an energy-saving mechanism. However, we did not find evidence for acclimation in this strategy – as members of both temperature treatments exhibited this pattern – nor that birds differed in their starting T_b among temperature treatments. The white-crowned sparrow (*Z. leucophrys*), another close relative of the junco, has been shown to lower its T_b by 3.6°C (Ketterson and King, 1977), but we found that juncos could lower their T_b by as much as 7°C and still recover normothermia during an acute cold trial. Although we did not assess potential consequences of hypothermia in this context, 7°C is well within the range of T_b reductions observed in other passerines (Mckechnie and Lovegrove, 2002). Furthermore, a nightly reduction in T_b of this magnitude is estimated to reduce the energy expenditure of *Parus* tits by up to 30% and increase their over-wintering survival by 58% (Brodin et al., 2017). Like other birds, however, juncos suffer impaired mobility at such low T_b (M. Stager, personal observation). Although rest-phase hypothermia may be especially useful at night when activity levels

Table 5. Highest-ranked models (with lowest AIC_c scores) in candidate set for effects of phenotypic variables on the maintenance of T_b using Cox proportional hazards models

Candidate model	*K*	AIC_c	ΔAIC_c	w_i
Cabinet+Endurance×M_{sum}+RMR	5	1007.9	0.0	0.23
Cabinet+Conductance+Endurance×M_{sum}+RMR	6	1009.2	1.3	0.12
Cabinet+Endurance×M_{sum}+RMR+Tarsus	6	1009.6	1.7	0.10
Cabinet+Endurance×M_{sum}+M_b+RMR	6	1009.6	1.7	0.10
Cabinet+Conductance+Endurance×M_{sum}+M_b+RMR	7	1010.9	3.0	0.05
Cabinet+Endurance×M_{sum}+M_b+RMR+Tarsus	7	1010.9	3.0	0.05
Cabinet+Conductance+Endurance×M_{sum}+RMR+Tarsus	7	1011.0	3.1	0.05
Cabinet+Endurance×M_{sum}	4	1011.2	3.3	0.04
Cabinet+Conductance+Endurance×M_{sum}	5	1011.3	3.4	0.04

Only models with ΔAIC_c <4 are reported. *K* indicates the number of parameters in each model; cabinet refers to the cabinet temperature during the cold trial.

are reduced, it alone may not be a good strategy to cope with cold temperatures during the day when birds need to eat, move and avoid predators (Brodin et al., 2017).

Juncos may thus be layering longer-term modifications – such as the observed changes in conductance – on top of these shorter-term mechanisms to arrive at the optimal phenotype for the challenge at hand. If widespread, this would provide birds with a host of strategies to employ, each of which may be useful over different time scales. As a result, in the face of increasing climatic variability, some birds may be well equipped to deal with potential mismatches between photoperiod and temperature that lead to thermoregulatory challenges in the cold. However, their ability to employ these different strategies is likely dependent on their access to sufficient food to fuel and maintain these phenotypic changes. Because food resources are also likely to vary in response to global change (Rafferty, 2017; Williams and Jackson, 2007), future work should investigate the complex interactions between environmental change, subsequent physiological responses and their energetic costs.

Acknowledgements
We are especially thankful to Phred Benham, Ryan Mahar, Nick Sly, Hannah Specht and Stanley Senner for their assistance in catching birds. We also thank Frank Moss for logistical assistance, Hailey Bunker for help with husbandry, and Keely Corder, Rena Schweizer, Jon Velotta, Cole Wolf, and four anonymous reviewers for comments on an earlier version of this paper.

Competing interests
The authors declare no competing or financial interests.

Author contributions
Conceptualization: M.S., Z.A.C.; Methodology: M.S., B.W.T.; Formal analysis: M.S.; Investigation: M.S.; Resources: M.S., N.R.S., B.W.T., Z.A.C.; Data curation: M.S.; Writing - original draft: M.S.; Writing - review & editing: N.R.S., B.W.T., Z.A.C.; Supervision: Z.A.C.; Project administration: M.S.; Funding acquisition: M.S., B.W.T., Z.A.C.

Funding
This work was supported by the National Science Foundation [GRFP to M.S., IOS-1656120 to B.W.T.] and the University of Montana [startup to Z.A.C.].

Supplementary information
Supplementary information available online at
http://jeb.biologists.org/lookup/doi/10.1242/jeb.221853.supplemental

References
Bennett, A. and Ruben, J. (1979). Endothermy and activity in vertebrates. *Science* **206**, 649-654. doi:10.1126/science.493968
Brodin, A., Nilsson, J.-Å. and Nord, A. (2017). Adaptive temperature regulation in the little bird in winter: predictions from a stochastic dynamic programming model. *Oecologia* **185**, 43-54. doi:10.1007/s00442-017-3923-3
Buckley, L. B., Khaliq, I., Swanson, D. L. and Hof, C. (2018). Does metabolism constrain bird and mammal ranges and predict shifts in response to climate change? *Ecol. Evol.* **8**, 12375-12385. doi:10.1002/ece3.4537
Cheviron, Z. A., Bachman, G. C. and Storz, J. F. (2013). Contributions of phenotypic plasticity to differences in thermogenic performance between highland and lowland deer mice. *J. Exp. Biol.* **216**, 1160-1166. doi:10.1242/jeb.075598
Crompton, A. W., Taylor, C. R. and Jagger, J. A. (1978). Evolution of homeothermy in mammals. *Nature* **272**, 333-336. doi:10.1038/272333a0
Danner, R. M., Greenberg, R. S., Danner, J. E. and Walters, J. R. (2015). Winter food limits timing of pre-alternate moult in a short-distance migratory bird. *FunctZEcol.* **29**, 259-267. doi:10.1111/1365-2435.12322
Dawson, W. R. and Carey, C. (1976). Seasonal acclimatization to temperature in cardueline finches. *J. Comp. Physiol. A* **112**, 317-333. doi:10.1007/BF00692302
Dawson, W. R. and O'Connor, T. P. (1996). Energetic features of avian thermoregulatory responses. In *Avian Energetics and Nutritional Ecology* (ed. C. Carey), pp. 85-124. Boston, MA: Springer US.
Dawson, W. R. and Smith, B. K. (1986). Metabolic acclimatization in the American goldfinch (*Carduelis tristis*). In *Living in the Cold: Physiological and Biochemical Adaptations* (ed. H. C. Heller), pp. 427-434. Amsterdam: Elsevier.
Douglas, T. K., Cooper, C. E. and Withers, P. C. (2017). Avian torpor or alternative thermoregulatory strategies for overwintering? *J. Exp. Biol.* **220**, 1341-1349. doi:10.1242/jeb.154633
Dutenhoffer, M. S. and Swanson, D. L. (1996). Relationship of basal to summit metabolic rate in passerine birds and the aerobic capacity model for the evolution of endothermy. *Physiol. Zool.* **69**, 1232-1254. doi:10.1086/physzool.69.5.30164255
Ferretti, A., Rattenborg, N. C., Ruf, T., McWilliams, S. R., Cardinale, M. and Fusani, L. (2019). Sleeping unsafely tucked in to conserve energy in a nocturnal migratory songbird. *Curr. Biol.* **29**, 2766-2772.e4. doi:10.1016/j.cub.2019.07.028
Gelman, A. (2008). Scaling regression inputs by dividing by two standard deviations. *Statist. Med.* **27**, 2865-2873. doi:10.1002/sim.3107
Grueber, C. E., Nakagawa, S., Laws, R. J. and Jamieson, I. G. (2011). Multimodel inference in ecology and evolution: challenges and solutions: multimodel inference. *J. Evol. Biol.* **24**, 699-711. doi:10.1111/j.1420-9101.2010.02210.x
Hohtola, E. (2002). Facultative and obligatory thermogenesis in young birds: a cautionary note. *Comp. Biochem. Physiol. A Mol. Integr. Physiol.* **131**, 733-739. doi:10.1016/S1095-6433(02)00011-9
Hohtola, E., Rintamäki, H. and Hissa, R. (1980). Shivering and ptiloerection as complementary cold defense responses in the pigeon during sleep and wakefulness. *J. Comp. Physiol. B* **136**, 77-81. doi:10.1007/BF00688626
Irving, L. and Krog, J. (1955). Temperature of skin in the Arctic as a regulator of heat. *J. Appl. Physiol.* **7**, 355-364. doi:10.1152/jappl.1955.7.4.355
Jimenez, A. G., Dillaman, R. M. and Kinsey, S. T. (2013). Large fibre size in skeletal muscle is metabolically advantageous. *Nat. Commun.* **4**, 2150. doi:10.1038/ncomms3150
Jimenez, A. G., O'Connor, E. S., Brown, K. J. and Briggs, C. W. (2019). Seasonal muscle ultrastructure plasticity and resistance of muscle structural changes during temperature increases in resident black-capped chickadees and rock pigeons. *J. Exp. Biol.* **222**, jeb201855. doi:10.1242/jeb.201855
Ketterson, E. D. and King, J. R. (1977). Metabolic and behavioral responses to fasting in the white-crowned sparrow *(Zonotrichia leucophrys gambelii*). *Physiol. Zool.* **50**, 115-129. doi:10.1086/physzool.50.2.30152551
Kolstad, E. W., Breiteig, T. and Scaife, A. A. (2010). The association between stratospheric weak polar vortex events and cold air outbreaks in the Northern Hemisphere. *Q.J.R. Meteorol. Soc.* **136**, 886-893. doi:10.1002/qj.620
Korhonen, K. (1981). Temperature in the nocturnal shelters of the redpoll (*Acanthis flammea* L.) and the Siberian tit (*Parus cinctus* Budd.) in winter. *Ann. Zool. Fenn.* **18**, 165-167.
Lighton, J. (2008). *Measuring Metabolic Rates: a Manual for Scientists*. New York: Oxford University Press.
Liknes, E. T. and Swanson, D. L. (2011). Phenotypic flexibility of body composition associated with seasonal acclimatization in passerine birds. *J. Therm. Biol.* **36**, 363-370. doi:10.1016/j.jtherbio.2011.06.010
Lima, S. L. (1985). Maximizing feeding efficiency and minimizing time exposed to predators: a trade-off in the black-capped chickadee. *Oecologia* **66**, 60-67. doi:10.1007/BF00378552
Londoño, G. A., Chappell, M. A., Jankowski, J. E. and Robinson, S. K. (2017). Do thermoregulatory costs limit altitude distributions of Andean forest birds? *Funct. Ecol.* **31**, 204-215. doi:10.1111/1365-2435.12697
Lovegrove, B. G. (2003). The influence of climate on the basal metabolic rate of small mammals: a slow-fast metabolic continuum. *J. Comp. Physiol. B* **173**, 87-112. doi:10.1007/s00360-002-0309-5
Marsh, R. L. and Dawson, W. R. (1989). Avian adjustments to cold. In *Animal Adaptation to Cold* (ed. L. C. H. Wang), pp. 205-253. Berlin, Heidelberg: Springer.
Mckechnie, A. E. and Lovegrove, B. G. (2002). Avian facultative hypothermic responses: a review. *The Condor* **104**, 705-724. doi:10.1093/condor/104.4.705
McWilliams, S. R. and Karasov, W. H. (2014). Spare capacity and phenotypic flexibility in the digestive system of a migratory bird: defining the limits of animal design. *Proc. R. Soc. B Biol. Sci.* **281**, 20140308. doi:10.1098/rspb.2014.0308
Middleton, A. L. A. (1986). Seasonal changes in plumage structure and body composition of the American goldfinch, *Carduelis tristis*. *Canadian Field Naturalist* **100**, 545-549.
Møller, A. P. (2015). The allometry of number of feathers in birds changes seasonally. *Avian Res.* **6**, 2. doi:10.1186/s40657-015-0012-3
Morris, D. (1956). The feather postures of birds and the problem of the origin of social signals. *Behaviour* **9**, 75-113. doi:10.1163/156853956X00264
Muñoz-Garcia, A., Cox, R. M. and Williams, J. B. (2008). Phenotypic flexibility in cutaneous water loss and lipids of the stratum corneum in house sparrows (*Passer domesticus*) following acclimation to high and low humidity. *Physiol. Biochem. Zool.* **81**, 87-96. doi:10.1086/522651
Nolan, V., , Jr, Ketterson, E. D., Cristol, D. A., Rogers, C. M., Clotfelter, E. D., Titus, R. C., Schoech, S. J. and Snajdr, E. (2002). Dark-eyed junco (*Junco hyemalis*). *Birds N. Am.* doi:10.2173/bna.716
O'Connor, T. P. (1995). Metabolic characteristics and body composition in house finches: effects of seasonal acclimatization. *J. Comp. Physiol. B* **165**, 298-305. doi:10.1007/BF00367313
Osváth, G., Daubner, T., Dyke, G., Fuisz, T. I., Nord, A., Pénzes, J., Vargancsik, D., Vágási, C. I., Vincze, O. and Pap, P. L. (2018). How feathered are birds? Environment predicts both the mass and density of body feathers. *Funct. Ecol.* **32**, 701-712. doi:10.1111/1365-2435.13019
Parr, N., Bishop, C. M., Batbayar, N., Butler, P. J., Chua, B., Milsom, W. K., Scott, G. R. and Hawkes, L. A. (2019). Tackling the Tibetan Plateau in a down suit:

insights into thermoregulation by bar-headed geese during migration. *J. Exp. Biol.* **222**, jeb203695. doi:10.1242/jeb.203695

Pavlovic, G., Weston, M. A. and Symonds, M. R. E. (2019). Morphology and geography predict the use of heat conservation behaviours across birds. *Funct. Ecol.* **33**, 286-296. doi:10.1111/1365-2435.13233

Petit, M. and Vézina, F. (2014). Reaction norms in natural Conditions: how does metabolic performance respond to weather variations in a small endotherm facing cold environments? *PLoS ONE* **9**, e113617. doi:10.1371/journal.pone.0113617

Petit, M., Lewden, A. and Vézina, F. (2013). Intra-seasonal flexibility in avian metabolic performance highlights the uncoupling of basal metabolic rate and thermogenic capacity. *PLoS ONE* **8**, e68292. doi:10.1371/journal.pone.0068292

Petit, M., Clavijo-Baquet, S. and Vézina, F. (2017). Increasing winter maximal metabolic rate improves intrawinter survival in small birds. *Physiol. Biochem. Zool.* **90**, 166-177. doi:10.1086/689274

Pyle, P. (1997). *Identification Guide to North American Birds, Part I: Columbidae to Ploceidae*. Bolinas, CA, USA: Slate Creek Press.

Rafferty, N. E. (2017). Effects of global change on insect pollinators: multiple drivers lead to novel communities. *Curr. Opin. Insect Sci.* **23**, 22-27. doi:10.1016/j.cois.2017.06.009

Rosenmann, M. and Morrison, P. (1974). Maximum oxygen consumption and heat loss facilitation in small homeotherms by He-O_2. *Am. J. Physiol.* **226**, 490-495. doi:10.1152/ajplegacy.1974.226.3.490

Saarela, S., Klapper, B. and Heldmaier, G. (1989). Thermogenic capacity of greenfinches and siskins in winter and summer. In *Physiology of Cold Adaptation in Birds* (ed. C. Bech and R. E. Reinertsen), pp. 115-122. Boston, MA: Springer US.

Stager, M., Pollock, H. S., Benham, P. M., Sly, N. D., Brawn, J. D. and Cheviron, Z. A. (2016). Disentangling environmental drivers of metabolic flexibility in birds: the importance of temperature extremes versus temperature variability. *Ecography* **39**, 787-795. doi:10.1111/ecog.01465

Swanson, D. L. (1990a). Seasonal variation in cold hardiness and peak rates of cold-induced thermogenesis in the dark-eyed junco (*Junco hyemalis*). *The Auk* **107**, 6.

Swanson, D. L. (1990b). Seasonal variation of vascular oxygen transport in the dark-eyed junco. *The Condor* **92**, 62-66. doi:10.2307/1368383

Swanson, D. L. (1991). Seasonal adjustments in metabolism and insulation in the dark-eyed junco. *The Condor* **93**, 538-545. doi:10.2307/1368185

Swanson, D. L. (1993). Cold tolerance and thermogenic capacity in dark-eyed Juncos in winter: geographic variation and comparison with American tree sparrows. *J. Therm. Biol.* **18**, 275-281. doi:10.1016/0306-4565(93)90014-K

Swanson, D. L. (2010). Seasonal metabolic variation in birds: functional and mechanistic correlates. In *Current Ornithology*, Vol. 17 (ed. C. F. Thompson), pp. 75-129. New York, NY: Springer New York.

Swanson, D. L. and Olmstead, K. L. (1999). Evidence for a proximate influence of winter temperature on metabolism in passerine birds. *Physiol. Biochem. Zool.* **72**, 566-575. doi:10.1086/316696

Swanson, D. L. and Vézina, F. (2015). Environmental, ecological and mechanistic drivers of avian seasonal metabolic flexibility in response to cold winters. *J. Ornithol.* **156**, 377-388. doi:10.1007/s10336-015-1192-7

Swanson, D. L., Thomas, N. E., Liknes, E. T. and Cooper, S. J. (2012). Intraspecific correlations of basal and maximal metabolic rates in birds and the aerobic capacity model for the evolution of endothermy. *PLoS ONE* **7**, e34271. doi:10.1371/journal.pone.0034271

Swanson, D., Zhang, Y., Liu, J.-S., Merkord, C. L. and King, M. O. (2014). Relative roles of temperature and photoperiod as drivers of metabolic flexibility in dark-eyed juncos. *J. Exp. Biol.* **217**, 866-875. doi:10.1242/jeb.096677

Vezina, F., Ruhs, E., O'Connor, E., Le Pogam, A., Regimbald, L., Love, O. and Jimenez, A. G. (2020). Consequences of being phenotypically mismatched with the environment: rapid muscle ultrastructural changes in cold-shocked black-capped chickadees (*Poecile atricapillus*). *Am. J. Physiol. Regul. Integr. Comp. Physiol.* **318**, R274-R283. doi:10.1152/ajpregu.00203.2019

Wiersma, P., Munoz-Garcia, A., Walker, A. and Williams, J. B. (2007). Tropical birds have a slow pace of life. *Proc. Natl Acad. Sci. USA* **104**, 9340-9345. doi:10.1073/pnas.0702212104

Williams, J. W. and Jackson, S. T. (2007). Novel climates, no-analog communities, and ecological surprises. *Front. Ecol. Envir.* **5**, 475-482. doi:10.1890/070037

Wolf, B. O. and Walsberg, G. E. (2000). The role of the plumage in heat transfer processes of birds. *Am. Zool.* **40**, 575-584. doi:10.1093/icb/40.4.575

Supplementary Materials

Table S1. Effect of respirometry unit on pre-acclimation RMR in (a) 2016 and (b) 2017 and on M_{sum} in (c) 2016 and (d) 2017. Unit A is reference for 2016 and Unit 3 is reference for 2017.

a.

Unit	β	SE	p
Unit B	-0.07	0.06	0.24
Unit C	0.12	0.05	0.04

b.

Unit	β	SE	p
Unit 1	0.13	0.11	0.21
Unit 4	-0.52	0.06	2.4×10^{-10}

c.

Unit	β	SE	p
Unit C	-0.17	0.15	0.25

d.

Unit	β	SE	p
Unit 1	7.94	0.58	$< 2 \times 10^{-16}$
Unit 4	-1.54	0.25	2.5×10^{-7}
Unit 5	4.62	0.34	$< 2 \times 10^{-16}$

Table S2. Cox proportional hazards model output when hypothermic state defined as < 37°C. **(a)** Effects of cabinet temperature, acclimation temperature treatment, and duration treatment. Negative β coefficients represent reduced risk of hypothermia. Hazards ratio (HR) is the exponent of the β coefficient. *Control* treatment is reference for Temperature effect. All continuous variables were standardized; bold indicates predictor variables with statistically significant effects on T_b maintenance. (b) Highest-ranked models (with lowest AIC_c scores) in candidate set for effects of phenotypic variables on the maintenance of T_b. Only models with $\Delta AIC_c < 4$ are reported. *K* indicates the number of parameters in each model. Cabinet refers to the cabinet temperature during the cold trial.

(a)

Variable	β	SE	HR	95% CI	*p*
Cabinet Temp.	**-3.70**	**0.49**	**0.02**	**-4.98, -2.41**	**1.7×10^{-8}**
Temp. Treatment	**-2.00**	**0.41**	**0.14**	**-3.13, -0.87**	**5.2×10^{-4}**
Duration Treatment	**-1.30**	**0.24**	**0.27**	**-1.99, -0.60**	**2.4×10^{-4}**

(b)

Candidate Model	*K*	AIC_c	ΔAIC_c	w_i
Cabinet + Conductance + Endurance × M_{sum} + RMR	6	989.3	0.0	0.13
Cabinet + Conduct. + M_b + Tarsus + Endurance × M_{sum} + RMR	8	989.3	0.0	0.13
Cabinet + Conductance + Endurance × M_{sum} + RMR + Tarsus	7	989.5	0.3	0.11
Cabinet + Endurance × M_{sum} + M_b + RMR + Tarsus	7	990.1	0.8	0.09
Cabinet + Conductance + Endurance x M_{sum} + M_b +RMR	7	990.2	1.0	0.08
Cabinet + Endurance × M_{sum} + RMR	5	990.4	1.2	0.07
Cabinet + Endurance × M_{sum} + RMR +Tarsus	6	990.4	1.2	0.07
Cabinet + Endurance × M_{sum} + M_b + RMR	6	991.2	2.0	0.05
Cabinet + Conductance + Endurance + M_{sum} + RMR	5	992.1	2.8	0.03
Cabinet + Conductance + Endurance × M_{sum} + M_b	6	992.2	2.9	0.03
Cabinet + Endurance + RMR + M_{sum}	4	992.5	3.2	0.03
Cabinet + Conductance + Endurance × M_{sum}	5	992.6	3.4	0.02
Cabinet + Conductance + Endurance × M_{sum} + M_b + Tarsus	7	992.8	3.6	0.02
Cabinet + Conductance + Endurance + M_b + RMR + M_{sum}	6	993.0	3.7	0.02

Table S3. Effect of thermal conductance assay date on average power input.

Date	β	SE	p
5/20/19	-1.24	17.21	0.94
5/21/19	21.89	16.39	0.19
5/22/19	4.57	17.21	0.80
5/23/19	13.39	16.76	0.43
5/24/19	- 1.01	20.84	0.96
5/27/19	9.40	20.84	0.65
6/6/19	26.99	18.50	0.37
6/7/19	21.50	16.76	0.46
6/8/19	-16.84	17.21	0.48
6/9/19	12.37	17.21	0.75
6/10/19	-12.25	17.21	0.12
6/11/19	-5.2	16.76	0.20

Table S4. Linear effects of *Cold* treatment, *Duration,* and their interaction on phenotypic traits before and after acclimation. Mass (M_b) is included as a covariate for metabolic traits. Delta (Δ) represents change over acclimation period (post- minus pre-acclimation) for traits that were measured at both time points. Metabolic rates are expressed as measures of oxygen consumption per (ml O_2^{-1}•min^{-1}); conductance expressed in mW; endurance in min; mass in g. Bolded significant effects after Bonferroni correction ($p < 0.004$). Sample sizes reported in Table 1.

	Phenotype	Intercept		M_b			Cold Treatment			Duration			Cold x Duration		
		β	SE	β	SE	p	β	SE	p	β	SE	p	β	SE	p
Pre	M_b	22.51	0.38				-0.32	0.54	0.55	-0.10	0.08	0.26	0.10	0.12	0.43
	Tarsus	19.92	0.14				0.07	0.20	0.73	0.04	0.03	0.25	0.01	0.04	0.79
	RMR	0.22	0.32	**0.05**	**0.01**	**7.2×10^{-4}**	0.05	0.08	0.49	0.00	0.01	0.68	-0.02	0.02	0.32
	M_{sum}	4.77	0.80	0.07	0.04	0.06	0.30	0.21	0.16	0.01	0.03	0.76	-0.05	0.05	0.25
	Endur.	39.39	18.41	-0.50	0.81	0.54	-1.49	4.91	0.76	-0.33	0.75	0.66	0.81	1.09	0.46
Post	M_b	23.08	0.40				-0.03	0.56	0.95	-0.20	0.09	0.03	0.14	0.13	0.27
	RMR	0.40	0.38	**0.05**	**0.02**	**3.6×10^{-3}**	-0.14	0.09	0.15	-0.03	0.02	0.05	0.03	0.02	0.19
	M_{sum}	5.09	1.76	0.08	0.07	0.31	**1.35**	**0.44**	**2.9×10^{-3}**	-0.09	0.07	0.20	-0.01	0.10	0.93
	Endur.	16.50	22.44	0.19	0.94	0.85	-4.66	5.62	0.41	1.43	0.91	0.12	-0.37	1.26	0.77
	Conduct.	308.62	7.96				30.10	11.28	9.0×10^{-3}	3.06	1.78	0.09	**-8.52**	**2.56**	**1.2×10^{-3}**
Δ	M_b	0.57	0.46				0.29	0.65	0.66	-0.10	0.10	0.32	0.04	0.15	0.76
	RMR	1.52	0.07	0.02	0.01	0.11	-0.15	0.10	0.14	-0.04	0.02	0.02	0.03	0.02	0.12
	M_{sum}	6.92	0.31	-0.11	0.07	0.09	**1.32**	**0.43**	**3.0×10^{-3}**	-0.12	0.07	0.07	0.01	0.10	0.94

Table S5. Data file. **(a)** Individual identifier, Temperature treatment, treatment Duration, Year, Sex, Tarsus, Masses, RMR, M_{sum}, Endurance, and Conductance for each individual (first sheet in attached xlsx file). (b) Body temperature data averaged over each one-minute interval of the post-acclimation acute cold trials with accompanying cabinet temperature for each individual used in Cox proportional hazards models (second sheet in attached xlsx file).

Click here to Download Table S5

Figure S1. Minimum temperature for North America using WorldClim data and winter junco distribution demarcated with white lines (approximated from Nolan et al., 2002).

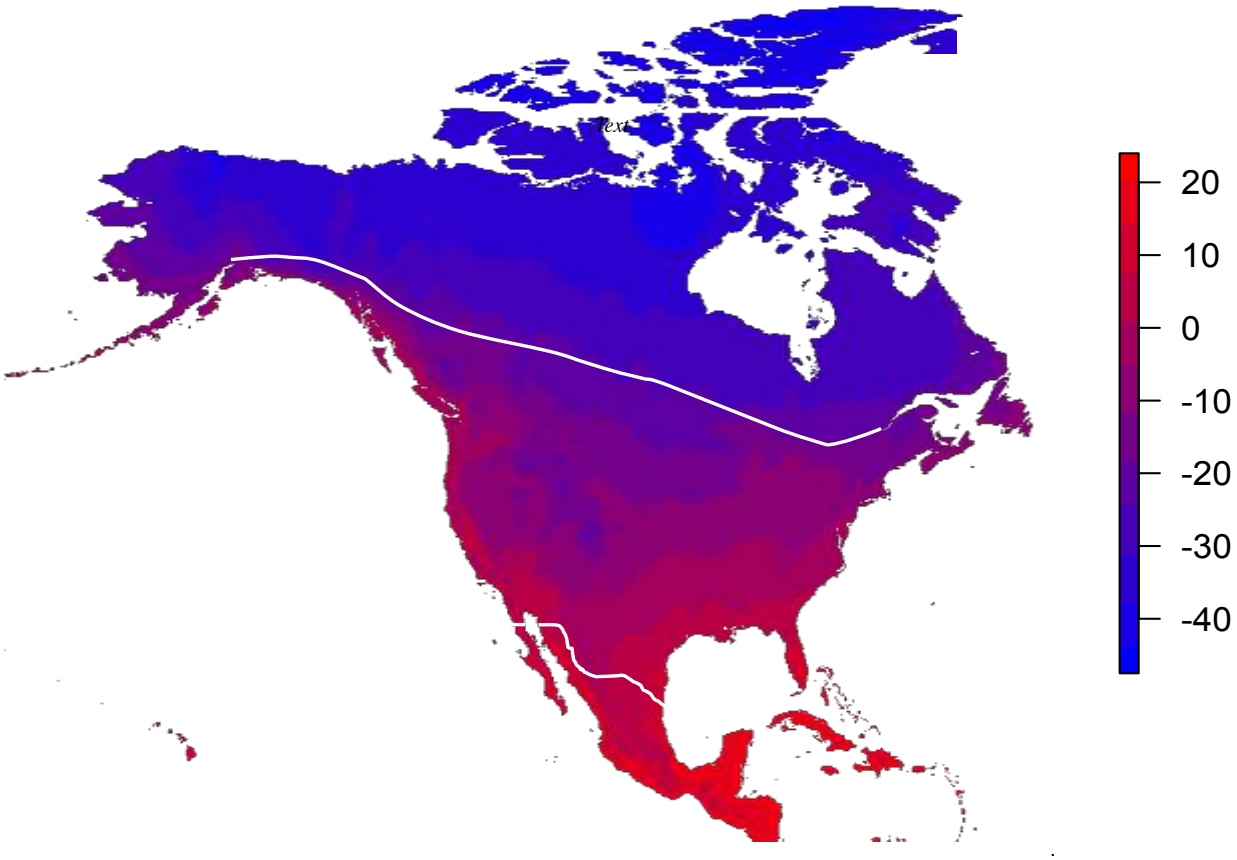

BIOLOGY LETTERS

royalsocietypublishing.org/journal/rsbl

Research

Cite this article: Stager M, Cheviron ZA. 2020 Is there a role for sarcolipin in avian facultative thermogenesis in extreme cold? *Biol. Lett.* **16**: 20200078.
http://dx.doi.org/10.1098/rsbl.2020.0078

Received: 12 February 2020
Accepted: 27 April 2020

Subject Areas:
cellular biology, ecology, molecular biology

Keywords:
sarco/endoplasmic reticulum Ca^{2+} ATPase, non-shivering thermogenesis, Ca^{2+} cycling, acclimation, thermogenic performance

Author for correspondence:
Maria Stager
e-mail: maria.stager@umontana.edu

Electronic supplementary material is available online at https://doi.org/10.6084/m9.figshare.c.4983299.

THE ROYAL SOCIETY PUBLISHING

Physiology

Is there a role for sarcolipin in avian facultative thermogenesis in extreme cold?

Maria Stager and Zachary A. Cheviron

Division of Biological Sciences, University of Montana, Missoula, MT 59812, USA

MS, 0000-0002-5635-580X

Endotherms defend their body temperature in the cold by employing shivering (ST) and/or non-shivering thermogenesis (NST). Although NST is well documented in mammals, its importance to avian heat generation is unclear. Recent work points to a prominent role for the sarco/endoplasmic reticulum Ca^{2+} ATPase (SERCA) in muscular NST. SERCA's involvement in both ST and NST, however, posits a tradeoff between these two heat-generating mechanisms. To explore this tradeoff, we assayed pectoralis gene expression of adult songbirds exposed to chronic temperature acclimations. Counter to mammal models, we found that cold-acclimated birds downregulated the expression of sarcolipin (*SLN*), a gene coding for a peptide that promotes heat generation by uncoupling SERCA Ca^{2+} transport from ATP hydrolysis, indicating a reduced potential for muscular NST. We also found differential expression of many genes involved in Ca^{2+} cycling and muscle contraction and propose that decreased *SLN* could promote increased pectoralis contractility for ST. Moreover, *SLN* transcript abundance negatively correlated with peak oxygen consumption under cold exposure (a proxy for ST) across individuals, and higher *SLN* transcript abundance escalated an individual's risk of hypothermia in acute cold. Our results therefore suggest that SLN-mediated NST may not be an important mechanism of—and could be a hindrance to—avian thermoregulation in extreme cold.

1. Introduction

In the face of thermal stress, endotherms can protect their body temperature (T_b) by employing heat-generating processes in the form of shivering thermogenesis (ST) and/or non-shivering thermogenesis (NST). The use of NST has been extensively described in mammals, which increase NST to regulate body temperature in the cold [1]. It is suspected that birds also use NST and, indeed, some juvenile birds increase NST with cold acclimation [2–4]. Nonetheless, few studies have explored the role of NST during cold acclimatization in adult birds.

Part of this discrepancy arises from uncertainty in the potential mechanism underlying avian NST. For instance, the mitochondrial uncoupling of oxidative phosphorylation from ATP synthesis is one well-characterized mechanism of mammalian NST. During this process, an uncoupling protein (UCP1) facilitates the leakage of protons across the mitochondrial membrane, which dissipates heat. In placental mammals, UCP1 is mainly expressed in brown adipose tissue (BAT) and cold acclimation is associated with BAT recruitment and an increased capacity for NST [5]. Although birds lack BAT, a role for mitochondrial uncoupling in the avian skeletal muscle has been proposed [6,7]. However, direct empirical support for a contribution of the avian UCP homologue (avUCP) to mitochondrial uncoupling is lacking [8,9].

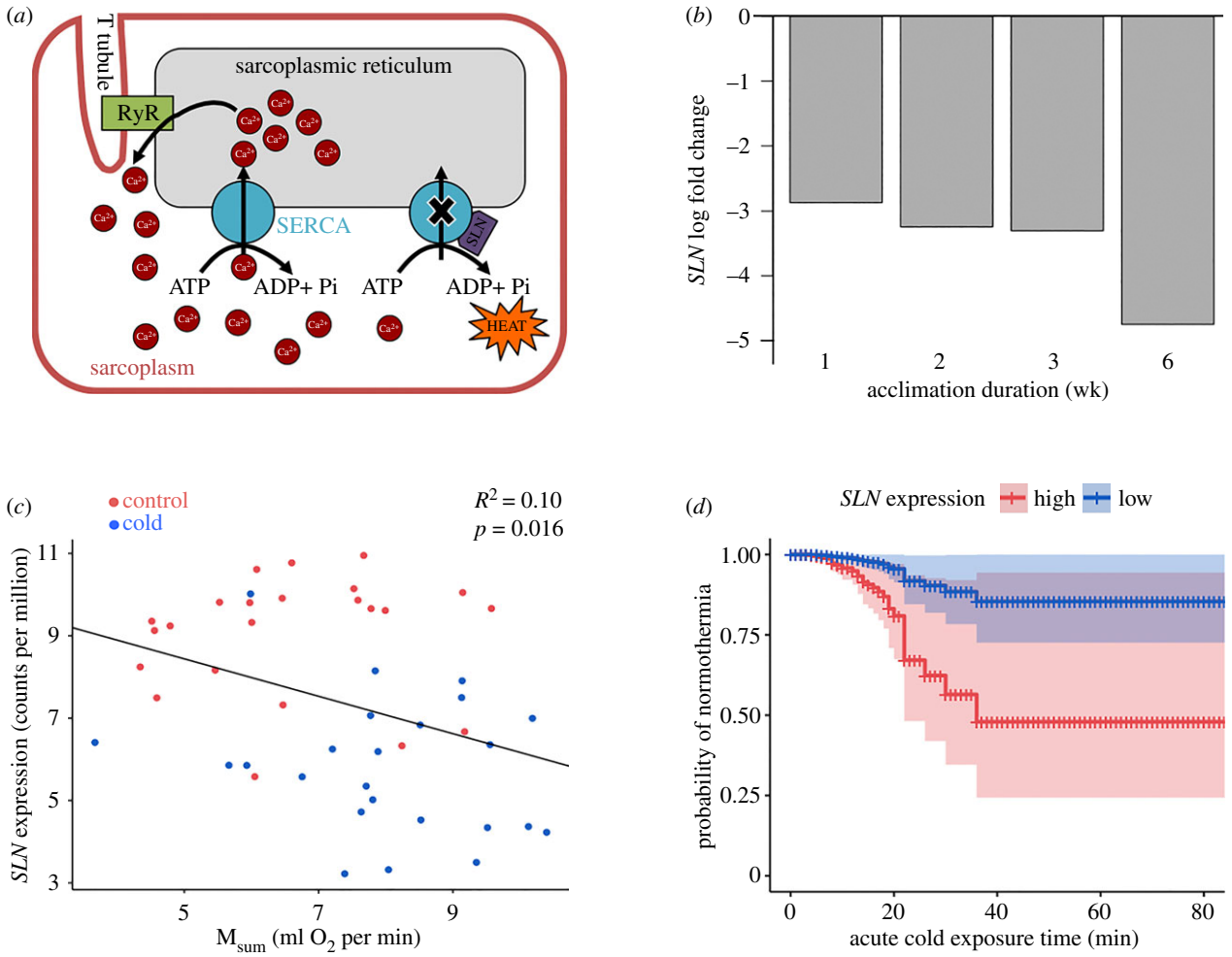

Figure 1. (*a*) Mechanism of heat generation via sarcolipin (SLN) in mammals. RyR, ryanodine receptor channel. (*b*) Magnitude of *SLN* expression change across sampling points. (*c*) Negative correlation between *SLN* transcript abundance and M_{sum}. (*d*) Effect of *SLN* expression on risk of hypothermia using best Cox proportional hazards model, with *SLN* transcript abundance represented as high or low (mean for control and cold treatments, respectively) and covariates held constant at mean values across individuals.

Instead, increasing evidence points to a role for the sarco/endoplasmic reticulum calcium ATPase (SERCA) in facilitating avian NST [10]. SERCA uses phosphate bond energy from ATP to move Ca^{2+} ions from the myocyte cytosol into the sarcoplasmic reticulum to create a Ca^{2+} gradient in resting striated muscle [11] (figure 1*a*). When present, the peptide sarcolipin (SLN) binds to SERCA and promotes uncoupling of Ca^{2+} transport from ATP hydrolysis, resulting in futile SERCA activity and heat production in mammals ([11], but see [12]). Overexpression of SLN in laboratory mice is associated with increased NST and decreased energy stores in the cold [13,14].

While SLN can enhance NST, it may also negatively impact ST. For instance, experimental increases in exogenous SLN result in reduced peak isometric force, lower rates of contraction and relaxation, and increased fatigue of the soleus in rats [15]. Because rapid muscular contractions require high Ca^{2+} cycling activity [16], SLN-associated reductions in Ca^{2+} cycling could similarly reduce shivering activity. These potentially antagonistic effects of SERCA on ST and NST therefore setup an obvious, yet unexplored tradeoff between heat-generating mechanisms.

We explored this tradeoff using transcriptome-wide patterns of gene expression to reveal the many co-occurring processes within the skeletal muscle of dark-eyed juncos (*Junco hyemalis*) exposed to chronic temperature acclimations. Juncos winter at high latitudes across North America [17] and we have previously shown that they increase their thermogenic performance with increasing duration of cold acclimation [18]. Here, we present the first evidence, to our knowledge, for *SLN* expression in the avian skeletal muscle. We predicted that if SLN-mediated NST is an advantageous mechanism of avian heat generation, birds should increase *SLN* expression in the cold. Alternatively, if shivering is the most important component of avian facultative thermogenesis, we expected cold-acclimated birds to decrease *SLN* expression. We further predicted that potential *SLN* differences would be accompanied by changes in the expression of genes related to ST muscle contraction, as well as whole-organism measures of thermogenic performance. Our results suggest that, if SLN-mediated NST occurs in adult birds, it has a minimal role in their acclimation to extreme cold, revealing exciting directions for future exploration of tradeoffs between these heat-generating mechanisms.

2. Methods

We have previously described our acclimation experiment and physiological assays in detail [18]. Briefly, in 2017 we exposed wild-caught, adult juncos from Missoula, MT to constant laboratory conditions for six weeks (18°C), then randomly assigned birds to cold (−8°C) or control (18°C) acclimation treatments lasting one, two, three or six weeks (electronic supplementary material, table S1). Following acclimations, we simultaneously

Table 1. Cox proportional hazards model estimates for the standardized effects of *SLN* transcript abundance and M_{sum} on the risk of hypothermia while controlling for variation in T_a ($n = 45$). Robust standard error (SE); likelihood-ratio test (LRT).

T_a			*SLN*			M_{sum}			*SLN* × M_{sum}			
β	SE	p	β	SE	p	β	SE	p	β	SE	p	LRT
−2.45	0.53	3.5×10^{-6}										48.64
−3.23	0.68	1.8×10^{-6}	1.12	0.97	0.25							53.34
−2.56	0.54	2.4×10^{-6}				−1.16	0.48	0.02				60.23
−3.41	0.65	1.5×10^{-7}	1.21	0.87	0.16	−1.15	0.49	0.02				64.84
−4.15	0.73	1.4×10^{-8}	1.68	0.80	0.04	−1.46	0.58	0.01	−3.13	1.15	6.3×10^{-3}	81.58

assayed an individual's core T_b (using a passive-integrated transponder tag inserted into the cloaca) and peak oxygen consumption (M_{sum} [ml O_2 per min]; using open-flow respirometry) during acute cold trials (short-term exposure to temperatures below −10°C in a heliox environment). Upon trial completion, we immediately euthanized individuals and harvested the pectoralis (the principal shivering muscle for small birds [19]). We flash froze tissues and stored them at −80°C.

To assay gene expression, we isolated mRNA from left pectoralis tissue of 47 randomly selected individuals (electronic supplementary material, table S2) using TRI Reagent (Sigma-Aldrich). The UT Austin Genomic Sequencing and Analysis Facility performed TagSeq [20] library preparation and sequencing. The 47 libraries were pooled in one lane and sequenced three times on an Illumina HiSeq 2500 platform, yielding 254 million reads. We filtered raw reads in accordance with [20] using publicly available scripts (https://github.com/z0on/tag415 based_RNAseq) and trimmed reads with the FASTX-toolkit (http://hannonlab.cshl.edu/fastx_toolkit/), resulting in $\mu = 1.46$ million reads per individual. We mapped these reads to the genome of the white-throated sparrow (*Zonotrichia albicollis*, a close junco relative), using bwa mem [21], with $\mu = 816\,600$ reads per individual mapped. Finally, we generated individual-level transcript abundances using featureCounts [22] for use in downstream analyses, which we conducted in R [23] (electronic supplementary material, table S3).

We performed differential expression analyses using package *edgeR* [24]. We first removed lowly expressed genes that occurred in fewer than 6 individuals, resulting in 12 249 genes in our dataset (electronic supplementary material, table S4). We then normalized read counts using *calcNormFactors*, estimated dispersion using *estimateDisp* and employed a generalized linear model [25] to test for differential expression among experimental treatments using *glmFit*, with cold acclimation duration as the main effect and all control treatments combined as the reference (false discovery rate [FDR] less than 0.05). We performed functional enrichment analysis on the list of differentially expressed (DE) genes using package *gprofiler2* [26] with the 12 249 genes as our background gene set (electronic supplementary material, table S5). To help explain the pattern of increasing thermogenic performance observed across the acclimation period [18], we asked whether each DE gene also differed in its magnitude of change across the acclimation duration by regressing its log fold change (from the fitted glm) on treatment duration (in weeks) using linear regressions ($p < 0.05$).

We related normalized *SLN* transcript abundance to phenotypic measures from [18], for each individual. We tested for an association between *SLN* and M_{sum} using a linear regression. To determine if *SLN* expression influenced thermoregulatory performance, we fit T_b data from acute cold trials to Cox proportional hazards regression models with the package *Survival* [27]. We created survival objects using an individual's hypothermic status ($T_b < 10\%$ of starting T_b) for each one-minute interval of the trial, then fit regressions using the function *coxph* with all terms clustered by individual to quantify the effects of *SLN* expression, M_{sum}, and their interaction on the risk of hypothermia. To account for variation in acute temperature stimulus among individuals, we also included ambient temperature (T_a) for each time event as a covariate (see [18] for details). We standardized each predictor variable according to [28] and removed from this analysis two individuals that ejected their T_b transponders before they became hypothermic.

Finally, we asked if cold-acclimated birds altered the expression of genes involved in skeletal muscle contraction. To do this, we mapped expression patterns onto the muscle contraction (MC) and excitation-contraction coupling (ECC) pathways identified in [29]. Pathways included multiple isoforms for many proteins and some genes were not present in the dataset (2 ECC genes) or annotated in the *Zonotrichia* genome (7 of 38 MC genes; 5 of 32 ECC), including those encoding SERCA1 and RyR1.

3. Results

We found 526 DE genes among temperature treatments (electronic supplementary material, table S6). Compared to control birds, juncos consistently upregulated 196 genes and downregulated 256 across cold groups. Fifty-seven DE genes showed patterns of increasing or decreasing fold change over the duration of cold acclimation, and the top among them was *SLN* (lowest FDR; electronic supplementary material, table S7). Normalized *SLN* transcript abundance decreased in the cold, with the magnitude of downregulation increasing with acclimation duration ($\beta = -0.37$, $p = 0.019$; figure 1*b*). *SLN* transcript abundance also negatively correlated with M_{sum} ($\beta = -0.45$, $p = 0.016$, $R^2 = 0.10$; figure 1*c*). The best model explaining risk of hypothermia in acute cold included T_a, *SLN* transcript abundance, M_{sum} and *SLN* × M_{sum} (table 1). A disparity in hypothermia risk emerges between high and low *SLN* expression when the other two variables are held constant, such that individuals with low expression better maintain T_b (figure 1*d*). Additionally, of the candidate skeletal muscle contraction genes present in our dataset, 5 of 31 genes in the MC pathway and 3 of 25 in the ECC pathway were DE (28% and 12% of represented proteins, respectively; figure 2; electronic supplementary material, table S8).

4. Discussion

Endogenous heat generation through either ST or NST can allow endotherms to maintain high T_b at low ambient

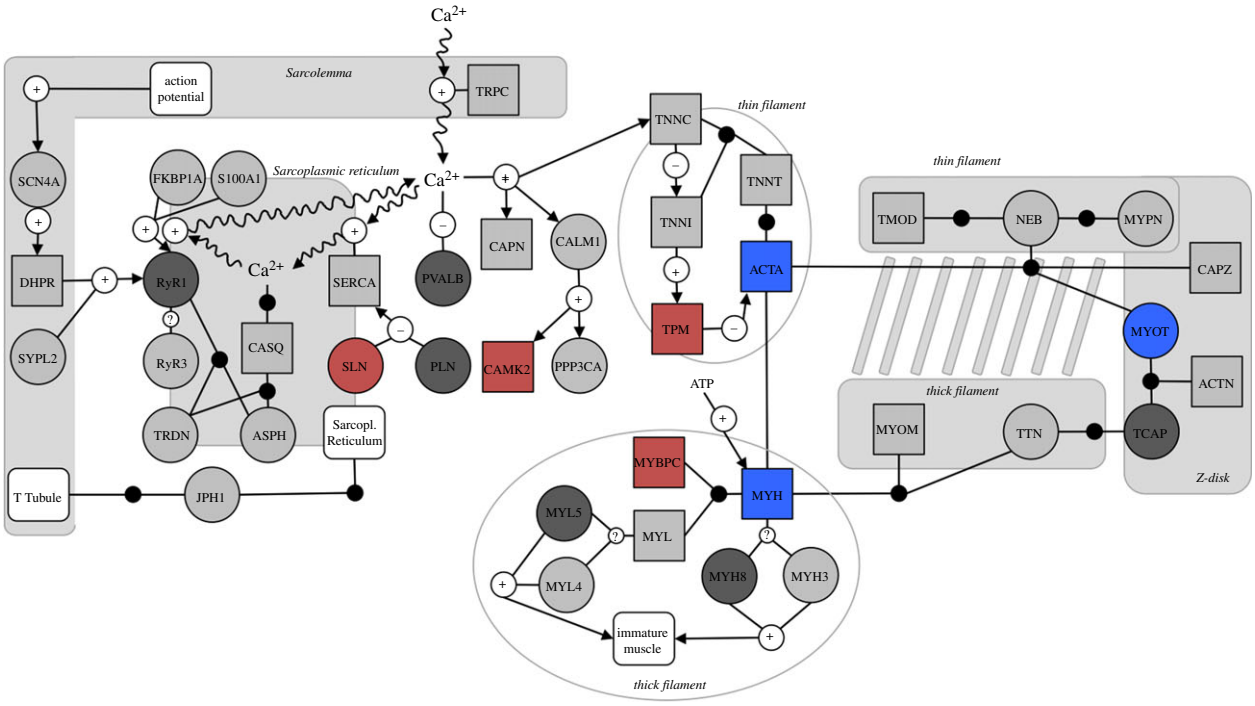

Figure 2. Expression changes in targeted skeletal muscle contraction pathways. Symbols represent genes (circles), gene complexes (squares), modules or functions (white squares), interactions (white circles; positive, negative or unknown) and binding (black circles) per [29]. Colours indicate upregulation (blue), downregulation (red) or no change (light grey) in the cold, or not present in the dataset (dark grey). See electronic supplementary material, table S7 for complete pathway details.

temperatures. Despite its established importance in mammalian thermoregulation, the adaptive significance of avian NST is difficult to determine because the evidence derives entirely from juvenile birds [30]. To address this gap, we used previously reported patterns of avian thermogenic performance to explore the use of facultative NST in wild, adult dark-eyed juncos following cold acclimation. We employed whole-transcriptome expression patterns to simultaneously examine multiple pathways related to ST and NST within the avian pectoralis. We provide novel evidence that *SLN* is expressed in adult birds; however, juncos downregulated *SLN* after acclimation to subzero temperatures, demonstrating that if SLN-mediated NST is used by birds, it is not important—and perhaps even counterproductive—to adult thermoregulation in extreme cold.

We attribute the pattern in *SLN* expression to the possible cost of uncoupling Ca^{2+} cycling for NST in the form of reduced muscle activity for ST. Indeed, the potential for NST to impair muscular function has been proposed as a hypothesis to explain the evolution of BAT-mediated NST in placental mammals [10,31]. It therefore follows that at truly cold temperatures, like those used here, birds should prioritize the process with the greatest heat-generating capacity. Importantly, *SLN*-mediated NST is estimated to produce only a small fraction (2%) of the heat generated during a single-muscle contraction [32]. Accordingly, we observed a tradeoff between *SLN* expression and M_{sum} across individuals. Over the course of acclimation, cold birds further decreased the expression of *SLN*, perhaps facilitating increases to ST.

In support of this idea, we found differential expression of several genes related to skeletal muscle contraction. Whether these expression differences resulted in increased muscle contractility is unknown, but several of the expression patterns we observed are consistent with this hypothesis. For instance, overexpression of β-tropomyosin (*TPM2*) in cardiac muscle is associated with a delay in relaxation [33] and juncos accordingly downregulated *TPM2* in the cold. Many additional DE genes are involved in striated muscle Ca^{2+} cycling, such as members of the adrenergic signalling pathway (*ADCY6*, *CREB5*, *CREM*, *KCNQ1*, *PLCB1*, *PPP2R2D* and *PPP2R5A*). We also observed expression changes in transcription factors (*MEF2C*, *EGR1* and *NFATC1*) that have been implicated in heightened striated muscle performance in mice (e.g. faster relaxation, increased contractility, reduced fatigability and enhanced force) [34]. Nonetheless, while our findings indicate that juncos are simultaneously incorporating several modifications that could improve ST in the cold, quantification of shivering (e.g. using electromyographic activity [4]) is necessary to verify the thermogenic effects of these expression patterns. Moreover, although juncos did not change the expression of a biomarker for mitochondrial abundance (citrate synthase, *CS*), measures of junco mitochondrial function are needed to fully address the potential effects of SLN on muscle energetics (e.g. [14]).

Previous work has demonstrated that cold-acclimated ducklings increase SERCA activity in the gastrocnemius, and this has been cited as evidence of increased capacity for NST [2,35]. We did not measure SERCA activity, but we did not find changes in the expression of SERCA2 or SERCA3 (*ATP2A2* and *ATP2A3*) with cold acclimation. There is likely functional differentiation between SERCA isoforms, with SERCA1 being implicated in NST and SERCA2a in ST [31,36]. However, the gene that encodes SERCA1 is not annotated in our reference genome. These discrepancies are difficult to interpret but it is possible that the relative benefit of NST differs among muscles and/or across life stages in birds.

Although limited to a single muscle in a single species, our work highlights a possible discrepancy in the utilization of NST among small birds and many mammals in the cold. This difference may emerge because mammals with BAT

can compartmentalize one mechanism of NST within a specialized organ, while for birds and other organisms lacking BAT, NST is constrained by the diverse functions of the skeletal muscle. Our evidence thus suggests a potential trade-off between shivering and non-shivering heat production in birds and emphasizes the need for direct measures of avian Ca^{2+} uncoupling. These results point to fruitful avenues for further investigation regarding the evolution of avian endothermy and the use of NST in seasonal acclimatization.

Ethics. This work was completed with approval from the University of Montana Institutional Animal Care and Use Committee (Protocol 010-16ZCDBS-020916).

Data accessibility. Raw sequence reads are available from the NCBI Sequence Read Archive (PRJNA612334).

Authors' contributions. M.S. and Z.A.C. conceived of the study; M.S. performed all data collection and analyses, and drafted the manuscript; Z.A.C. contributed edits to the manuscript. Both authors gave final approval for publication and are accountable for its content.

Competing interests. We declare we have no competing interests.

Funding. This work was supported by the National Science Foundation [GRF to M.S.] and the University of Montana [startup to Z.A.C.].

Acknowledgements. We thank Grant McClelland, Nathan Senner, Cheviron laboratory members and four anonymous reviewers for feedback on this manuscript.

References

1. Janský L. 1973 Non-shivering thermogenesis and its thermoregulatory significance. *Biol. Rev.* **48**, 85–132. (doi:10.1111/j.1469-185X.1973.tb01115.x)
2. Dumonteil E, Barre H, Meissner G. 1995 Expression of sarcoplasmic reticulum Ca^{2+} transport proteins in cold-acclimating ducklings. *Am. J. Physiol. Cell Physiol.* **269**, C955–C960. (doi:10.1152/ajpcell.1995.269.4.C955)
3. Barre H, Geloen A, Chatonnet J, Dittmar A, Rouanet JL. 1985 Potentiated muscular thermogenesis in cold-acclimated muscovy duckling. *Am. J. Physiol. Regul. Integr. Comp. Physiol.* **249**, R533–R538. (doi:10.1152/ajpregu.1985.249.5.R533)
4. Teulier L, Rouanet J-L, Rey B, Roussel D. 2014 Ontogeny of non-shivering thermogenesis in Muscovy ducklings (*Cairina moschata*). *Comp. Biochem. Physiol. A: Mol. Integr. Physiol.* **175**, 82–89. (doi:10.1016/j.cbpa.2014.05.012)
5. Cannon B, Nedergaard J. 2004 Brown adipose tissue: function and physiological significance. *Physiol. Rev.* **84**, 277–359. (doi:10.1152/physrev.00015.2003)
6. Duchamp C. 1993 Skeletal muscle as the major site of nonshivering thermogenesis in cold-acclimated ducklings. *Am. J. physiol.* **265**, R1076–R1083. (doi:10.1152/ajpregu.1993.265.5.r1076)
7. Raimbault S *et al*. 2001 An uncoupling protein homologue putatively involved in facultative muscle thermogenesis in birds. *Biochem. J.* **353**, 441–444. (doi:10.1042/bj3530441)
8. Emre Y, Hurtaud C, Ricquier D, Bouillaud F, Hughes J, Criscuolo F. 2007 Avian UCP: the killjoy in the evolution of the mitochondrial uncoupling proteins. *J. Mol. Evol.* **65**, 392–402. (doi:10.1007/s00239-007-9020-1)
9. Walter I, Seebacher F. 2009 Endothermy in birds: underlying molecular mechanisms. *J. Exp. Biol.* **212**, 2328–2336. (doi:10.1242/jeb.029009)
10. Rowland LA, Bal NC, Periasamy M. 2015 The role of skeletal-muscle-based thermogenic mechanisms in vertebrate endothermy: non-shivering thermogenic mechanisms in evolution. *Biol. Rev.* **90**, 1279–1297. (doi:10.1111/brv.12157)
11. Periasamy M, Huke S. 2001 SERCA pump level is a critical determinant of Ca^{2+} homeostasis and cardiac contractility. *J. Mol. Cell. Cardiol.* **33**, 1053–1063. (doi:10.1006/jmcc.2001.1366)
12. Mall S, Broadbridge R, Harrison SL, Gore MG, Lee AG, East JM. 2006 The presence of sarcolipin results in increased heat production by Ca^{2+}-ATPase. *J. Biol. Chem.* **281**, 36 597–36 602. (doi:10.1074/jbc.M606869200)
13. Bal NC *et al*. 2012 Sarcolipin is a newly identified regulator of muscle-based thermogenesis in mammals. *Nat. Med.* **18**, 1575–1579. (doi:10.1038/nm.2897)
14. Maurya SK, Herrera JL, Sahoo SK, Reis FCG, Vega RB, Kelly DP, Periasamy M. 2018 Sarcolipin signaling promotes mitochondrial biogenesis and oxidative metabolism in skeletal muscle. *Cell Reports* **24**, 2919–2931. (doi:10.1016/j.celrep.2018.08.036)
15. Tupling AR, Asahi M, MacLennan DH. 2002 Sarcolipin overexpression in rat slow twitch muscle inhibits sarcoplasmic reticulum Ca^{2+} uptake and impairs contractile function. *J. Biol. Chem.* **277**, 44 740–44 746. (doi:10.1074/jbc.M206171200)
16. Rome LC, Lindstedt SL. 1998 The quest for speed: muscles built for high-frequency contractions. *Physiology* **13**, 261–268. (doi:10.1152/physiologyonline.1998.13.6.261)
17. Nolan Jr V, Ketterson ED, Cristol DA, Rogers CM, Clotfelter ED, Titus RC, Schoech SJ, Snajdr E. 2002 Dark-eyed Junco (*Junco hyemalis*). *Birds N. Am.* (doi:10.2173/bna.716)
18. Stager M, Senner NR, Tobalske BW, Cheviron ZA. 2020 Body temperature maintenance acclimates in a winter-tenacious songbird. *J. Exp. Biol.* **223**, jeb221853. (doi:10.1242/jeb.221853)
19. Yacoe M, Dawson W. 1983 Seasonal acclimatization in American goldfinches: the role of the pectoralis muscle. *Am. J. Physiol. Regul. Integr. Comp. Physiol.* **245**, R265–R271. (doi:10.1152/ajpregu.1983.245.2.R265)
20. Lohman BK, Weber JN, Bolnick DI. 2016 Evaluation of TagSeq, a reliable low-cost alternative for RNAseq. *Mol. Ecol. Resour.* **16**, 1315–1321. (doi:10.1111/1755-0998.12529)
21. Li H. 2013 Aligning sequence reads, clone sequences and assembly contigs with BWA-MEM. *ArXiv* 1303. (https://arxiv.org/abs/1303.3997)
22. Liao Y, Smyth GK, Shi W. 2014 FEATURECOUNTS: an efficient general purpose program for assigning sequence reads to genomic features. *Bioinformatics* **30**, 923–930. (doi:10.1093/bioinformatics/btt656)
23. R Core Team. 2018 *R: The R project for statistical computing*. Vienna, Austria: R Foundation for Statistical Computing. See https://www.r-project.org/.
24. Robinson MD, McCarthy DJ, Smyth GK. 2010 edgeR: a Bioconductor package for differential expression analysis of digital gene expression data. *Bioinformatics* **26**, 139–140. (doi:10.1093/bioinformatics/btp616)
25. McCarthy DJ, Chen Y, Smyth GK. 2012 Differential expression analysis of multifactor RNA-Seq experiments with respect to biological variation. *Nucleic Acids Res.* **40**, 4288–4297. (doi:10.1093/nar/gks042)
26. Reimand J, Kolde R, Arak T. 2018 gProfileR: interface to the 'g:Profiler' toolkit. R package version 0.6.7. See https://cran.r-project.org/web/packages/gProfileR/index.html.
27. Therneau T. 2015 A package for survival analysis in S. version 2.38. See https://cran.r-project.org/web/packages/survival/citation.html.
28. Gelman A. 2008 Scaling regression inputs by dividing by two standard deviations. *Statist. Med.* **27**, 2865–2873. (doi:10.1002/sim.3107)
29. Smith LR, Meyer G, Lieber RL. 2013 Systems analysis of biological networks in skeletal muscle function. *WIREs Syst. Biol. Med.* **5**, 55–71. (doi:10.1002/wsbm.1197)
30. Hohtola E. 2002 Facultative and obligatory thermogenesis in young birds: a cautionary note. *Comp. Biochem. Physiol. A: Mol. Integr. Physiol.* **131**, 733–739. (doi:10.1016/S1095-6433(02)00011-9)
31. Nowack J, Giroud S, Arnold W, Ruf T. 2017 Muscle non-shivering thermogenesis and its role in the evolution of endothermy. *Front. Physiol.* **8**, 889. (doi:10.3389/fphys.2017.00889)
32. Campbell KL, Dicke AA. 2018 Sarcolipin makes heat, but is it adaptive thermogenesis? *Front. Physiol.* **9**, 714. (doi:10.3389/fphys.2018.00714)
33. Muthuchamy M, Grupp IL, Grupp G, Toole BAO, Kier AB, Boivin GP, Neumann J, Wieczorek DF. 1995 Molecular and physiological effects of overexpressing striated muscle β-tropomyosin in the adult murine heart.

J. Biol. Chem. **270**, 30593–30603. (doi:10.1074/jbc.270.51.30593).

34. Scharf M *et al*. 2013 Mitogen-activated protein kinase-activated protein kinases 2 and 3 regulate SERCA2a expression and fiber type composition to modulate skeletal muscle and cardiomyocyte function. *Mol. Cell. Biol.* **33**, 2586–2602. (doi:10.1128/MCB.01692-12)
35. Dumonteil E, Barre H, Meissner G. 1993 Sarcoplasmic reticulum Ca^{2+}-ATPase and ryanodine receptor in cold-acclimated ducklings and thermogenesis. *Am. J. Physiol. Cell Physiol.* **265**, C507–C513. (doi:10.1152/ajpcell.1993.265.2.C507)
36. de Meis L, Arruda AP, Carvalho DP. 2005 Role of sarco/endoplasmic reticulum Ca^{2+}-ATPase in thermogenesis. *Biosci. Rep.* **25**, 181–190. (doi:10.1007/s10540-005-2884-7)

The architecture of phenotypic flexibility within a complex trait: an empirical case study using avian thermogenic performance

Maria Stager, Luke R. Wilde, and Zachary A. Cheviron

ABSTRACT

Reversible modifications to trait values can allow individuals to match their phenotypes to changing environmental conditions, a phenomenon known as phenotypic flexibility. A system's capacity for flexibility may be determined by its underlying architecture, and these relationships can have important implications for both organismal adaptation and the evolvability of acclimatization responses. Theory provides two possible alternatives to explain the ways in which lower-level traits respond to environmental challenges and contribute to phenotypic flexibility in complex, whole-organism traits: symmorphosis predicts correspondence between structure and demand across all levels of a physiological system, while the alternative predicts that influence is concentrated in select elements of a physiological network. Here we provide a rich dataset — composed of 20 sub-organismal, physiological traits paired with whole-organism metabolic rates for 106 adult Dark-eyed Juncos (*Junco hyemalis*) — to explore the mechanistic basis of phenotypic flexibility in complex traits. When exposed to synthetic temperature cues, these individuals have previously been shown to increase their thermogenic capacity (M_{sum}) and enhance their ability to maintain their body temperature in the cold. We show that the relationships among a number of the traits that contribute to M_{sum} varied as the environmental context changed. Moreover, variation in M_{sum} in response to temperature acclimation was correlated with only a handful of subordinate phenotypes. As a result, avian thermogenic flexibility does not appear to be a symmorphotic response. If this is generally true of complex traits, it suggests that simple and reversible modifications can significantly impact whole-organism performance, and thus that the evolution of phenotypic flexibility in a single component part could impart flexibility for the entire system.

INTRODUCTION

The ability to match an organism's phenotype to changing conditions across its life can be key to fitness in variable environments (Piersma and van Gils, 2011). Such reversible modification of an individual's trait value (phenotypic flexibility) is ubiquitous across life forms and among traits (Piersma and Drent, 2003). However, the proper matching of trait value to the demands of the environment is not guaranteed (Mills et al., 2013). Identifying the causes of variation in flexibility among individuals can therefore inform our understanding of species' resilience to environmental change (Norin and Metcalfe, 2019). In particular, many flexible phenotypes are complex whole-organism responses that are underlain by many lower-level, subordinate traits (Schulte et al., 2011). Determining how the underlying architecture influences the system's capacity for flexibility has important implications for understanding both organismal adaptation and the evolvability of the physiological response. For instance, in order to modify these whole-organism responses, must an individual change all subordinate phenotypes in concert or is control instead focused in just a few of these traits?

Support for concerted change derives from the evolutionary principle of symmorphosis, which states that within biological systems structural design should meet functional demand (Taylor and Weibel, 1981). This congruence between structure and function implies optimization across all levels of a physiological pathway such that no one part is operating in excess. As a

result, symmorphosis predicts that parameters will exhibit an invariant ratio (i.e., constant correlations among traits) under all perturbations to the system, and empirical tests using aerobic performance have shown varying degrees of support across and within individuals (e.g., Weibel et al., 1991). However, because each component of the physiological network would need to be fine-tuned simultaneously (Dudley and Gans, 1991), this configuration could constrain the scope or rate of the flexible response.

Alternatively, we might expect that particular elements of the physiological response might be more flexible than others. In contrast to symmorphosis, this would imply that excess capacity exists in physiological systems (Diamond and Hammond, 1992). Because there are costs associated with trait modification, traits with the greatest net fitness gain should be the most flexible (Murren et al., 2015). The cost of adjusting a phenotypic value results from not only the energy directly required for trait production, but also the pleiotropic nature of many physiological traits. As with genetic pleiotropy, physiological pleiotropy can either facilitate or constrain phenotypic responses to selection (Dantzer and Swanson, 2017). It therefore follows that changing a highly pleiotropic trait may be either (1) more costly, if many downstream traits have to be changed reactively, or (2) more efficient than fine-tuning each trait individually. Depending on the structure of the physiological network, the former scenario may look much like symmorphosis. However, in the case of the latter, selection may only act on a single element to positively influence the capacity of the entire network.

Our ability to effectively evaluate these potential avenues of flexible architecture is limited by our knowledge of how organisms coordinate flexible responses in the wild. Because physiological systems are complex, it is challenging to measure all traits at once and, at the same time, traits may be responding to different environmental cues (Westneat et al., 2019). One well-studied system that lends itself to mechanistic evaluation is thermogenic flexibility — the ability to reversibly alter endogenous heat production, which is used by many small temperate birds to maintain a relatively constant body temperature (T_b) throughout the year (Cooper and Swanson, 1994; Liknes and Swanson, 1996; Marsh and Dawson, 1989; Petit et al., 2013; Swanson, 1990; Swanson and Olmstead, 1999). In the winter, birds can theoretically increase their shivering thermogenesis by enhancing a variety of subordinate traits (see Swanson, 2010 for a review). These flexible modifications fall within four broad levels of physiological organization related to aerobic performance: (1) the size and structure of thermogenic muscle; (2) the supply of metabolic substrate and (3) oxygen to and within the muscle; and (4) the muscle's cellular aerobic capacity. Each level is, in turn, composed of multiple traits for which there is evidence for avian seasonal acclimatization and/or cold acclimation (Figure 1). Many of these potential modifications may be accompanied by concomitant growth in maintenance costs. Indeed, basal metabolic rate also increases in the cold for many birds (McKechnie, 2008; Weathers and Caccamise, 1978), perhaps as a byproduct of other physiological changes (Swanson, 1991; Swanson, 2010). Failure to achieve adequate thermogenic capacity can have dramatic consequences for endothermic fitness (Hayes and O'Connor, 1999; Petit et al., 2017) such that thermogenic flexibility mediates a balance between thermoregulation and its associated energetic costs in response to changing climatic selective pressures (Swanson, 2010). Thus, thermogenic flexibility may profoundly influence endothermic physiological adaptation to temperate climates (Swanson and Garland, Jr., 2009).

Despite evidence for modifications to each of these subordinate traits across species, though, often only a few traits are measured in any given study (but see Vézina et al., 2017). In order to understand the relative contribution of these subordinate traits to avian thermogenic

flexibility, they must instead be evaluated simultaneously. To address this knowledge gap, we conducted a large acclimation experiment aimed at investigating the mechanisms underlying thermogenic flexibility in the Dark-eyed Junco (*Junco hyemalis*). Juncos overwinter at high latitudes across North America and show increases in peak thermogenesis (the maximum metabolic rate under cold exposure; M_{sum}) and cold tolerance in winter (Swanson, 1990). We exposed juncos to temperature treatments of varying duration (from one to nine weeks) and previously reported that cold-acclimated juncos increased their M_{sum} and the ability to maintain their T_b during acute cold exposure (Stager et al., 2020). Here we add 20 additional organ- and tissue-level phenotypes for these same individuals to explore the degree to which flexibility in subordinate physiological traits contributed to thermogenic flexibility. Specifically, we assayed body composition, organ size, muscle histology, blood parameters, and mitochondrial enzyme activities of the pectoralis representing indices of all four of the levels of physiological organization laid out above. We predicted that if avian thermogenic flexibility is a symmorphotic response, birds should make changes to traits across all four physiological levels concurrently. If, instead, control of this flexible response is concentrated in key parts of the physiological cascade, we expected birds to make changes to only a subset of traits. This comprehensive line of inquiry allows us to characterize the avian thermogenic response to cold in unprecedented detail and assess the relative contributions of component traits to whole-organism performance.

METHODS

Acclimations treatments

The methods for capture, acclimation, and metabolic assays have been previously described (Stager et al., 2020). Briefly, we captured adult juncos near the end of the breeding season in Missoula County, Montana, USA (~47.0°N, -113.4°W) in 2016 and 2017. We transferred birds to husbandry facilities at the University of Montana and housed them individually in common conditions for 42 days (18°C, 10h light : 14h dark), which we refer to as the "adjustment period." We verified that breeding traits (brood patches and cloacal protuberances) were not present after this six-week adjustment period. For five additional males not included in the study, we confirmed by dissection that testes had regressed before the acclimations began.

After the adjustment period, we randomly assigned individuals to one of ten experimental groups: we subjected them to one of two temperature treatments, *Cold* (-8°C) or *Control* (18°C), lasting 1, 2, 3, 6, or 9 weeks in duration. Photoperiod was maintained at a constant 10L: 14D in all treatments and food and water were supplied ad libitum. We did not repeat the *Week 9* treatments in 2017, thus final samples sizes are $n = 12$ per treatment, except $n_{Control\_1} = 11$, $n_{Control\_9} = 6$, $n_{Cold\_9} = 5$.

Metabolic assays

We assayed M_{sum} and resting metabolic rate (RMR) using open-flow respirometry at three sampling points: capture, before and after acclimations (referred to as pre- and post-acclimation, respectively). Data for pre- and post-acclimation measures are published in (Stager et al., 2020). We assayed RMR in the evening on the day of capture and M_{sum} the following morning using methods identical to those detailed for pre-acclimation assays (see Stager et al., 2020 for details). In brief, birds were placed in a modified 1-L plastic Nalgene container for metabolic trails. RMR trials were conducted in the dark at 27°C over 3 h with ambient, dried air pumped in at 500 ml/min. Three individuals were assayed at once such that we rotated among

individuals every 20 min for recording. M_{sum} trials were conducted at -5°C for ≤ 1 hr using heliox (21% O_2, 79% He) at 750 ml/min. For both trials, the outflow from the animal's chamber was dried, scrubbed of CO_2, and dried again before the O_2 concentration was quantified using a Foxbox (Sable Systems). We quantified O_2 consumption according to Lighton (2008). We defined RMR as the lowest O_2 consumption averaged over a 10-min period and M_{sum} as the highest O_2 consumption averaged over a 5-min period.

Body composition assays

Body mass (M_b) was quantified before each metabolic measurement began. In 2016, we additionally measured M_b on two dates during the adjustment period (roughly one week and two weeks after capture) to assess mass gain as birds acclimated to captivity. As a structural index of size, we measured the length of both tarsi (± mm) post hoc and calculated the mean tarsus length for each individual. One individual was missing its left foot at capture; thus, the right tarsus was used as the mean.

Immediately before each M_{sum} trial, we also assayed body composition using quantitative magnetic resonance (EchoMRI Whole Body Composition Analyzer). This allows for rapid quantification of fat, lean, and water masses without sedation (Guglielmo, 2010). We quantified body composition three times for each individual—at capture, before and after acclimation—which allows us to use lean mass as a proxy for organ and muscle masses during the first two time points when destructive sampling was not possible. We calibrated the instrument daily before measurements began. We also assayed an oil standard at the beginning and end of a day's measurements. We used the variation in the standard measures across the day's two time points to calculate a daily rate of drift for each fat, lean, and water masses. Individual measures were then linearly corrected using this rate of drift (slope) and the initial deviation from the standard measure (intercept). We report fat mass, lean mass, free water, and total water in grams.

Blood parameters

Directly following the pre- and post-acclimation M_{sum} trials, we extracted blood from the brachial vein to quantify blood O_2 parameters. We first collected 10 µl of whole blood in a cuvette to assay hemoglobin concentration (g/dL) using a Hemocue Hb 201+ analyzer. To quantify hematocrit levels, we collected ~50 µl of blood, centrifuged it for 5 min, and measured the proportion of packed red blood cells to total blood volume.

Post-acclimation, we collected an additional blood sample from the jugular vein. To quantify, erythrocyte number we mixed 10 µl whole blood with 1990 µl of 0.85% saline and later imaged 10 µl of solution on a Neubauer hemocytometer. We randomly selected one of the twenty-five central grid cells (0.04 mm^2) in which to count erythrocytes. Samples that were not imaged within 5 days of blood collection were removed from analysis due to degradation of the sample. We centrifuged the remaining blood sample to separate the red blood cells, then pipetted off the plasma, flash-froze and stored it at -80°C for future assays.

As an index of fat mobilization capacity, we quantified plasma lipid metabolites by endpoint assay on a microplate spectrophotometer at a later date. Assays were run according to Guglielmo et al. (2002a) in 400 µl flat-bottom 96 well polystyrene microplates. We thawed plasma and diluted samples three-fold with 0.9% NaCl. We first measured free glycerol concentration (5 µl plasma, 240 µl free glycerol Sigma reagent A) at 37°C and A540. We then added 60 µl triglyceride (Sigma reagent B) and read absorbance at the same spectrophotometer conditions to quantify total triglyceride concentrations. Samples were run in duplicate and

standard curves were included for each plate. Intra-assay and inter-assay coefficients of variation were 0.35 and 0.34 for total triglycerides and 0.24 and 0.36 for glycerol, respectively. True triglyceride concentration (TRIG) was calculated as total triglyceride minus glycerol (mmol L^{-1}).

Organ masses

At the end of the acclimation treatments, immediately following the final M_{sum} trial and blood extraction, we euthanized individuals using cervical dislocation. We excised the left pectoralis for enzyme assays and the right pectoralis for histological purposes (see below). We weighed organs with a 0.0001 g precision balance (Mettler Toledo ME104). We excised the heart, removed major vessels, fat, and blood before weighing it, and similarly preserved it for histology. We harvested the liver, right kidney, and lungs, trimmed fat, blotted blood on the surface, weighed each (wet mass), and then dried them at 60°C for 48 h before quantifying dry mass. Lungs were not completely exsanguinated, thus blood content likely contributed to mass. Right and left lung masses did not differ (t-test: $t = -0.67$, $df = 206$, $p = 0.50$) and are reported as total lung mass. In 2017, we additionally harvested the gizzard (proventriculus removed), intestines (from gizzard to cloaca; small and large combined), spleen, and pancreas in the same way. Gonads were regressed in all cases and were not weighed. We report wet mass for heart, and dry mass for all other organs (spleen not shown in text).

Due to the difficulty of quantifying total muscle mass directly, we approximated muscle size with data from 2017 individuals. First, we totaled all wet organ masses and subtracted this value from lean mass. We did this multiplying kidney mass by two and using a proportionally constant estimate of brain mass from the literature based on an individual's mass at capture because we did not expect brain mass to change with acclimation. We used the remaining value as an index of wet muscle mass and assumed 75% water content to arrive at a rough estimate of dry muscle mass. This estimate includes other organs not measured here that may have responded to our acclimation treatments (e.g., esophagus, crop, proventriculus). To validate this measure, we separately estimated the water content of muscle by calculating water composition for each organ (wet minus dry masses) and subtracting these values, as well as the mass attributed to free water, water in fat, and water in other tissues (i.e., bones, skin, feathers) from the total water mass for each individual. To do this, we approximated brain mass as before, and estimated that brain and heart (for which we did not quantify dry mass) were composed of 77% and 75% water, respectively (Graber and Graber, 1965; Hughes, 1974). We also assumed that adipose stores were composed of 10% water and that M_b not assigned to lean, fat, or free water could be attributed to bones, skin, and feathers, for which we estimated 20% water content. Though rough approximations, these independent estimates of dry muscle mass and water content of the muscle are strongly correlated (Pearson's correlation: $r = 0.84$, $p = 5.8 \times 10^{-14}$).

Muscle histology

The pectoralis is the principle muscle used for shivering in small birds (Yacoe and Dawson, 1983). In 2017, we excised the middle section of the right pectoralis, coated it with embedding medium (OCT compound), froze it in a bath of isopentane, and stored the sample at -80°C until sectioning. We sectioned pectoralis tissue (10 μm) transverse to muscle fiber length at -20°C using a Leica CM1950 Cryostat. We mounted sections on poly-L-lysine–coated slides, air-dried and stored them at -80°C until staining occurred. To identify capillaries, we stained for alkaline phosphatase activity. We first incubated slides at room temperature for ~2 h then fixed them in acetone for 5 min and allowed them to air dry. We stained slides in assay buffer (1.0 mM

nitroblue tetrazolium, 0.5 mM 5-bromo-4-chloro-3-in- doxyl phosphate, 28 mM $NaBO_2$, and 7 mM $MgSO_4$) at pH 9.3 for 1 h. We imaged muscle sections using light microscopy and used stereological quantification methods to make unbiased measurements (Weibel 1979; Egginton 1990). For a randomly selected subset (200 mm^2) of the image, we then quantified capillary number relative to muscle fiber count and capillary density (per mm^2). We analyzed three regions for each sample to account for heterogeneity across the tissue.

Enzyme assays

Upon excision, we flash froze the left pectoralis in liquid nitrogen, stored it at -80°C, and later used it to quantify activities of carnitine palmitoyl transferase (CPT; an indicator of fatty acid transport into the mitochondrial membrane), beta hydroxyacyl Co-A dehydrogenase (HOAD; an indicator of fatty acid oxidation capacity), and citrate synthase (CS; an indicator of maximal cellular metabolic intensity) according to Guglielmo et al., (2002b). We combined 100 mg frozen pectoralis tissue with 9 volumes ice-cold homogenization buffer (20 mM Na_2HPO_4, 0.5 mM EDTA, 0.2% fatty acid-free BSA, 0.1% Triton X-100, and 50% glycerol at pH 7.4). We homogenized tissues for 3 min at high speed using a Qiagen TissueLyser with adapter sets cooled to -20°C. We further diluted crude muscle homogenates to 1:100 with homogenization buffer, divided samples, and stored aliquots at -80°C until assays were performed. Maximal enzyme activities were quantified using a microplate spectrophotometer. All assays were performed in duplicate, in 400 µl flat-bottom 96 well polystyrene microplates at 39°C, with a reaction volume of 200 µl. Assay conditions were: 50 mM Tris buffer pH 8.56, 7.5 mM carnitine, 0.035 mM palmitoyl-CoA, 0.15 mM DTNB, and 20 µl diluted homogenate for CPT; 50 mM imidazole pH 7.96, 1 mM EDTA, 0.1 mM aceto-acetyl-CoA, 0.2 mM NADH, and 20 µl diluted homogenate for HOAD; and 50 mM Tris buffer pH 8.56, 0.75 mM oxaloacetic acid, 0.10 mM acetyl-CoA, 0.15 mM 5,5 -dithiobis(2- nitrobenzoic acid) (DTNB), and 2 µl diluted homogenate for CS. Activities ($\mu mol \bullet min^{-1}$) were calculated from A412 ($\varepsilon = 13.6$) for CS and CPT and from A340 ($\varepsilon = 6.22$) for HOAD. Week 9 individuals were not included for CPT and CS assays.

Statistical analyses

We performed all analyses in the statistical environment R (R Core Team, 2018). We performed analysis of variance tests to verify that the ten treatment groups did not differ in trait values either at capture or before acclimation (Tables S1). To quantify the rate of mass gain across the adjustment period, we employed the repeated measures of M_b obtained in 2016 in a linear mixed model with days in captivity as a fixed effect and individual as a random effect. We used pairwise t-tests to assess changes in body composition that occurred between capture and the pre-acclimation assays.

To compare the relative degree of change among phenotypic traits in response to temperature acclimation, we first standardized each phenotypic variable (by subtracting the mean and dividing by two standard deviations) using the package *arm* (Gelman, 2008). We tested for effects of Treatment, Duration, and their interaction on phenotypic measures using linear models. In all cases, Treatment × Duration terms were not significant (Table S2) and thus models without the interaction are presented in the text. We also used linear models to test for an effect of *Year* on phenotypic measures that were repeated in both years of the study. We established significance after Bonferroni corrections for multiple testing.

We tested for pairwise associations between all phenotypic traits for a given sampling period with Pearson's correlation tests. In order to determine the relative influence of subordinate phenotypes on M_{sum}, we utilized the variation in traits exhibited across temperature treatments post-acclimation and performed regressions of standardized trait values on M_{sum}. Rather than including all possible traits, we used only those identified with Pearson's correlations to be associated with post-acclimation M_{sum}. Including single terms in each model allowed us to maximize sample sizes for each trait and avoid complications associated with combining terms, like lean mass, which is a composite trait and would therefore be redundant to measures of muscle and organ masses.

RESULTS

At capture

At capture, 10 of 15 pairwise trait combinations (67%) showed correlations. Juncos that were structurally larger were also heavier and carried more lean mass (Figure 2a), but all birds had very little fat (Table S3). Differences did not exist in body size or composition between years, yet individuals exhibited slightly higher metabolic rates in 2017 (Table S4). M_{sum} positively correlated with M_b, lean mass, and RMR (Figure 2a).

Prior to acclimation

Our six-week adjustment period successfully reduced variation in M_{sum} among individuals ($var_{Capture}$ = 2.11 vs. var_{Pre} = 0.36 ml $O_2 \bullet min^{-1}$). Juncos rapidly increased M_b over this time (Table S3), with birds gaining 0.10 g per day in 2016. Most of this mass gain can be attributed to growth in adipose stores, though birds did increase lean mass to a lesser degree (Table S3). Individuals gained more M_b — particularly fat mass — during the six-week adjustment period in 2017 than in 2016 (Table S4). Importantly, treatment groups did not differ at capture or before acclimations for any of the phenotypic traits assayed (Table 1; Table S1).

Immediately prior to acclimation, 13 of 28 pairwise trait combinations (46%) exhibited correlations (Figure 2b). Only 3 of these associations were present at capture. M_{sum} correlated positively with hematocrit alone.

After acclimation

Several trait values were modified in response to cold acclimation. Although M_b did not vary among treatments, juncos adjusted body composition in the cold (Table 1). Cold-acclimated individuals exhibited 0.73 g more lean mass and 0.92 g less fat mass compared to *Control* individuals. This difference in lean mass can, in part, be attributed to growth of the digestive tract in *Cold* birds, which increased the size of their gizzard, intestines, and pancreas by 39%, 49%, and 28% respectively relative to *Control* birds. Cold-acclimated juncos additionally enlarged the size of their heart by 15% compared with *Control* individuals. Both lung mass and kidney mass increased in the cold, but these trends were not significant after correction for multiple testing. Liver mass, which decreased over time in both temperature treatments, was the only trait to show a significant effect of treatment duration. In contrast, muscle, blood, and enzymatic parameters exhibited little flexibility among treatments.

After acclimation, 52 of 276 pairwise trait combinations (19%) exhibited correlations (Figure 2c). Of these associations, 7 were also observed at capture and 4 were observed before acclimation. Only 3 associations were common to all three contexts: RMR and M_b; fat mass and M_b; and lean mass and tarsus length. Six traits correlated positively with M_{sum} after acclimation,

and most involved organ masses that had not been measured at prior sampling points. Lean and heart masses showed the strongest influence on M_{sum}, exhibiting effects equal in magnitude and direction (Table 2).

DISCUSSION

Phenotypic flexibility allows individuals to change trait values in order to match their phenotypes with fluctuations in environmental conditions. Although many whole-organism phenotypes are composed of a complex network of subordinate traits, the ways in which these lower-level traits respond to environmental challenges and contribute to phenotypic flexibility has been little explored. We previously demonstrated that adult Dark-eyed Juncos increased their thermogenic capacity (M_{sum}) in response to synthetic temperature cues, and that this increase corresponded with an enhanced ability to maintain T_b in the cold (Stager et al., 2020). Here we add measures of 20 additional sub-organismal, physiological traits for the same individuals, several of which were measured repeatedly in the same individuals, providing a rich dataset for exploring the mechanistic basis of phenotypic flexibility. We show that the relationships among a number of these traits varied as the environmental context changed. Moreover, variation in M_{sum} in response to temperature acclimation was correlated with only a handful of subordinate phenotypes. Our results thus indicate that avian thermogenic flexibility is not a symmorphotic response, but rather that adjustments to thermogenic flexibility are concentrated in a few subordinate traits. If this is a general feature of complex traits, it suggests that the evolution of phenotypic flexibility in a single component part could impart flexibility for the system as a whole, thereby enabling simple and reversible modifications to significantly impact whole-organism performance in response to environmental change.

Phenotypic responses to cold

We found that in response to very cold temperatures, juncos increased lean mass by enlarging the size of several major organs and simultaneously decreased adipose stores relative to *Control* birds. These traits changed rapidly and plateaued within the first week of cold exposure such that increased duration of the temperature treatment had little effect on trait values. Juncos were thus able to respond on shorter timescales to a significant environmental stressor than had previously been appreciated (see also Stager et al., 2020).

Intriguingly though, many other traits that have been previously implicated in avian thermogenic flexibility remained unchanged. For example, we hypothesized that increased thermogenic capacity might be achieved by augmenting the fuels supporting aerobic metabolism — either directly from food processing or from reserves. While we cannot address the former, counter to the latter idea, juncos had lower adipose depots in the cold, similar to cold-acclimated White-throated Sparrows (*Zonotrichia albicollis*; McWilliams and Karasov, 2014). This change in body composition could result from cold-acclimated individuals burning fat faster than they were able to store it. Accordingly, we observed that juncos gained, on average, only 0.10 g of M_b per day at 18°C during the adjustment period, which is likely not enough to overcome rates of overnight mass loss at cold temperatures (e.g., Ketterson and Nolan, 1978).

Consequently, with fat stores likely being quickly diminished, *Cold* birds may have instead maintained their fuel supplies by increasing food consumption. Many birds accompany higher food intake with growth to their digestive track, which allows individuals to process larger food quantities more quickly without losses to digestive efficiency (McWilliams and Karasov, 2001). In support of this, although we did not quantify food intake, we did find that

birds increased the size of their gizzard, intestine, and pancreas within the first week of cold acclimation. Likewise, White-throated Sparrows grew their intestines within 2-12 d of cold exposure (-20°C), and their larger digestive tracks facilitated greater digestive capacity and increased feeding rates in the absence of reciprocal changes in nutrient uptake per unit of intestine (McWilliams and Karasov, 2014). If true of juncos as well, at high rates of energy use, this could enable them to efficiently use digestive products without spending energy to convert fuels to/from stored adipose. However, we did not observe increases in fat transporters either in the blood or within the muscle. The fact that all traits did not change suggests that many traits may harbor spare capacity (*sensu* McWilliams and Karasov, 2001) such that they can accommodate larger demands without significantly adjusting their trait value.

Ultimately, our treatments lasted up to two months and birds were exposed to a fairly extreme temperature stimulus such that the phenotypic responses shown here are not likely to have been constrained by time or insufficient severity of the cue. Additionally, junco M_{sum} plateaued within one week of cold acclimation (Stager et al., 2020). As a result, any discrepancies between our findings and those shown in wild birds may follow from the fact that winter acclimatization likely involves the combination of several environmental cues. We focused on temperature specifically because previous work has shown that junco M_{sum} responds to variation in temperature rather than photoperiod (Swanson et al., 2014). This had the benefit of allowing us to isolate the phenotypic responses that underlie thermogenic performance in order to decompose this complex trait. Nonetheless, it means that we may have missed certain hormonal changes and subsequent physiological responses that are likely tied to photoperiod or variation in resource abundance and availability, and thus associated with the "winter phenotype." We cannot therefore discount the fact that a different environmental cue — or several coinciding cues — may induce maximal output at every level through the regulation of trait changes (i.e., symmorphosis).

Variation in trait associations across time

Even though our acclimation treatment targeted responses to cold alone, an unintended outcome of our experimental setup is that several environmental variables changed throughout the course of the investigation as a whole. For instance, juncos were nearing the end of their breeding season when they were captured, which is typically considered a "lean" time of the annual cycle. In addition to defending territories and provisioning young, they were likely contending with variation in temperatures, precipitation, food availability, and predation pressures in the wild. These stressors are reflected in the poor body condition of our birds at capture. In contrast, during the adjustment period in the lab environment, breeding traits quickly regressed following exposure to an artificially short photoperiod, and birds were housed individually with ad libitum food under mild temperatures (albeit, outside of their thermoneutral zone). These conditions therefore represented a more benign environment than that experienced by wild juncos at this time of year, and the standard conditions removed inter-individual variation. When we next induced temperature changes, we did so in the absence of variation in photoperiod or food availability, after birds had already adjusted to captivity. The phenotypic responses that we observed during this period are therefore reflective of the isolated effect of cold temperatures. Thus, because birds must respond to changes in their environment across many different axes in the wild, these three contexts let us explore how consistently traits may be associated.

In total, we quantified 253 pairwise trait correlations among individuals, 28 of which we measured two or more times per individual (e.g., at capture, before acclimation, and after acclimation). Many of these relationships varied in either strength or direction across the three sampling periods. For example, fat and lean masses, which correlated positively at capture, correlated negatively after six weeks of captivity. All individuals were thus capable of storing adipose in this setting. At this same time point, though, other trait correlations that existed at the time of capture were absent, perhaps due to the reduced phenotypic variation following the adjustment period. Ultimately, of the original trait associations exhibited at capture, 70% did not persist across the subsequent sampling points.

Notably, the traits that correlated with M_{sum} also changed across time, such that ratios between subordinate traits and aerobic performance were not invariant to perturbation, as would be predicted by symmorphosis. Lean mass correlated with M_{sum} both at capture and after, but not before, acclimation. Meanwhile, RMR and M_b correlated with M_{sum} only at capture and not once birds had adjusted to captivity. Collectively, these results point to the importance of environmental context in evaluating phenotypic contributions to performance and, more broadly, imply that relationships between flexible phenotypic and performance traits — which are often used as indices of fitness — may change across time.

Symmorphosis?

Previous work has indicated that symmorphosis may be generally applicable to the limits of avian aerobic performance (Seymour et al., 2008; Suarez, 1998; Swanson, 2010). However, because most studies focus on the contribution of oxygen transport alone, they could also be interpreted as demonstrating that correlations exist across only *some* of the physiological pathways associated with aerobic performance (Swanson, 2010). In comparison, we did not observe correlations among the many parameters quantified within the oxygen supply pathway, but we did see associations between several traits related to fuel transport. In addition to correlations among many of the digestive organs, these organs positively correlated with heart mass, and plasma triglyceride concentrations positively correlated with intestinal mass and with CPT activity, as well. Together this indicates that higher digestive capacity was likely met with higher fuel transport capacity.

In its strictest sense, though, symmorphosis predicts that all components within a system should change in concert such that no one element is operating in excess (Weibel et al., 1991). We did not find support for this hypothesis in that juncos achieved higher thermogenic capacity in the cold without simultaneously adjusting each subordinate trait. Juncos instead enhanced M_{sum} by concurrently modifying five traits that fall within three levels of biological organization (Figure 1) — including the masses of the muscle, certain digestive organs, and the heart; however, they did not alter lower-level indices of cellular aerobic capacity that we measured here.

Growing larger organs may seem like a costly and time-consuming investment for a small bird to make if an alternative possibility is to increase the expression of key metabolic enzymes. Though we did not quantify their cost of production, surprisingly, none of these organ sizes correlated with RMR, suggesting that larger organs were not associated with higher maintenance costs as predicted (e.g., Chappell et al., 1999; Vézina et al., 2017). Moreover, sizeable growth in these traits was achieved within one week of cold exposure indicating that these modifications are induced on seemingly short time scales rather than preemptive to

seasonal temperature changes. Thus, in order to fully understand the costs of trait production as they relate to reversible modification, de-acclimation studies are also needed.

Of any single trait, heart mass exhibited the largest effect on M_{sum}. Unfortunately, though, we did not quantify as many traits in the first year of the study as we did in the second. This may have reduced our power to detect associations among traits and appropriately assess their relative influence on M_{sum}. For instance, the strong influence of lean mass (measured in both years) on M_{sum}, in combination with the strong correlations between lean mass and muscle (r = 0.82) and intestinal (r =0.40) masses in 2017, is suggestive that these phenotypes likely influenced M_{sum} in 2016, as well. If so, their effects may have outweighed that of heart mass across all individuals. This would not be surprising as the potential benefit of larger muscles to facilitate shivering is clear, and the advantage of larger intestine, pancreas, and kidney masses likely derives from a greater digestive and excretory capacity to fuel aerobic performance, as discussed above. However, cardiac function is involved in both the fuel and oxygen supply pathways, suggesting that enhancements to this one component could have dual benefits. Increased heart size may therefore be an especially efficient way to increase flux across multiple parts of the physiological network.

Conclusions

Understanding how organisms flexibly alter physiological responses can help us understand their capacity to cope with a changing environment (Stillman, 2003). Taken together, our results indicate that flexibility in a whole-organism performance phenotype can be modified quickly by altering a handful of underlying traits of large effect. If this is a generalizable feature of phenotypic flexibility, it may help explain its ubiquity across many morphological, physiological, and behavioral traits. We thus urge future studies to continue exploring how flexibility in performance traits is achieved and to develop a cost-benefit framework that can help put into context why some traits are flexible, while others are not.

Acknowledgements

We are especially thankful to Nathan Senner, Phred Benham, Ryan Mahar, and Nicholas Sly for their help in catching birds. We thank Chris Guglielmo for sharing his plasma metabolite assay protocols; Jesse Loewecke, Catie Ivy, and Lou Herritt for histology assistance; Frank Moss for logistical assistance; Hailey Bunker for help with husbandry; Alex Gerson and Francois Vézina for helpful advice after the initial year of data collection; as well as Keely Corder, Ryan Mahar, Rena Schweizer, Jon Velotta, and Cole Wolf for feedback on an earlier draft of this manuscript.

Funding

This work was funded by the National Science Foundation (GRFP to M.S.) and the University of Montana (startup funds to Z.A.C.).

Ethics

All procedures were approved by the University of Montana Animal Care Committee (Protocol 010-16ZCDBS-020916). Birds were collected with permission from Montana Fish Wildlife & Parks (permits 2016-013 and 2017-067-W, issued to M.S.) and the US Fish & Wildlife Service (permit MB84376B-1 to M.S.).

Author Contributions
M.S. and Z.A.C. conceived of the study; L.W. performed histological sectioning, staining, and imaging; M.S. performed acclimations, all other assays and data collection, and analyses, and drafted the manuscript; Z.A.C. contributed edits to the manuscript.

REFERENCES

Chappell, M. A., Bech, C. and Buttemer, W. A. (1999). Aerobic capacity in house sparrows. *Journal of Experimental Biology* **202**, 2269–2279.

Cooper, S. J. and Swanson, D. L. (1994). Seasonal acclimatization of thermoregulation in the Black-Capped Chickadee. *The Condor* **96**, 638–646.

Dantzer, B. and Swanson, E. M. (2017). Does hormonal pleiotropy shape the evolution of performance and life history traits? *Integr Comp Biol* **57**, 372–384.

Diamond, J. and Hammond, K. (1992). The matches, achieved by natural selection, between biological capacities and their natural loads. *Experientia* **48**, 551–557.

Dudley, R. and Gans, C. (1991). A critique of symmorphosis and optimality models in physiology. *Physiological Zoology* **64**, 627–637.

Gelman, A. (2008). Scaling regression inputs by dividing by two standard deviations. *Statist. Med.* **27**, 2865–2873.

Graber, R. R. and Graber, J. W. (1965). Variation in avian brain weights with special reference to age. *The Condor* **67**, 300–318.

Guglielmo, C. G. (2010). Move that fatty acid: fuel selection and transport in migratory birds and bats. *Integrative and Comparative Biology* **50**, 336–345.

Guglielmo, C. G., O'Hara, P. D. and Williams, T. D. (2002a). Extrinsic and intrinsic sources of variation in plasma lipid metabolites of free-living Western Sandpipers. **119**, 10.

Guglielmo, C. G., Haunerland, N. H., Hochachka, P. W. and Williams, T. D. (2002b). Seasonal dynamics of flight muscle fatty acid binding protein and catabolic enzymes in a migratory shorebird. *American Journal of Physiology-Regulatory, Integrative and Comparative Physiology* **282**, R1405–R1413.

Hayes, J. P. and O'Connor, C. S. (1999). Natural selection on thermogenic capacity of high-altitude deer mice. *Evolution* **53**, 1280–1287.

Hughes, M. R. (1974). Water content of the salt glands and other avian tissues. *Comp Biochem Physiol A Comp Physiol* **47**, 1089–1093.

Ketterson, E. D. and Nolan, V. (1978). Overnight weight loss in Dark-Eyed Juncos (Junco hyemalis). *The Auk* **95**, 755–758.

Lighton, J. (2008). *Measuring metabolic rates: a manual for scientists.* New York: Oxford University Press.

Liknes, E. T. and Swanson, D. L. (1996). Seasonal variation in cold tolerance, basal metabolic rate, and maximal capacity for thermogenesis in White-breasted Nuthatches *Sitta carolinensis* and Downy Woodpeckers *Picoides pubescens*, two unrelated arboreal temperate residents. *Journal of Avian Biology* **27**, 279.

Marsh, R. L. and Dawson, W. R. (1989). Avian adjustments to cold. In *Animal Adaptation to Cold* (ed. Wang, L. C. H.), pp. 205–253. Berlin, Heidelberg: Springer.

McKechnie, A. E. (2008). Phenotypic flexibility in basal metabolic rate and the changing view of avian physiological diversity: a review. *J Comp Physiol B* **178**, 235–247.

McWilliams, S. R. and Karasov, W. H. (2001). Phenotypic flexibility in digestive system structure and function in migratory birds and its ecological significance. *Comparative Biochemistry and Physiology Part A: Molecular & Integrative Physiology* **128**, 577–591.

McWilliams, S. R. and Karasov, W. H. (2014). Spare capacity and phenotypic flexibility in the digestive system of a migratory bird: defining the limits of animal design. *Proc. R. Soc. B* **281**, 20140308.

Mills, L. S., Zimova, M., Oyler, J., Running, S., Abatzoglou, J. T. and Lukacs, P. M. (2013). Camouflage mismatch in seasonal coat color due to decreased snow duration. *PNAS* **110**, 7360–7365.

Murren, C. J., Auld, J. R., Callahan, H., Ghalambor, C. K., Handelsman, C. A., Heskel, M. A., Kingsolver, J. G., Maclean, H. J., Masel, J., Maughan, H., et al. (2015). Constraints on the evolution of phenotypic plasticity: limits and costs of phenotype and plasticity. *Heredity* **115**, 293–301.

Norin, T. and Metcalfe, N. B. (2019). Ecological and evolutionary consequences of metabolic rate plasticity in response to environmental change. *Philosophical Transactions of the Royal Society B: Biological Sciences* **374**, 20180180.

Petit, M., Lewden, A. and Vézina, F. (2013). Intra-seasonal flexibility in avian metabolic performance highlights the uncoupling of basal metabolic rate and thermogenic capacity. *PLoS ONE* **8**, e68292.

Petit, M., Clavijo-Baquet, S. and Vézina, F. (2017). Increasing winter maximal metabolic rate improves intrawinter survival in small birds. *Physiological and Biochemical Zoology* **90**, 166–177.

Piersma, T. and Drent, J. (2003). Phenotypic flexibility and the evolution of organismal design. *Trends in Ecology & Evolution* **18**, 228–233.

Piersma, T. and van Gils, J. A. (2011). *The Flexible Phenotype: A Body-centred Integration of Ecology, Physiology, and Behaviour*. Oxford University Press.

R Core Team (2018). R: The R project for statistical computing. *R Foundation for Statistical Computing, Vienna, Austria*.

Schulte, P. M., Healy, T. M. and Fangue, N. A. (2011). Thermal performance curves, phenotypic plasticity, and the time scales of temperature exposure. *Integr Comp Biol* **51**, 691–702.

Seymour, R. S., Runciman, S. and Baudinette, R. V. (2008). Development of maximum metabolic rate and pulmonary diffusing capacity in the superprecocial Australian Brush Turkey Alectura lathami: An allometric and morphometric study. *Comparative Biochemistry and Physiology Part A: Molecular & Integrative Physiology* **150**, 169–175.

Stager, M., Swanson, D. L. and Cheviron, Z. A. (2015). Regulatory mechanisms of metabolic flexibility in the dark-eyed junco (Junco hyemalis). *Journal of Experimental Biology* **218**, 767–777.

Stager, M., Senner, N. R., Tobalske, B. W. and Cheviron, Z. A. (2020). Body temperature maintenance acclimates in a winter-tenacious songbird. *J Exp Biol* **223**, jeb221853.

Stillman, J. H. (2003). Acclimation capacity underlies susceptibility to climate change. *Science* **301**, 65–65.

Suarez, R. K. (1998). Oxygen and the upper limits to animal design and performance. *Journal of Experimental Biology* **201**, 1065–1072.

Swanson, D. L. (1990). Seasonal variation in cold hardiness and peak rates of cold-induced thermogenesis in the Dark-Eyed Junco (Junco hyemalis). *The Auk* **107**, 6.

Swanson, D. L. (1991). Seasonal adjustments in metabolism and insulation in the Dark-Eyed Junco. *The Condor* **93**, 538–545.

Swanson, D. L. (2010). Seasonal metabolic variation in birds: functional and mechanistic correlates. In *Current Ornithology Volume 17* (ed. Thompson, C. F.), pp. 75–129. New York, NY: Springer New York.

Swanson, D. L. and Garland, Jr., T. (2009). The evolution of high summit metabolism and cold tolerance in birds and its impact on present-day distributions. *Evolution* **63**, 184–194.

Swanson, D. L. and Olmstead, K. L. (1999). Evidence for a proximate influence of winter temperature on metabolism in passerine biirds. *Physiological and Biochemical Zoology* **72**, 566–575.

Swanson, D., Zhang, Y., Liu, J.-S., Merkord, C. L. and King, M. O. (2014). Relative roles of temperature and photoperiod as drivers of metabolic flexibility in dark-eyed juncos. *Journal of Experimental Biology* **217**, 866–875.

Taylor, C. R. and Weibel, E. R. (1981). Design of the mammalian respiratory system. I. Problem and strategy. *Respir Physiol* **44**, 1–10.

Vézina, F., Gerson, A. R., Guglielmo, C. G. and Piersma, T. (2017). The performing animal: causes and consequences of body remodeling and metabolic adjustments in red knots facing contrasting thermal environments. *American Journal of Physiology-Regulatory, Integrative and Comparative Physiology* **313**, R120–R131.

Weathers, W. W. and Caccamise, D. F. (1978). Seasonal acclimatization to temperature in monk parakeets. *Oecologia* **35**, 173–183.

Weibel, E. R., Taylor, C. R. and Hoppeler, H. (1991). The concept of symmorphosis: a testable hypothesis of structure-function relationship. *Proceedings of the National Academy of Sciences* **88**, 10357–10361.

Westneat, David. F., Potts, L. J., Sasser, K. L. and Shaffer, J. D. (2019). causes and consequences of phenotypic plasticity in complex environments. *Trends in Ecology & Evolution* **34**, 555–568.

Yacoe, M. and Dawson, W. (1983). Seasonal acclimatization in American goldfinches: the role of the pectoralis muscle. *American Journal of Physiology-Regulatory, Integrative and Comparative Physiology* **245**, R265–R271.

Table 1. Linear effects of *Cold* treatment and *Duration* on standardized values of phenotypic traits. Significant effects after correction for 36 tests ($p < 0.0014$) bolded. Metabolic rates, body mass, and tarsus lengths for pre- and post-acclimation from Stager et al. (2020).

			Treatment			Duration			
	Trait	***n***	***β***	**SE**	**p**	***β***	**SE**	***p***	**R^2**
Capture	M_{sum}	86	0.05	0.11	0.66	-0.02	0.02	0.42	0.01
	RMR	99	0.04	0.10	0.66	0.00	0.02	0.93	0.00
	Tarsus length	106	0.09	0.10	0.33	0.04	0.02	0.07	0.04
	M_b	106	-0.03	0.10	0.73	0.02	0.02	0.32	0.01
	Lean mass	98	-0.05	0.11	0.66	0.04	0.02	0.08	0.03
	Fat mass	98	0.15	0.10	0.14	0.05	0.02	7.2×10^{-3}	0.09
Pre-acclimation	M_{sum}	103	0.08	0.10	0.42	-0.02	0.02	0.43	0.01
	RMR	106	-0.02	0.10	0.85	-0.03	0.02	0.09	0.03
	M_b	106	0.01	0.10	0.94	-0.02	0.02	0.41	0.01
	Lean mass	105	-0.06	0.10	0.51	0.04	0.02	0.02	0.06
	Fat mass	105	0.09	0.10	0.34	-0.04	0.02	0.03	0.05
	Hemoglobin	106	-0.01	0.10	0.91	0.00	0.02	0.95	0.00
	Hematocrit	100	0.01	0.10	0.92	0.00	0.02	0.96	0.00
Post-acclimation	**M_{sum}**	105	**0.45**	**0.09**	**1.0×10^{-6}**	-0.04	0.02	0.03	0.24
	RMR	105	-0.02	0.10	0.84	-0.04	0.02	0.04	0.04
	M_b	106	0.14	0.10	0.14	-0.04	0.02	0.04	0.06
	Lean mass	106	**0.47**	**0.09**	**2.9×10^{-7}**	-0.02	0.02	0.25	0.24
	Muscle mass	51	0.02	0.14	0.88	0.08	0.04	0.05	0.08
	Fiber density	51	-0.08	0.14	0.60	-0.03	0.04	0.49	0.02
	Fat mass	106	**-0.31**	**0.09**	**7.2×10^{-4}**	-0.05	0.02	4.2×10^{-3}	0.16
	Gizzard mass	51	**0.57**	**0.12**	**1.1×10^{-5}**	-0.03	0.03	0.36	0.34
	Intestine mass	51	**0.72**	**0.09**	**9.7×10^{-10}**	-0.05	0.03	0.07	0.56
	Pancreas mass	51	**0.43**	**0.12**	**7.7×10^{-4}**	-0.09	0.03	7.5×10^{-3}	0.31
	Liver mass	106	0.15	0.09	0.08	**-0.09**	**0.02**	**1.5×10^{-6}**	0.22
	Kidney mass	104	0.28	0.09	3.7×10^{-3}	-0.02	0.02	0.20	0.10
	Plasma TRIG	61	0.22	0.12	0.08	-0.05	0.03	0.07	0.11
	Plasma glycerol	64	0.14	0.12	0.25	0.06	0.03	0.06	0.07
	Heart mass	106	**0.61**	**0.08**	**3.4×10^{-12}**	0.02	0.14	0.41	0.38
	Lung mass	106	0.25	0.09	9.3×10^{-3}	0.00	0.02	0.92	0.06
	Hemoglobin	106	0.16	0.10	0.10	0.01	0.02	0.58	0.03
	Hematocrit	105	0.20	0.10	0.04	0.00	0.02	0.93	0.04
	Erythrocyte count	58	-0.11	0.13	0.40	0.05	0.04	0.15	0.05
	Capillary density	51	-0.09	0.14	0.55	0.01	0.04	0.81	0.01
	Pectoralis CPT	95	0.06	0.10	0.59	-0.01	0.03	0.69	0.00
	Pectoralis HOAD	95	-0.05	0.10	0.61	0.02	0.03	0.40	0.01
	Pectoralis CS	95	0.16	0.10	0.12	0.04	0.03	0.15	0.05

Table 2. Effects of standardized phenotypic traits on M_{sum} post-acclimation.

	Phenotypic Trait	*n*	*β*	SE	*p*	R^2
Post-acclimation	Lean mass	105	1.26	0.26	3.5×10^{-6}	0.19
	Heart mass	105	1.25	0.27	1.0×10^{-5}	0.17
	Muscle mass	50	1.11	0.46	0.02	0.11
	Kidney mass	103	0.71	0.29	0.02	0.06
	Intestine mass	50	1.14	0.46	0.02	0.12
	Pancreas mass	50	1.15	0.46	0.02	0.12

Figure 1. (a) Schematic of potential physiological adjustments to enhance thermogenic capacity. (B) Detail of the fuel and oxygen supply pathways as they feed into cellular aerobic metabolism. Modified from Stager et al. (2015). (c) Evidence for winter acclimatization and cold acclimation in small birds for each trait from the literature. Increased (+), decreased (-), or no change (nc).

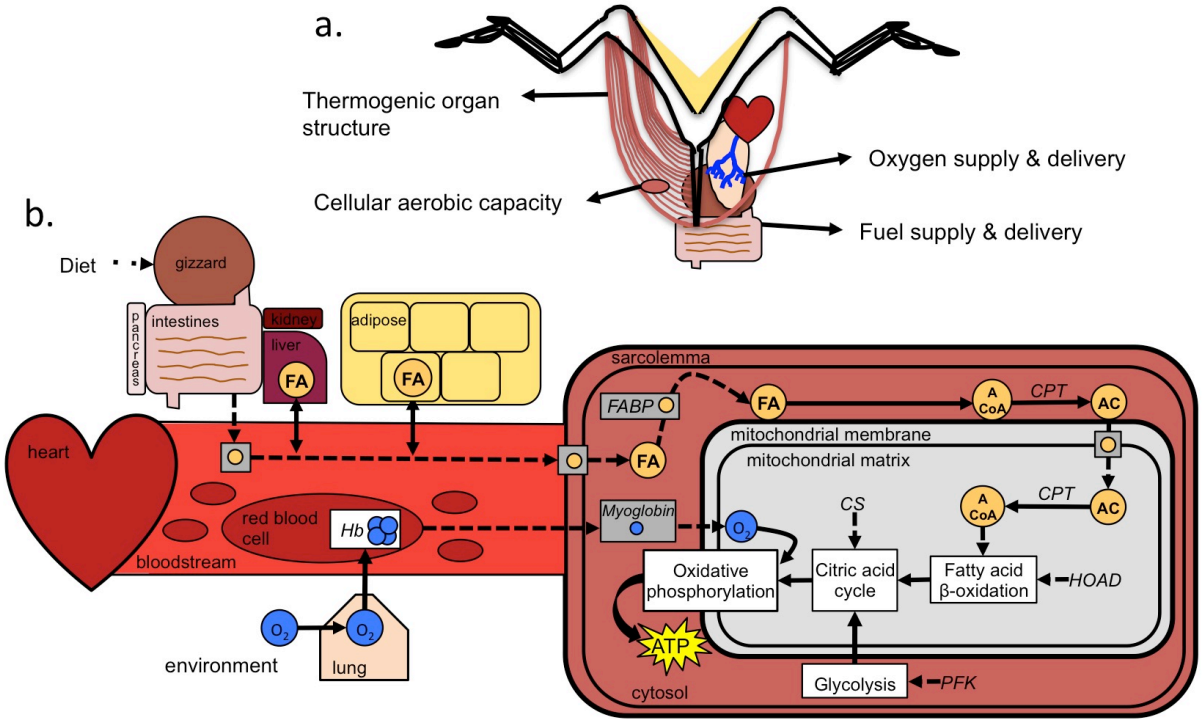

Level	Trait	Winter Acclimatization		Cold Acclimation	
Thermogenic organ structure	Pectoralis mass	+	Liknes and Swanson, 2011a	+ nc	Vézina et al., 2017 Swanson et al., 2014
	Pectoralis fiber size	+	Jimenez et al., 2019	+	Vezina et al., 2020
Fuel supply & delivery	Digestive organ size			+	McWilliams and Karasov, 2014; McWilliams et al. 1999
	Adipose stores	+	King 1972; Laplante et al., 2019	+ -	Rogers, 1995 McWilliams and Karasov, 2014
	Plasma triglycerides	nc	Swanson and Thomas, 2007		
	Pectoralis FABP	+/nc	Liknes 2005	+	Stager et al., 2015
	Pectoralis CPT	+	Liknes et al., 2014	+	Swanson et al., 2014
Oxygen supply & delivery	EO_2	+	Arens and Cooper, 2005		
	Heart size	+	Liknes 2005	+	Swanson et al., 2014
	Hemoglobin	+	Clemens, 1990	-	Niedojadlo et al., 2018
	Hematocrit	+	Swanson, 1990b; deGraw et al. 1979; Fair et al., 2007		
	Erythrocyte count	+	Breuer et al., 1995		
	Pectoralis capillarity	nc	Carey et al. 1978	+	Mathieu-Costello et al., 1998
	Pectoralis myoglobin	+	Chaffee et al., 1965		
Cellular aerobic capacity	Mitochondrial density			+	Mathieu-Costello et al., 1994; Mathieu-Costello et al., 1998
	Pectoralis PFK	+ nc	Yacoe and Dawson, 1983 Liknes 2005		
	Pectoralis HOAD	+ +/nc	Carey 1989; O'Connor 1995b Liknes 2005	+	Swanson et al., 2014
	Pectoralis CS	+	Liknes and Swanson, 2011b	nc	Swanson et al., 2014
	Pectoralis CCO	+	Zheng et al. 2008		

Figure 2. Pairwise trait correlations at (a) capture, (b) before acclimation, and (c) after acclimation. Colors correspond to Pearson's correlation coefficients (positive = red; negative = blue); asterisks indicate significance. Underlying values shown in Tables S5-S7.

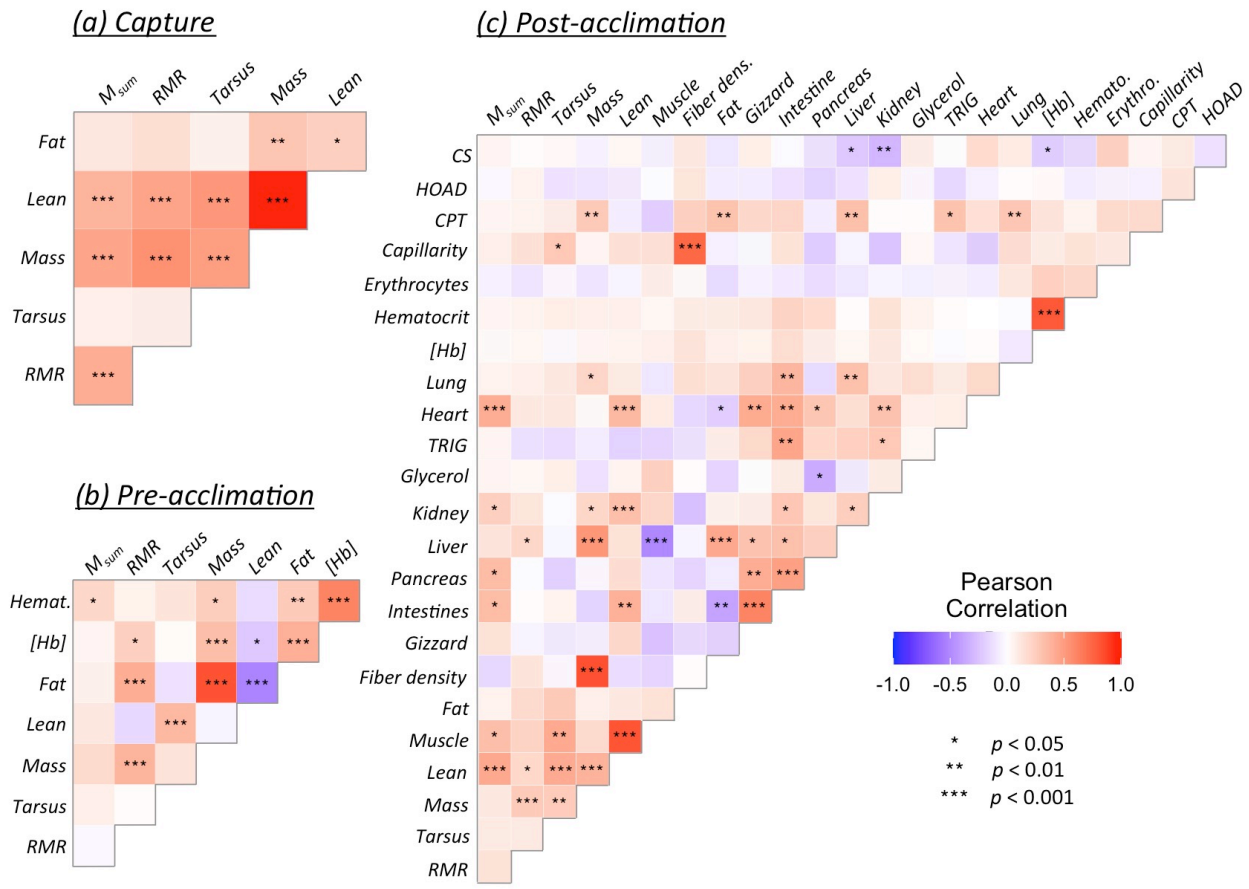

Table S1. Results from ANOVAs to determine if the ten treatment groups differed in physiological parameters at (a) capture and (b) before acclimation treatments.

(a)

Variable	*n*	df	F	*p*
M_{sum}	86	9	1.17	0.33
RMR	99	9	0.62	0.78
Tarsus	106	9	1.62	0.12
M_b	106	9	1.25	0.28
M_{lean}	98	9	0.97	0.48
M_{fat}	98	9	1.74	0.09
M_{fH2O}	98	9	0.49	0.88

(b)

Variable	*n*	df	F	*p*
M_{sum}	103	9	1.74	0.09
RMR	106	9	1.09	0.38
M_b	106	9	0.46	0.90
M_{lean}	105	9	1.27	0.26
M_{fat}	105	9	0.93	0.50
M_{fH2O}	105	9	1.12	0.36
Hemoglobin	106	9	0.21	0.99
Hematocrit	100	9	0.63	0.77

Table S2. Linear effects of *Cold* Treatment, *Duration,* and their interaction on standardized phenotypic traits. Body mass, tarsus lengths, and metabolic rates for pre- and post-acclimation from Stager et al. (2020). Bolded significant effects after Bonferroni correction for 36 models ($p < 0.0014$).

			Treatment			**Duration**			**Treat x Duration**		
	Trait	***n***	**β**	**SE**	**p**	**β**	**SE**	**p**	**β**	**SE**	**p**
Canture	RMR	99	0.13	0.18	0.48	0.01	0.03	0.76	-0.02	0.04	0.58
	M_{sum}	86	-0.15	0.20	0.46	0.04	0.03	0.17	0.05	0.05	0.24
	Tarsus Length	106	0.06	0.17	0.73	0.03	0.03	0.25	0.01	0.04	0.79
	M_b	106	0.06	0.17	0.72	0.03	0.03	0.24	-0.03	0.04	0.50
	M_{lean}	98	-0.15	0.18	0.41	0.02	0.03	0.38	0.03	0.04	0.49
	M_{fat}	98	0.27	0.17	0.12	0.07	0.03	0.01	-0.03	0.04	0.40
Pre-acclimation	RMR	106	0.08	0.17	0.65	-0.02	0.03	0.45	-0.03	0.04	0.49
	M_{sum}	103	0.24	0.18	0.18	0.00	0.03	0.88	-0.04	0.04	0.29
	M_b	106	-0.10	0.17	0.55	-0.03	0.03	0.26	0.03	0.04	0.43
	M_{lean}	105	-0.12	0.17	0.47	0.04	0.03	0.17	0.02	0.04	0.67
	M_{fat}	105	0.12	0.17	0.50	-0.04	0.03	0.15	-0.01	0.04	0.87
	Hemoglobin	106	-0.05	0.17	0.76	-0.01	0.03	0.80	0.01	0.04	0.76
	Hematocrit	100	-0.03	0.18	0.87	0.00	0.03	0.88	0.01	0.04	0.79
Post-acclimation	RMR	105	-0.24	0.17	0.16	-0.07	0.03	0.01	0.06	0.04	0.11
	M_{sum}	105	0.44	0.15	4.0×10^{-3}	-0.04	0.02	0.11	0.00	0.03	0.98
	M_b	106	-0.01	0.17	0.95	-0.06	0.03	0.03	0.04	0.04	0.27
	M_{lean}	106	0.33	0.15	0.03	-0.04	0.02	0.11	0.04	0.03	0.26
	M_{fat}	106	-0.36	0.16	0.02	-0.06	0.02	0.02	0.01	0.04	0.69
	Hemoglobin	106	0.05	0.17	0.76	0.00	0.03	0.88	0.03	0.04	0.43
	Hematocrit	105	0.04	0.17	0.83	-0.02	0.03	0.46	0.04	0.04	0.25
	Erythrocyte count	58	0.01	0.27	0.97	0.07	0.05	0.16	-0.04	0.07	0.61
	Capillary density	51	0.04	0.28	0.90	0.03	0.06	0.59	-0.04	0.08	0.61
	Fiber density	51	0.28	0.27	0.32	0.03	0.06	0.56	-0.12	0.08	0.14
	Heart mass	106	**0.46**	**0.13**	**9.0×10^{-4}**	0.00	0.02	0.91	0.04	0.03	0.18
	Lung mass	106	0.35	0.17	0.04	0.01	0.03	0.67	-0.03	0.04	0.47
	Liver mass	106	0.08	0.15	0.60	**-0.10**	**0.02**	**9.5×10^{-5}**	0.02	0.03	0.56
	Kidney mass	104	-0.01	0.16	0.94	-0.06	0.03	0.02	0.08	0.04	0.03
	Gizzard mass	51	0.65	0.05	6.0×10^{-3}	-0.02	0.05	0.74	-0.03	0.06	0.67
	Intestine mass	51	**0.82**	**0.18**	**5.9×10^{-5}**	-0.03	0.04	0.40	-0.03	0.05	0.53
	Pancreas mass	51	0.54	0.23	0.02	-0.07	0.05	0.13	-0.04	0.07	0.57
	Muscle mass	51	-0.32	0.26	0.23	0.02	0.05	0.31	0.11	0.08	0.13
	CPT	95	-0.06	0.20	0.75	-0.03	0.04	0.43	0.04	0.06	0.48
	HOAD	95	-0.03	0.20	0.90	0.03	0.04	0.48	-0.01	0.06	0.87
	CS	95	0.22	0.19	0.26	0.05	0.04	0.21	-0.02	0.05	0.71
	Plasma TRIG	61	0.26	0.23	0.27	-0.05	0.04	0.20	0.01	0.06	0.85
	Plasma glycerol	64	0.12	0.23	0.59	0.05	0.04	0.16	0.01	0.06	0.92

Table S3. Body composition (in grams) across time points. Mean ± SD and two-sample t-test results.

Trait	Capture	Pre-Acclimation	t	df	*p*
M_b	17.45 ± 1.24	22.60 ± 1.57	-25.2	193	$<2.2 \times 10^{-16}$
Lean mass	14.03 ± 1.01	14.70 ± 0.93	-4.9	197	1.7×10^{-6}
Fat mass	0.08 ± 0.11	3.60 ± 1.65	-21.8	105	$<2.2 \times 10^{-16}$
Free water mass	0.33 ± 0.04	0.32 ± 0.06	0.5	177	0.64
Total water mass	11.40 ± 1.18	11.98 ± 0.88	-3.9	179	1.3×10^{-4}

Table S4. Linear effects of *Year* on standardized trait values for phenotypes measured in both years of the study. Bolded significant effects after Bonferroni correction for 33 models ($p < 0.0015$).

	Phenotype	*n*	β	SE	p	Adjusted R^2
Capture	**RMR**	99	**0.52**	**0.09**	**3.0×10^{-8}**	0.27
	M_{sum}	86	**0.57**	**0.09**	**8.9×10^{-9}**	0.32
	Tarsus Length	106	-0.17	0.10	0.08	0.02
	M_b	106	0.04	0.10	0.69	-0.01
	M_{lean}	98	0.03	0.10	0.80	-0.01
	M_{fat}	98	-0.10	0.10	0.24	0.00
	M_{fH2O}	98	0.02	0.10	0.82	-0.01
Pre-acclimation	**RMR**	106	**0.54**	**0.08**	**1.8×10^{-9}**	0.29
	M_{sum}	102	-0.11	0.10	0.27	0.00
	M_b	106	**0.42**	**0.09**	**6.4×10^{-6}**	0.17
	M_{lean}	105	**-0.59**	**0.08**	**2.1×10^{-11}**	0.35
	M_{fat}	105	**0.75**	**0.06**	**$< 2 \times 10^{-16}$**	0.56
	M_{fH2O}	105	-0.09	0.10	0.37	0.00
	Hemoglobin	106	**0.41**	**0.09**	**9.4×10^{-6}**	0.16
	Hematocrit	100	0.16	0.10	0.10	0.02
Post-acclimation	RMR	105	0.11	0.10	0.25	0.00
	M_{sum}	105	0.15	0.10	0.13	0.01
	M_b	106	-0.07	0.10	0.50	-0.01
	M_{lean}	106	-0.20	0.10	0.04	0.03
	M_{fat}	106	0.03	0.10	0.77	-0.01
	M_{fH2O}	106	0.14	0.10	0.14	0.01
	Hemoglobin	106	-0.10	0.10	0.31	0.00
	Hematocrit	105	-0.25	0.09	0.01	0.05
	Erythrocyte count	58	-0.08	0.17	0.63	-0.01
	Heart mass	106	**0.31**	**0.09**	**1.1×10^{-3}**	0.09
	Lung mass	106	0.13	0.10	0.17	0.01
	Liver mass	106	0.24	0.09	0.01	0.05
	Kidney mass	104	0.16	0.10	0.10	0.02
	CPT	95	0.18	0.10	0.08	0.02
	HOAD	95	0.08	0.10	0.44	0.00
	CS	95	-0.03	0.10	0.76	-0.01
	Plasma TRIG	61	0.23	0.10	0.03	0.06
	Plasma glycerol	64	-0.11	0.13	0.39	0.00

Table S5. Pearson's correlation coefficients for all pairwise trait associations at the capture.

Variable 1	Variable 2	*r*	p
M_{sum}	RMR	0.38	4.1×10^{-4}
M_{sum}	Tarsus	0.12	0.25
RMR	Tarsus	0.09	0.40
M_{sum}	Mass	0.36	6.3×10^{-4}
RMR	Mass	0.54	1.3×10^{-8}
Tarsus	Mass	0.49	1.1×10^{-7}
M_{sum}	Lean	0.28	0.01
RMR	Lean	0.44	1.1×10^{-5}
Tarsus	Lean	0.52	3.1×10^{-8}
Mass	Lean	0.96	8.1×10^{-57}
M_{sum}	Fat	0.05	0.66
RMR	Fat	0.15	0.16
Tarsus	Fat	0.07	0.51
Mass	Fat	0.29	3.5×10^{-3}
Lean	Fat	0.24	0.02

Table S6. Pearson's correlation coefficients for all pairwise trait associations at the end of the adjustment period (pre-acclimation).

Variable 1	Variable 2	*r*	p
M_{sum}	RMR	0.41	2.0×10^{-5}
M_{sum}	Tarsus	-0.17	0.08
RMR	Tarsus	-0.01	0.92
M_{sum}	Mass	0.26	0.01
RMR	Mass	0.46	9.5×10^{-7}
Tarsus	Mass	0.14	0.15
Msum	Lean	-0.31	1.4×10^{-3}
RMR	Lean	-0.23	0.02
Tarsus	Lean	0.36	1.5×10^{-4}
Mass	Lean	-0.04	0.70
M_{sum}	Fat	0.45	2.1×10^{-6}
RMR	Fat	0.52	1.8×10^{-8}
Tarsus	Fat	-0.12	0.22
Mass	Fat	0.83	2.0×10^{-27}
Lean	Fat	-0.52	1.1×10^{-8}
M_{sum}	Hemoglobin	0.27	6.9×10^{-3}
RMR	Hemoglobin	0.32	9.8×10^{-4}
Tarsus	Hemoglobin	0.02	0.86
Mass	Hemoglobin	0.33	5.2×10^{-4}
Lean	Hemoglobin	-0.23	0.02
Fat	Hemoglobin	0.40	1.92×10^{-5}
M_{sum}	Hematocrit	0.03	0.76
RMR	Hematocrit	0.11	0.28
Tarsus	Hematocrit	0.13	0.19
Mass	Hematocrit	0.25	0.01
Lean	Hematocrit	-0.14	0.16
Fat	Hematocrit	0.26	0.01
Hemoglobin	Hematocrit	0.62	7.4×10^{-12}

Table S7. Pearson's correlation coefficients for all pairwise trait associations post-acclimation.

Variable 1	Variable 2	*r*	p
M_{sum}	RMR	0.27	0.01
M_{sum}	Tarsus	-0.10	0.30
RMR	Tarsus	0.08	0.41
Msum	Mass	-0.02	0.84
RMR	Mass	0.25	0.01
Tarsus	Mass	0.26	0.01
M_{sum}	Lean	-0.05	0.63
RMR	Lean	0.16	0.09
Tarsus	Lean	0.42	5.9×10^{-6}
M_{sum}	Lean	0.39	4.4×10^{-5}
M_{sum}	Muscle	0.27	0.06
RMR	Muscle	0.22	0.12
Tarsus	Muscle	0.43	1.5×10^{-3}
Mass	Muscle	0.18	0.20
Lean	Muscle	0.82	3.3×10^{-13}
M_{sum}	Fiber_density	0.20	0.15
RMR	Fiber_density	0.18	0.20
Tarsus	Fiber_density	0.27	0.05
Mass	Fiber_density	0.08	0.59
Lean	Fiber_density	0.11	0.44
Muscle	Fiber_density	0.15	0.30
M_{sum}	Fat	-0.04	0.72
RMR	Fat	0.13	0.17
Tarsus	Fat	-0.03	0.75
Mass	Fat	0.83	4.6×10^{-28}
Lean	Fat	-0.14	0.16
Muscle	Fat	-0.17	0.23
Fiber_density	Fat	0.01	0.97
M_{sum}	Gizzard	0.08	0.57
RMR	Gizzard	-0.04	0.79
Tarsus	Gizzard	-0.09	0.51
M_{sum}	Gizzard	-0.07	0.61
Lean	Gizzard	0.20	0.16
Muscle	Gizzard	-0.26	0.07
Fiber_density	Gizzard	-0.16	0.28
Fat	Gizzard	-0.20	0.16
M_{sum}	Intestine	0.24	0.09

RMR	Intestine	0.01	0.97
Tarsus	Intestine	0.06	0.70
Mass	Intestine	-0.18	0.22
Lean	Intestine	0.40	3.9×10^{-3}
Muscle	Intestine	-0.10	0.50
Fiber_density	Intestine	0.09	0.54
Fat	Intestine	-0.39	0.01
Gizzard	Intestine	0.62	1.4×10^{-6}
M_{sum}	Pancreas	0.17	0.23
RMR	Pancreas	-0.01	0.94
Tarsus	Pancreas	-0.19	0.17
Mass	Pancreas	-0.03	0.82
Lean	Pancreas	0.17	0.24
Muscle	Pancreas	-0.11	0.45
Fiber_density	Pancreas	-0.18	0.22
Fat	Pancreas	-0.08	0.58
Gizzard	Pancreas	0.42	2.2×10^{-3}
Intestine	Pancreas	0.48	3.4×10^{-4}
M_{sum}	Liver	0.24	0.01
RMR	Liver	0.23	0.02
Tarsus	Liver	-0.03	0.76
Mass	Liver	0.53	6.4×10^{-9}
Lean	Liver	0.14	0.14
Muscle	Liver	-0.51	1.5×10^{-4}
Fiber_density	Liver	-0.04	0.79
Fat	Liver	0.44	2.4×10^{-6}
Gizzard	Liver	0.31	0.03
Intestine	Liver	0.32	0.02
Pancreas	Liver	0.24	0.09
M_{sum}	Kidney	0.17	0.08
RMR	Kidney	0.15	0.14
Tarsus	Kidney	-0.02	0.87
Mass	Kidney	0.21	0.03
Lean	Kidney	0.33	7.3×10^{-4}
Muscle	Kidney	0.21	0.14
Fiber_density	Kidney	-0.26	0.07
Fat	Kidney	0.07	0.49
Gizzard	Kidney	0.09	0.54
Intestine	Kidney	0.28	0.04
Pancreas	Kidney	0.13	0.37

Liver	Kidney	0.25	0.01
M_{sum}	Glycerol	-0.08	0.53
RMR	Glycerol	0.02	0.89
Tarsus	Glycerol	0.08	0.53
Mass	Glycerol	-0.12	0.34
Lean	Glycerol	0.05	0.69
Muscle	Glycerol	0.24	0.17
Fiber_density	Glycerol	0.00	0.98
Fat	Glycerol	-0.17	0.18
Gizzard	Glycerol	0.00	0.99
Intestine	Glycerol	0.10	0.56
Pancreas	Glycerol	-0.34	0.04
Liver	Glycerol	-0.09	0.50
Kidney	Glycerol	0.10	0.42
M_{sum}	TRIG	0.26	0.04
RMR	TRIG	-0.09	0.48
Tarsus	TRIG	-0.14	0.29
Mass	TRIG	-0.08	0.57
Lean	TRIG	-0.18	0.16
Muscle	TRIG	-0.17	0.33
Fiber_density	TRIG	-0.12	0.48
Fat	TRIG	0.09	0.49
Gizzard	TRIG	0.19	0.27
Intestine	TRIG	0.45	0.01
Pancreas	TRIG	0.20	0.26
Liver	TRIG	0.23	0.07
Kidney	TRIG	0.28	0.03
Glycerol	TRIG	0.04	0.78
M_{sum}	Heart	0.35	2.1×10^{-4}
RMR	Heart	0.15	0.13
Tarsus	Heart	0.12	0.20
Mass	Heart	0.03	0.78
Lean	Heart	0.35	1.9×10^{-4}
Muscle	Heart	0.10	0.50
Fiber_density	Heart	-0.16	0.27
Fat	Heart	-0.20	0.04
Gizzard	Heart	0.43	1.8×10^{-3}
Intestine	Heart	0.42	2.3×10^{-3}
Pancreas	Heart	0.28	0.04
Liver	Heart	0.16	0.10

Kidney	Heart	0.31	1.6×10^{-3}
Glycerol	Heart	0.08	0.55
TRIG	Heart	0.08	0.52
M_{sum}	Lung	0.12	0.21
RMR	Lung	0.09	0.36
Tarsus	Lung	0.11	0.25
Mass	Lung	0.21	0.03
Lean	Lung	0.11	0.27
Muscle	Lung	-0.10	0.49
Fiber_density	Lung	0.16	0.26
Fat	Lung	0.14	0.15
Gizzard	Lung	0.24	0.09
Intestine	Lung	0.37	0.01
Pancreas	Lung	-0.15	0.30
Liver	Lung	0.31	1.0×10^{-3}
Kidney	Lung	0.12	0.22
Glycerol	Lung	0.17	0.18
TRIG	Lung	0.11	0.41
Heart	Lung	0.19	0.05
M_{sum}	Hemoglobin	-0.02	0.85
RMR	Hemoglobin	0.02	0.81
Tarsus	Hemoglobin	-0.02	0.81
Mass	Hemoglobin	0.05	0.61
Lean	Hemoglobin	0.05	0.59
Muscle	Hemoglobin	0.07	0.60
Fiber_density	Hemoglobin	0.14	0.33
Fat	Hemoglobin	0.08	0.43
Gizzard	Hemoglobin	0.06	0.65
Intestine	Hemoglobin	0.17	0.24
Pancreas	Hemoglobin	0.09	0.53
Liver	Hemoglobin	0.04	0.69
Kidney	Hemoglobin	0.12	0.23
Glycerol	Hemoglobin	0.02	0.85
TRIG	Hemoglobin	-0.02	0.90
Heart	Hemoglobin	0.01	0.91
Lung	Hemoglobin	-0.09	0.35
M_{sum}	Hematocrit	-0.16	0.10
RMR	Hematocrit	0.02	0.84
Tarsus	Hematocrit	0.08	0.39
Mass	Hematocrit	0.08	0.43

Lean	Hematocrit	0.08	0.43
Muscle	Hematocrit	0.04	0.78
Fiber_density	Hematocrit	0.10	0.49
Fat	Hematocrit	0.10	0.31
Gizzard	Hematocrit	0.12	0.41
Intestine	Hematocrit	0.22	0.12
Pancreas	Hematocrit	0.18	0.22
Liver	Hematocrit	0.00	0.97
Kidney	Hematocrit	0.14	0.15
Glycerol	Hematocrit	0.06	0.64
TRIG	Hematocrit	0.02	0.90
Heart	Hematocrit	0.00	1.00
Lung	Hematocrit	-0.01	0.89
Hemoglobin	Hematocrit	0.81	0.00
M_{sum}	RBC	-0.08	0.57
RMR	RBC	-0.11	0.41
Tarsus	RBC	-0.03	0.80
Mass	RBC	-0.11	0.42
Lean	RBC	-0.04	0.77
Muscle	RBC	0.09	0.55
Fiber_density	RBC	0.03	0.86
Fat	RBC	-0.15	0.27
Gizzard	RBC	-0.05	0.74
Intestine	RBC	-0.09	0.57
Pancreas	RBC	-0.14	0.34
Liver	RBC	-0.10	0.46
Kidney	RBC	-0.04	0.78
Glycerol	RBC	-0.07	0.69
TRIG	RBC	-0.06	0.73
Heart	RBC	-0.07	0.60
Lung	RBC	0.12	0.36
Hemoglobin	RBC	0.23	0.08
Hematocrit	RBC	0.20	0.13
M_{sum}	Capillarity	0.32	0.02
RMR	Capillarity	0.15	0.29
Tarsus	Capillarity	0.28	0.05
Mass	Capillarity	0.05	0.74
Lean	Capillarity	0.15	0.29
Muscle	Capillarity	0.16	0.26
Fiber_density	Capillarity	0.74	6.6×10^{-10}

Fat	Capillarity	-0.06	0.68
Gizzard	Capillarity	-0.03	0.81
Intestine	Capillarity	0.14	0.32
Pancreas	Capillarity	-0.21	0.14
Liver	Capillarity	-0.05	0.75
Kidney	Capillarity	-0.24	0.09
Glycerol	Capillarity	0.03	0.86
TRIG	Capillarity	-0.11	0.54
Heart	Capillarity	-0.21	0.15
Lung	Capillarity	0.17	0.23
Hemoglobin	Capillarity	0.10	0.48
Hematocrit	Capillarity	0.14	0.32
RBC	Capillarity	0.12	0.43
M_{sum}	CPT	0.16	0.11
RMR	CPT	0.08	0.46
Tarsus	CPT	0.10	0.35
Mass	CPT	0.27	0.01
Lean	CPT	-0.07	0.50
Muscle	CPT	-0.20	0.16
Fiber_density	CPT	0.24	0.09
Fat	CPT	0.30	2.7×10^{-3}
Gizzard	CPT	0.20	0.16
Intestine	CPT	0.21	0.14
Pancreas	CPT	-0.07	0.63
Liver	CPT	0.32	1.6×10^{-3}
Kidney	CPT	0.01	0.95
Glycerol	CPT	0.00	0.98
TRIG	CPT	0.30	0.02
Heart	CPT	0.15	0.14
Lung	CPT	0.29	0.01
Hemoglobin	CPT	0.14	0.19
Hematocrit	CPT	0.06	0.58
RBC	CPT	0.19	0.16
Capillarity	CPT	0.18	0.20
M_{sum}	HOAD	0.06	0.59
RMR	HOAD	0.07	0.50
Tarsus	HOAD	-0.12	0.24
Mass	HOAD	-0.11	0.31
Lean	HOAD	-0.09	0.38
Muscle	HOAD	-0.01	0.96

Fiber_density	HOAD	0.13	0.38
Fat	HOAD	-0.07	0.52
Gizzard	HOAD	-0.07	0.62
Intestine	HOAD	-0.12	0.40
Pancreas	HOAD	-0.18	0.20
Liver	HOAD	-0.12	0.26
Kidney	HOAD	0.08	0.44
Glycerol	HOAD	-0.03	0.80
TRIG	HOAD	-0.16	0.22
Heart	HOAD	-0.06	0.58
Lung	HOAD	0.01	0.94
Hemoglobin	HOAD	0.02	0.85
Hematocrit	HOAD	-0.07	0.51
RBC	HOAD	-0.05	0.69
Capillarity	HOAD	-0.06	0.69
CPT	HOAD	0.13	0.21
M_{sum}	CS	-0.01	0.91
RMR	CS	0.00	0.99
Tarsus	CS	0.03	0.76
Mass	CS	-0.05	0.63
Lean	CS	0.03	0.74
Muscle	CS	-0.06	0.66
Fiber_density	CS	0.11	0.42
Fat	CS	-0.10	0.36
Gizzard	CS	0.08	0.58
Intestine	CS	-0.02	0.90
Pancreas	CS	-0.12	0.38
Liver	CS	-0.23	0.02
Kidney	CS	-0.30	2.9×10^{-3}
Glycerol	CS	0.09	0.50
TRIG	CS	-0.01	0.94
Heart	CS	0.18	0.08
Lung	CS	0.10	0.36
Hemoglobin	CS	-0.21	0.05
Hematocrit	CS	-0.17	0.11
RBC	CS	0.24	0.07
Capillarity	CS	0.05	0.73
CPT	CS	0.11	0.31
HOAD	CS	-0.12	0.26

The environmental drivers of variation in *Junco* physiological flexibility

Maria Stager, Nathan R. Senner, David L. Swanson, and Zachary A. Cheviron

ABSTRACT

Phenotypic flexibility allows individuals to reversibly modify their trait values to match fluctuating environmental conditions across their lifetime. Theory predicts that the relative degree of flexibility exhibited by an individual will positively correlate with the environmental heterogeneity it experiences yet there are few empirical examples to support this. To help uncover the mechanisms driving geographic variation in physiological flexibility, we integrated assays of population genetic variation with whole-organism measures of thermogenic performance and indices of environmental heterogeneity for individuals in the genus *Junco*. We combined measures of thermogenic capacity for close to 300 individuals collected across the United States, more than 28,000 single nucleotide polymorphisms genotyped in 192 individuals, and laboratory acclimation experiments replicated on five *Junco* populations. We found that across their range, juncos: (1) differed in their thermal performance responses to temperature variation *in situ*; (2) exhibit intra-specific variation in their degree of thermogenic flexibility that correlates with the heterogeneity of their native thermal environment; and (3) harbor genetic variation that also correlates with temperature heterogeneity. Together, these results suggest that thermogenic flexibility may play a key role in local adaptation in this broadly distributed lineage.

INTRODUCTION

Phenotypic plasticity — the ability of a single genotype to produce multiple trait values in response to an environmental cue — can be important for colonizing and persisting in novel environments (Price et al. 2003; Ghalambor et al. 2007; Crispo 2008). As a result, the role of plasticity in adaptation to environmental variation has received significant attention (e.g., Tienderen 1991; West-Eberhard 2003; Scheiner 2013). These studies have documented standing genetic variation in plastic responses (Pigliucci 2005), and that plasticity can evolve in response to natural selection (Nussey et al. 2005). Because adaptive plasticity should increase fitness in variable environments, theory predicts that the magnitude of plasticity that individuals exhibit should positively correlate with the amount of environmental heterogeneity they experience (Moran 1992; Sultan and Spencer 2002; Ernande and Dieckmann 2004).

Empirical evaluations of this prediction provide conflicting levels of support for it, but most have focused on traits that are developmentally plastic (i.e., those that undergo environmentally-induced but irreversible changes to a trait value). For instance, morphological plasticity varies with diet breadth among ecotypes of threespine stickleback (Day et al. 1994). Similarly, plasticity in development time positively correlates with spatial variation in the pool-drying regimes in the common frog (*Rana temporana*; Lind and Johansson 2007). Analagous patterns have been shown in plants as well. In a bindweed (*Convolvulus chilensis*), plasticity in leaf morphology and functional traits varies with interannual variation in rainfall (Gianoli and González-Teuber 2005). Conversely, plasticity for thermal tolerance limits is not associated with latitudinal or thermal seasonality in *Drosophila* (Overgaard et al. 2011; van Heerwaarden et al. 2014; Sørensen et al. 2016). Disparities among studies may arise from differences in the relationship between the temporal scale of environmental heterogeneity and the time period over

which a trait value may be determined, thus traits that can be modified repeatedly may respond to intra-annual environmental heterogeneity more strongly.

Unlike developmental plasticity, phenotypic flexibility — the ability to reversibly modify trait values — provides repeated opportunities to match phenotypes to environmental change across an individual's lifetime, especially in long-lived organisms (Piersma and Drent 2003; Piersma and van Gils 2011). Flexibility is predicted to evolve in environments characterized by frequent and predictable environmental variation (Botero et al. 2015). This flexibility is ubiquitous to morphological, physiological, and behavioral traits and can represent an adaptive acclimatization response. Determining the causes and consequences of variation in flexibility among individuals is therefore crucial to our understanding of adaptation, evolution, and species' resilience to environmental change. Yet few empirical tests exist that explore whether the degree of flexibility exhibited among populations corresponds to environmental heterogeneity (but see Cavieres and Sabat 2008; Fangue et al. 2009).

If environmental heterogeneity structures variation in adaptive plasticity/flexibility across a species' range, we would therefore also expect to find that environmental heterogeneity structures genetic variation as well. This is because the local selective regime is influenced by rates of gene flow among habitats, which can be determined by spatial features of the environment (Lenormand 2002; Kawecki and Ebert 2004). However, to date, no study has accounted for population genetic variation while simultaneously quantifying relationships among plasticity/flexibility and environmental heterogeneity. Failure to account for non-independence among populations (due to shared common ancestry and ongoing gene flow) when analyzing intraspecific patterns of phenotypic variation can obscure true relationships among variables of interest (Stone et al. 2011). Strong tests of this prediction will therefore include multiple populations from across an environmental continuum within a population genetic framework.

To uncover the drivers of geographic variation in phenotypic flexibility, we investigated the flexible capacity of a key physiological trait in a temperate songbird, the Dark-eyed Junco (*Junco hyemalis*). Juncos are particularly well suited to investigations of phenotypic flexibility due to the extensive phenotypic variation they exhibit and the broad range of environments they occupy (Nolan, Jr. et al. 2002). The *J. hyemalis* lineage is comprised of five distinct morphotypes and 14 subspecies that inhabit a variety of habitats (Figure 1) and exhibit conspicuous differences in life history, migratory tendency, physiology, size, song, plumage, and behavior (Miller 1941; Nolan, Jr. et al. 2002; Ketterson and Atwell 2016). This diversity is thought have arisen since the most recent glacial maxima when *J. hyemalis* diverged from *J. phaeonotus fulvescens* of southern Mexico and subsequently expanded its range across North America (Milá et al. 2007; Friis et al. 2016). While environmental factors partition genetic variation within a subset of *J. hyemalis* taxa (Friis et al. 2018), the major *J. hyemalis* morphotypes are not strongly differentiated from one another (Friis et al. 2016) suggesting that considerable phenotypic diversity persists in the face of high rates of gene flow. The role that environmental conditions thus play in driving the diversification of this lineage remain unclear.

Juncos have also been the subject of intense physiological study. Many *J. hyemalis* groups winter at temperate latitudes, and temperate environments place a premium on endogenous heat production in small homeothermic endotherms to maintain a relatively constant body temperature (Mcnab 2002). As a result, resident birds — including juncos (Swanson 1990a) — increase their thermogenic capacity (the ability to generate heat; quantified as the peak metabolic rate under cold exposure, M_{sum}) in winter via a number of physiological modifications that enhance shivering thermogenesis (Swanson 2010). This heightened thermogenic capacity is

associated with a reduced risk of hypothermia for juncos in the cold (Stager et al. 2020), and a failure to achieve adequate thermogenic output can have dire consequences for organismal fitness (Hayes and O'Connor 1999; Petit et al. 2017). Increases in thermogenic performance are also accompanied by changes occurring at lower hierarchical levels of biological organization (Swanson 1990b; Stager and Cheviron 2020; Chapter 3). Thus, a higher thermogenic capacity may be energetically costly to maintain due to the additional metabolic machinery required (Vezina et al. 2020). Phenotypic flexibility in thermogenic capacity could therefore help mediate a balance between thermoregulation and its associated maintenance costs in response to fluctuating selective pressures (Swanson 2010). Accordingly, laboratory acclimations in *J. h. hyemalis* and *J. h. montanus* have shown rapid changes in thermogenic capacity in response to changes in temperature (Swanson et al. 2014; Stager et al. 2020). Nonetheless, it remains unclear whether an individual's capacity for thermogenic flexibility is influenced by the degree of thermal variability it experiences throughout the year.

To explore the factors influencing variation in thermogenic flexibility, we drew upon natural variation that exists across the *Junco* distribution. We first surveyed *in situ* geographic variation in *Junco* thermogenic capacity to determine which environmental indices structure variation in this trait. We then characterized fine-scale, range-wide population genetic structure within the *Junco* genus to determine whether it is influenced by the same climatic indices. Finally, we performed a laboratory acclimation experiments on five *Junco* populations that differ in their annual thermal regimes to test whether environmental heterogeneity predicts the degree of thermogenic flexibility (Figure S1). This approach allows us to combine measures of physiological flexibility with indices of climatic variation while controlling for nonindependence among populations. We predicted that junco populations that experience greater seasonal temperature variation would exhibit higher thermogenic flexibility than those from more thermally stable regions. By combining these approaches, our results shed light on the ecological conditions that promote the evolution of increased flexibility and address long-standing hypotheses in the field of evolutionary biology.

METHODS

In situ data and analysis

In situ sampling

We captured juncos by mist net at sites in Arizona, Colorado, Illinois, Montana, New Mexico, New York, South Dakota, and Wyoming, spanning 16° in latitude and 37° in longitude (Figure 1; Table S1). We classified individuals into known morphotypes based on plumage (Gray-headed, Oregon, Pink-sided, Slate-colored, and Yellow-eyed). These morphs have distinct breeding distributions: Gray-headed Juncos (*J. hyemalis caniceps*) breed in Colorado, Nevada, New Mexico and Utah; Oregon Juncos (*J. h. montanus, J. h. oreganus*, *J. h. pinosus, J. h. shufeldti,* and *J. h. thurberi*) breed in the western United States from southern California to southcentral Alaska and as far east as western Montana; Pink-sided Juncos (*J. h. mearnsi*) breed in eastern Montana, Wyoming, and Idaho; Slate-colored Juncos (*J. h. hyemalis*) breed across northern North America from Alaska to Nova Scotia and south through the Great Lakes region; and Yellow-eyed Juncos (*J. phaeonotus palliatus*) breed on disjunct mountain tops in southeastern Arizona, southwestern New Mexico, and northern Mexico (Miller 1941; Nolan, Jr. et al. 2002; Sullivan 2018; Figure 1). However, the wintering ranges overlap for many morphs.

In situ metabolic assays

We assayed M_{sum} of captured birds using open-flow respirometry near the site of capture. All measurements were made within 48 h of capture to avoid the effects of captivity on metabolic rates, though most were completed within 24 h. Body mass (M_b) was quantified before each measurement began. M_{sum} trials were conducted during the birds' light cycle. A single individual was placed in a metabolic chamber in a dark, temperature-controlled environment. We pumped dry heliox gas (21% O_2, 79% He) first through copper coils (for cooling) and then through the animal's chamber at 750 ml/min (Sable Systems Mass Flow Meter). We subsampled the outflow current, dried it (Drierite), scrubbed it of CO_2 using ascarite, and dried it again before quantifying the O_2 concentration using a FoxBox (Sable Systems). Trials were conducted using static cold exposure (-5°C) for CO, IL, MT, NM, NY, and WY birds and sliding cold exposure (starting at -8°C) for AZ and SD birds; however, both methods have been shown to produce similar estimates of M_{sum} (Swanson et al. 1996). Trials ended after 1 h or a plateau in O_2 consumption was reached, whichever occurred first. We also sampled a blank chamber before and after trials to account for potential fluctuations in baseline, ambient air.

We used custom R scripts to quantify M_{sum} as the highest O_2 consumption averaged over a 5-min period. We discarded measures characterized by large drift in baseline O_2 (owing to ambient temperature fluctuations affecting the Fox Box) or inconsistent flow rates resulting in a total sample size of $n = 292$ individuals. Following measurements, birds were subject to different fates: either released with a USGS band (SD and AZ), exposed to acclimation experiments (MT; Stager et al. 2020), or immediately euthanized and deposited in museums (all other locations). Metabolic data from SD have been previously published (Swanson et al. 2012) and data from MT are included in Chapter 3.

Environmental data for in situ sampling sites

To account for an individual's recent acclimatization history, we retrieved weather data associated with each collection site (rounded to the nearest tenth of a degree latitude/longitude) from the DayMet dataset using the R package *daymetr* (Hufkens et al. 2018). This dataset is composed of daily weather parameters estimates derived from interpolation and extrapolation from meteorological observations for 1km x 1km gridded surfaces over North America (Thornton et al. 2016). We downloaded daily estimates of minimum temperature (T_{min}), maximum temperature (T_{max}), precipitation (prcp), water vapor pressure (wvp), and daylength (dayl) for the 7 d prior to each individual's capture date. We additionally calculated daily temperature range (T_{d_range}) as $T_{max} - T_{min}$. We selected a conservative potential acclimatization window of 7 d because we do not know how long juncos were present at a site before sampling occurred given their migratory nature. We also retrieved elevation (elev) for each site using the package *googleway* (Cooley et al. 2018).

Analyses for in situ data

All analyses were conducted in R version 4.0.2 (R Core Team 2018). To determine whether junco M_{sum} varied with environmental variation, we constructed seven linear models with M_b, morphotype (morph), and a single environmental variable (T_{min}, T_{max}, T_{range}, prcp, dayl, wvp, or elev) as main effects. We first standardized continuous predictor variables according to Gelman (2008) using the package *arm*. We used AICc to evaluate model fits among environmental variables and with that of a null model (including only M_b and morph as predictors) at $\Delta AICc > 2$. As an indicator of differences in flexibility, for the best model we

additionally tested for an interaction between environment and morph to determine if populations differed in their response to environmental cues. We reran the model with each morph as the reference and summarized results across these five variants.

Population genetic data

Sampling, sequencing, and SNP generation

For phylogeographic reconstruction, we obtained muscle tissue samples (n = 192) from museum specimens collected across the breeding distribution of all *Junco* species and subspecies (Figure 1). This included 2-30 individuals per taxonomic unit sampled from 94 geographic localities representing the majority of U.S. counties, Canadian provinces, and Mexican states for which tissue samples exist (Table S2). We then employed restriction-site-associated DNA (RAD)-sequencing, which offers a reduced representation of the genome that can be mined for thousands of single-nucleotide polymorphisms (SNPs) among individuals (Baird et al. 2008; Davey and Blaxter 2010).

We extracted whole genomic DNA from each sample using a Qiagen DNeasy Blood and Tissue extraction Kit and prepared RAD-libraries according to (Parchman et al. 2012). Briefly, we digested whole genomic DNA with two restriction enzymes (EcoRI and Mse1), ligated adaptor sequences with unique barcodes for each individual, performed PCR amplification, and then performed automated size selection of 300–400 bp fragments (Sage Science Blue Pippen). We split paired geographic samples between the two libraries such that all taxa were represented in each library of 96, pooled individuals. Libraries were sequenced on separate flow-cell lanes of an Illumina HiSeq 4000 at UC Berkeley's V.C. Genomics Sequencing Lab. This resulted in over 300 million, 100-nt single-end reads per lane with a mean of 2.05 million reads per individual. We removed 6 individuals that failed to sequence (< 100,000 reads/individual, comprising 5 *J. hyemalis* and 1 *J. insularis*).

We demultiplexed reads, removed inline barcodes, and performed quality filtering (removed Phred score < 10) using *process_radtags* in STACKS ver. 2.1 (Catchen et al. 2011). This resulted in final reads of μ = 92 bp in length. We used *bwa mem* (Li 2013) to align reads to the *J. h. carolinensis* genome (Friis et al. 2018), which we downloaded from NCBI (Accession GCA_003829775.1). An average of 91% of reads mapped and mapping success did not differ among *Junco* species. We then executed the STACKS pipeline to call SNPs using the function *ref_map.pl* and exported the resulting 2,904,961 SNPs in vcf format.

We filtered the dataset using *vcftools* (Danecek et al. 2011) in two ways. First, we removed sites with mean depth of coverage across all individuals < 4 (*--min-meanDP*) and > 50 (*--max-meanDP*), minimum minor allele frequency *(--min_maf*) < 0.02, > 50% missing data (*--max-missing*), Hardy-Weinburg equilibrium < 0.0001 *(--hwe*), and indels *(--remove-indels*). We then removed 9 individuals with > 60% missing data (*--remove*). Finally, we removed sites with > 5% missing data (*--max-missing*) resulting in 29,806 biallelic SNPs across 177 individuals for our full dataset. Second, we excluded 13 individuals from 4 divergent lineages (*J. vulcani, J. p. alticola, J. p. bairdi, and J. p. fulcescens*; see below) and then repeated the same filtering steps, resulting in 32,818 biallelic SNPs. We exported both datasets (referred to as full and subset, respectively) in plink.raw format for downstream analyses.

Population genetic structure

We visualized population genetic structure using a principal component analysis (PCA) on the full SNP dataset with the R package *adegenet* ver 2.1.1 (Jombart et al. 2020). Because

PCA requires no missing data, we first imputed missing SNP data using the most common genotype for n = 139,744 sites (2.6% of total sites). We assigned taxonomy according to the classification provided by the lending museums (likely based on morphology and geographic origin). Unsurprisingly, the pattern of clustering reflected divergence of northern junco forms (*J. hyemalis, J. insularis*, and northern *J. phaeonotus*) from lineages previously identified to be "ancestral" (*J. vulcani, J. p. alticola, J. p. bairdi, J. p. fulvescens*; Friis et al. 2016). We therefore excluded these taxa and performed the PCA anew on our subset data. We again imputed n = 147,962 missing sites (2.7% of total sites). We summarized variation for each individual as PC scores from the first two axes.

Genotype-environment association analyses

To determine if environmental variation structures genetic variation across *Juncos*, we employed our subset SNP dataset in a redundancy analysis (RDA) following a vignette provided in Forester et al. (2018). RDA is a multivariate ordination technique that has been used to identify multiple candidate loci and several environmental predictors simultaneously (Forester et al. 2016; Forester et al. 2018). Because RDA does not tolerate missing data, we again used the imputed dataset.

We downloaded interpolated monthly climate data corresponding to the site of origin for each specimen from WorldClim (Hijmans et al. 2005) at a resolution of 2.5' using the R package *raster* (Hijmans et al. 2020). This included all 19 Bioclim variables, but we excluded highly correlated variables ($r \geq 0.70$) resulting in 7 retained variables. We used these 7 climatic variables as predictors in an RDA executed with the package *vegan* (Oksanen et al. 2019). We removed one additional variable with variance inflation factor > 5 to reduce multicollinearity such that the final model contained mean diurnal temperature range (BIO2), maximum temperature of the warmest month (BIO5), temperature annual range (BIO7), mean temperature of the wettest quarter (BIO8), annual precipitation (BIO12), and precipitation seasonality (BIO15). We assessed the significance of the full model at $p \leq 0.05$ after 999 permutations of the genotype data and retained significant constrained axes at $p \leq 0.05$ after 99 permutations of the genotype data. We estimated the total proportion of genomic variation explained by each climatic variable using variance partitioning as implemented in *vegan*. We then identified candidate SNPs for environmental adaptation as those outside of a 3 standard deviation cutoff from the mean loading and characterized each candidate SNP by the predictor variable with which it had the strongest correlation. We additionally performed a partial RDA in which we accounted for background population structure by conditioning the relationship between population genetic variation and the 6 climatic variables on the PC scores from the first two axes of our PCA and repeated the RDA procedure.

Acclimation experiments

Population sampling for acclimation experiments

Our ability to connect *Junco* populations to native climatic regimes is restricted by our limited knowledge of junco movements across the year. For our acclimation treatments, we therefore focused on populations that likely remain resident to one narrow geographic area in order to reliably reconstruct climatic histories. We combined information gained from a literature search, eBird sightings, and expert opinion (*pers. comm.* David Swanson and Tom Martin) to identify five focal populations for phenotypic sampling that (1) were likely to be non-migratory, (2) represented different morphological subspecies, and (3) maximized variation in annual

temperature range within the United States. These populations include the White-winged Junco (*J. h. aikeni*) of the Black Hills, a coastal population of Oregon Junco (*J. h. shufeldti*), a highland population of Red-backed Junco (*J. h. dorsalis*), a sky island population of Yellow-eyed Junco (*J. p. palliatus*), and a well-studied, urban population of Oregon Junco (*J. h. thurberi*; Yeh and Price 2004). However, it is possible that some of these populations exhibit seasonal, altitudinal migrations within their geographic area of residence, e.g., *J. p. palliatus* (Lundblad and Conway 2020).

We captured ≤ 25 individuals from each focal population. Capture periods differed for each population in order to increase the likelihood that individuals were resident year-round, as well as due to time and permitting constraints. For instance, one partially migratory population (*J. h. aikeni*) with distinct morphological features was caught in the winter to ensure that the individuals used were non-migratory. The other four populations, which bred in areas where other, morphologically similar juncos over-winter, were captured in the breeding season when other subspecies were not present. Specifically, *J. h. shufeldti* (n = 20) were captured 14-15 July 2018 in Coos and Douglas Counties, OR; *J. p. palliatus* (n = 24) were captured 27 July 2018 in Cochise County, AZ; *J. h. dorsalis* (n = 25) were captured 30-31 July 2018 in Coconino County, AZ; *J. h. aikeni* (n = 15) were captured 6-9 March 2019 in Lawrence County, SD; and *J. h. thurberi* (n = 20) were captured 22-26 July 2019 in San Diego County, CA.

Acclimation treatments

Within days of capture, we ground-transported all birds to facilities at the University of Montana where birds were housed individually under common conditions (23°C with 12 h dark: 12 h light) for ≥ 8 weeks (μ = 62 d, range = 56-70 d). We have previously determined that a period of 6 wk is sufficient to reduce variation in metabolic traits among individuals (Chapter 3). Following this adjustment period, we assayed M_{sum} (see below). We allowed birds ~24 h to recover and then randomly assigned individuals from each population into treatment groups and exposed them to either cold (3°C) or control (23°C) temperatures. Treatments lasted 21 d in duration. Constant 12 h dark: 12 h light days were maintained for the duration of the experiment, and food and water were supplied *ad libitum*. The diet consisted of a 2:1 ratio by weight of white millet and black oil sunflower seed, supplemented with ground dog food, live mealworms, and water containing vitamin drops (Wild Harvest D13123 Multi Drops). These experimental conditions were chosen based on previous work in *J. h. hyemalis* exposed to the same temperatures, which revealed substantial increases in M_{sum} over the same duration (Swanson et al. 2014).

Brood patches and cloacal protuberances were not present after the adjustment period. At the end of treatments, we euthanized individuals using cervical dislocation. Gonads, identified during dissection, were regressed in all but one *J. h. dorsalis* individual post-acclimation.

Eight individuals died during the capture-transport and adjustment periods (1 *J. h. dorsalis,* 4 *J. h. shufeldti*, 1 *J. h. thurberi,* and 2 *J. p. palliatus*). Additionally, one *J. h. thurberi* individual exhibited lethargy upon introduction to the cold treatment, died within the first 24 h of cold acclimation, and was removed from analyses. This resulted in a total sample size of n = 95 individuals.

Metabolic assays for acclimation experiments

We quantified M_{sum} in a temperature-controlled cabinet using open-flow respirometry both before and after acclimation treatments as described above. We measured body mass (M_b)

immediately before each assay. M_{sum} trials were conducted at -5°C for pre-acclimation measures and -15°C for post-acclimation measures. We removed one *J. h. thurberi* individual from all analyses due to an equipment malfunction, which made the post-acclimation measure unusable. Because trials occurred at various times throughout the day, we tested for, but did not find, a linear effect of trial start time on M_{sum} either before or after acclimation ($p_{pre} = 0.61$, $p_{post} = 0.78$).

Climate data for acclimation populations

We reconstructed the annual thermal regime experienced by a population using interpolated monthly climate data downloaded from the WorldClim dataset (Hijmans et al. 2005). Specifically, we extracted the annual temperature range variable (Bio7) at a resolution of 2.5' for the site of capture, which we refer to as T_{range}. Focal populations varied in T_{range} by 21°C (Figure 1).

Pair-wise genetic distance

We estimated patterns of genetic differentiation (pairwise F_{ST}) for each of the five focal taxa. In the absence of population genetic data for the acclimated individuals, we selected 4-7 individuals from the population genetic dataset that originated in the region of our acclimation sampling sites. We used SNP data from these individuals to calculate weighted Weir's theta (Weir and Cockerham 1984) in *vcftools*. We employed identical pairwise F_{ST} for all individuals within a focal population.

Using these values, we then performed a partial mantel test to ascertain that environmental distance and genetic distance do not covary among our sampling sites. We estimated pair-wise environmental differences among the five sites as the Euclidean distance for 10 WorldClim variables (after removing redundant variables at $r \geq 0.70$ from the original 19 WorldClim variables). We simultaneously controlled for geographic distance, estimated as pairwise geodesic distance among sampling sites with package *geosphere* (Hijmans et al. 2019). We employed these indices of pairwise genetic, environmental, and geographic distance in a partial mantel test with the package *vegan* (Oksanen et al. 2019).

Analyses for acclimation data

We first verified that phenotypic differences did not exist among treatment groups before acclimations began by regressing pre-acclimation trait values on temperature treatment for each phenotype (M_b and M_{sum}). To evaluate whether environmental variation corresponded with flexibility, we related climatic data to M_{sum} for each population while simultaneously incorporating population demography. We used Markov Chain Monte Carlo generalized linear mixed models that allow for Bayesian approaches (Hadfield and Nakagawa 2010; Stone et al. 2011) with the *MCMCglmm* package (Hadfield 2010). We constructed a model to explain variation in ΔM_{sum} (post- minus pre-acclimation, to control for pre-treatment differences among individuals) with temperature treatment, T_{range}, and treatment × T_{range} interaction as main effects and pairwise F_{ST} as a random effect. We standardized all continuous predictor variables according to (Gelman 2008). We used default priors and ran models for 1,000,000 iterations with a burn-in of 10,000 and a thinning interval of 100.

To maximize the power of our modest sample size, we also separated the two treatment groups and investigated relationships with T_{range} in each subset. Thus, we quantified the effect of T_{range} on post-acclimation M_{sum} while including pre-acclimation M_{sum} and M_b as covariates and pairwise F_{ST} as a random effect for each Cold and Control birds. We again standardized all

continuous predictor variables and ran models with default priors for 1,000,000 iterations with a burn-in of 10,000 and thinning interval of 100.

RESULTS AND DISCUSSION

Geographic variation in thermogenic performance

Although several studies have characterized broad-scale *inter*specific patterns in endothermic thermogenic performance (e.g., Naya et al. 2012; Stager et al. 2016; Buckley et al. 2018), little is known about the potential for or the underlying environmental correlates of *intra*specific variation in thermogenic performance. We assayed M_{sum} for 292 juncos at 8 sites across the U.S. and correlated recent weather data to patterns of *in situ* variation (Figure 1). The number of individuals, number of sampling days, seasons, and years varied across sites with 86 total site-days of environmental variation and 5 morphotypes included in our dataset (Table S1).

Geographic variation in M_{sum} corresponded to environmental variation with three weather variables outperforming the null model (Table S3). The best model included mass (M_b), daily temperature range (T_{d_range}), morphotype, and a T_{d_range}× morphotype interaction and explained 49% of the variation in M_{sum} (Table 1). While M_b positively correlated with M_{sum}, this model also showed a persistent effect of morphotype on M_{sum} after controlling for differences in M_b, with Oregon Juncos exhibiting the lowest and Slate-colored Juncos the highest M_{sum} values. This could suggest local adaptation in thermogenic performance among populations. However, we cannot rule out plastic responses to the developmental environment or acclimatization to more recent climatic conditions in these *in situ* measures.

Accordingly, juncos that experienced larger T_{d_range} in the week prior to capture also had the highest M_{sum}, indicating that they may be responding to short-term heterogeneity in their thermal environment. This is consistent with recent laboratory findings showing that *J. h. montanus* can make substantial changes to M_{sum} within one week of exposure to a low temperature stimulus (Stager et al. 2020). Moreover, junco M_{sum} did not correlate with daylength (Table S3), a finding corroborated by previous work showing that *J. h. hyemalis* does not alter M_{sum} in response to simulated photoperiod cues in the lab (Swanson et al. 2014). The T_{d_range}× morph interaction term was also significant for several comparisons indicating that populations respond differentially to temperature variation in the wild (Table 1; Table S4). This suggests that *Junco* populations may differ in their physiological flexibility and that variation in the temperature range across their distribution may play an important role in shaping this flexibility.

Environmental structuring of population genetic variation

The spatial structure of the environment can also influence rates of gene flow among habitats and is therefore an important component determining the selective regime acting on local populations (Lenormand 2002; Kawecki and Ebert 2004). To understand how environmental variables might structure *Junco* population genetic variation, we generated 29,806 biallelic SNPs from 192 individuals that were selected to maximize geographic and environmental variance while representing all recognized *Junco* species/subspecies (Figure 1). Major clusters identified by PCA corresponded to the 'Sky Island' lineages of central America (*J. vulcani*), southern Mexico (*J. p. alticola* and *J. p. fulvescens*), and southern Baja (*J. p. bairdi*; Figure S2). Since we also did not sample these lineages phenotypically, we therefore excluded these four taxa to focus on *Junco* lineages of North America. We found subtle structuring across this group with the first three PC axes explaining 4.5% of the total variance: (1) *J. p. phaeonotus* and *J. p. palliatus* of Mexico (2) *J. h. dorsalis* of the southwestern U.S., (3) *J. h. pontilis* and (4)

J. h. townsendi of northern Baja, and (5) *J. insularis* of Guadalupe Island grouped into largely separate clusters. However, other *J. hyemalis* taxa did not comprise nonoverlapping genetic clusters (Figure S2), perhaps reflecting the rapid expansion of this lineage over the last ~20,000 years (Milá et al. 2007; Friis et al. 2016).

In instances where populations are not clearly distinguishable and environmental gradients are continuous, genotype-environment association methods can aid in the detection of signatures of natural selection (Jones et al. 2013). In particular, redundancy analysis (RDA) is a powerful multivariate tool for identifying even weak correlations between genetic and environmental data (Forester et al. 2018). We thus performed an RDA to quantify the population genetic variance that partitions with climatic indices both with and without controlling for background genetic structure. Six RDA axes explained 5.6% of the total genetic variance in the nonconditioned model, and 4.0% in the model controlling for background genetic structure (Table S5). Permutation tests confirmed the significance of the constraining variable effects in both cases ($p < 0.001$) and the first 4 RDA axes in the nonconditioned model were significant ($p < 0.001$). In both models, precipitation seasonality and annual temperature range loaded strongly and oppositely on the first two axes, while annual precipitation and mean diurnal temperature range loaded strongly and oppositely on axis 4 and on axis 3 in the unconditioned model and conditioned model, respectively. The variance partition analysis showed that temperature range explained 1.1% of total genetic variability, more than any other climatic variable (Table S6). Additionally, we detected 450 outlier SNPs exhibiting associations with the first 4 axes in the conditioned model. Of these, 60 and 90 outlier SNPs corresponded most strongly to mean diurnal temperature range and annual temperature range, respectively. This complements our above finding that physiological variation is structuring with temperature range. However, it is not known whether these sites are involved in conferring flexibility and in-depth genome scans are necessary to reveal the genomic architecture underlying thermogenic flexibility.

Our results also show that some taxa, like the widespread *J. h. hyemalis*, occupy large swaths of orthogonal space, and that many taxa overlap in climatic breadth. Recent work by Friis et al. (2018) instead found that Oregon Junco taxa exhibited distinct environmental partitioning across their distribution. However, in that study, each taxon was only sampled from a single site meaning that patterns of environmental and geographic distance may be largely confounded (Wang and Bradburd 2014). Our dataset encompasses far more environmental variation across varying geographic distances and thus uniquely highlights the role of seasonal and diurnal climatic variation in structuring junco population genetic variation.

Flexible responses to temperature acclimation treatments

To test whether phenotypic flexibility in thermogenic capacity correlated with environmental heterogeneity, we performed an acclimation experiment on individuals from five populations across the western U.S. Following the results of *in situ* sampling, we selected these focal populations to maximize variation in the temperature range they experienced across the year. Genetic differentiation among populations (F_{ST}) ranged from 0.013 to 0.053 (Table S7), while pairwise environmental and genetic distances did not covary among these populations (partial Mantel test: $r = -0.58$, $p = 0.93$) allowing us to simultaneously tease apart the effects of both factors.

Prior to acclimation, temperature treatment groups did not differ in M_{sum} or M_b (Table S8). However, both traits did positively correlate with native temperature range. We therefore controlled for individual differences in pre-acclimation M_{sum} in subsequent analyses. Per our

prediction, we expected to find a significant interaction between temperature range and treatment. When looking at changes in M_{sum} over the course of the experiment (ΔM_{sum} - measured as the difference between post- and pre acclimation measures), we found that cold-acclimated birds increased M_{sum} and birds from more variable thermal environments also exhibited higher ΔM_{sum} (Figure 3). These effects were similar in magnitude ($\beta = 0.65$ and 0.61, respectively) but the interaction term for these two variables was slightly weaker and nonsignificant ($\beta = 0.43$, $p = 0.10$). However, cold birds also increased M_b ($\beta = 0.71$, p = 5.6 x 10^{-6}; Figure S3) and this may obscure patterns contributing to variation in ΔM_{sum}. Moreover, control birds would have ideally maintained a consistent M_{sum} between the beginning and end of acclimation in all populations but that was not the case. In fact, *J. h. thurberi* control birds exhibited a reduction in M_{sum} over the course of the acclimation period. This pattern in the control birds is difficult to explain and may reflect the vagaries of measurement error and small sample size.

We therefore tested for effects of temperature range on M_{sum} separately for both treatment groups while controlling for an individual's pre-acclimation measure. In cold-acclimated juncos, we found that M_{sum} strongly correlated with temperature range ($\beta = 0.94$, $p < 0.01$) and to a lesser degree pre-acclimation M_{sum} ($\beta = 0.51$, $p = 0.04$), but the correlation with M_b was nonsignificant ($\beta = 0.58$, $p = 0.09$). In contrast, in control birds we found that pre-acclimation M_{sum} explained most of the variance in post-acclimation M_{sum} ($\beta = 1.07$, $p < 1$ x 10^{-4}), with M_b explaining more variation ($\beta = 0.57$, $p = 0.01$) than temperature range ($\beta = 0.50$, $p = 0.05$). Significance aside, the effect size of temperature range on changes in M_{sum} in cold birds is nearly twice that of control birds while accounting for individual differences in size and pre-acclimation M_{sum}. Our results therefore provide support for the prediction that the degree of flexibility in M_{sum} is correlated with native T_{range} in cold-acclimated juncos. Populations from more variable climates exhibited the greatest increase in M_{sum} in the cold, while populations from less variable climates exhibited little or no change in M_{sum}. Future work exploring these patterns would benefit from including larger sample sizes and more populations encompassing higher degrees of environmental variation.

Conclusions

Our multifaceted approach integrated measures of population genetic variation with whole-organism measures of physiological performance and indices of environmental variation to help elucidate the mechanisms driving variation in physiological flexibility among populations. We provide evidence that temperature variation drove patterns of intra-specific variation in thermal performance and found that junco populations responded differentially to weather cues *in situ*. This pattern was replicated in the laboratory. Thermogenic flexibility in juncos correlated with the heterogeneity of their native thermal environment. Moreover, range-wide population genetic variation was also correlated with climatic variation, providing evidence that environmental heterogeneity may be an important selective force driving junco population divergence. Together, these results suggest that physiological flexibility may play a key role in local adaptation in this broadly distributed lineage.

These results contrast with previous work in ectotherms that indicates that plasticity/flexibility in thermal physiology does not correspond to environmental heterogeneity (Overgaard et al. 2011; van Heerwaarden et al. 2014; Gunderson and Stillman 2015; Sørensen et al. 2016). While the cause of this disparity is not clear, one aspect that has largely been overlooked in these studies is the role of historical demographic processes in shaping adaptive plasticity/flexibility. Gene flow (Riechert 1993), colonization history (Beall 2007), population

size (Leimu and Fischer 2008), and the standing genetic variation of founding individuals (Barrett and Schluter 2008) are all important factors shaping adaptive outcomes (Benham and Cheviron 2020). For example, although gene flow can constrain adaptive divergence (Riechert 1993), high gene flow among selective regimes is predicted to favor increased plasticity/flexibility in order to aid offspring that experience a dissimilar environment from their parents (Sultan and Spencer 2002; Crispo 2008; Lind et al. 2011). Though *J. hyemalis* taxa exhibited low levels of population genetic differentiation, it is not yet clear how patterns of gene flow may influence flexibility in this system. Comprehensive studies that simultaneously incorporate both contemporary ecological conditions and population demographic processes are necessary to fully flesh out the role of environment heterogeneity in structuring plasticity/flexibility.

There are also several biological differences between ectotherms and endotherms that may contribute to disparities in evolutionary patterns of phenotypic plasticity/flexibility. In general, many ectotherms rely on behavioral thermoregulatory mechanisms and possess a number of avoidance strategies (e.g., diapause or hibernation, migration) that may be used to buffer against environmental extremes (Kearney et al. 2009). Thus, the amount of thermal heterogeneity that an individual or population experience may not correspond to broad-scale climatic patterns across the year. Endotherms maintain a relatively constant body temperature in comparison, despite sometimes large temperature differentials with their ambient environment (Mcnab 2002). While many endotherms also exhibit hibernation and migratory behaviors, small songbirds that reside year-round in temperate regions, like juncos, are particularly exposed to thermal heterogeneity (Swanson 2010). These differences may lead to divergent selection pressures on flexibility and thermal performance traits among taxonomic groups.

This study greatly expands our knowledge of endothermic responses to environmental alteration and their capacity for thermal acclimatization. Understanding flexibility in organismal thermal tolerances is important for predicting population growth/decline, making habitat delineations, and modeling disease transmission (Miazgowicz et al. 2020), and is especially relevant in light of ongoing global climate change. Although many recent macrophysiological approaches characterizing potential organismal responses to climatic change employ a single metric of thermal tolerance and treat it as a canalized trait across a species' range (Sunday et al. 2014; Gunderson and Stillman 2015; Riddell et al. 2019), our results highlight the capacity for populations to vary geographically in their physiological response to environmental cues. When coupled with datasets like ours, biophysical models that incorporate intraspecific patterns in acclimatization will improve our ability to predict organismal responses to climate warming.

ETHICS

This work was completed with approval from the U.S. Fish and Wildlife Service (MB84376B-1 to M.S.; MB01543B-0 to Z.A.C.; MB# to D.L.S.; MB06336A-4 to Matthew Carling; MB45239B-0 to Timothy Grieves; MB757670-1 to David Winkler; and MB094297-0 to Chris Witt,), the State of Arizona Game and Fish Department (E19253811 to M.S. and # to D.L.S.), the State of California Department of Fish and Wildlife (13971 to M.S.), Colorado Parks and Wildlife (10TRb2030A15 to Matthew Carling), the Illinois Department of Natural Resources (NH13.5667 to Z.A.C.), the Montana Department of Fish Wildlife and Parks (2016-013 and 2017-067-W to M.S.), the New Mexico Department of Game & Fish (#3217 to Chris Witt), the New York State Division of Fish, Wildlife, & Marine Resources (LCP 1477 to David Winkler), the Oregon Department of Fish and Wildlife (108-18 to M.S.), the State of South Dakota

Department of Game, Fish, and Parks (13 to M.S. and # to D.L.S.), Wyoming Game and Fish (#754 to Matthew Carling), and the Institutional Animal Care and Use Committees at Cornell University (2001-0051 to David Winkler), the University of Illinois (13385 to Z.A.C.), the University of Montana (010-16ZCDBS-020916 and 030-18ZCDBS-052918 to Z.A.C.), the University of South Dakota (# to D.L.S),the University of Wyoming (A-3216-01 to Matthew Carling).

ACKNOWLEDGMENTS
We are indebted to the many natural history museums that contributed tissue loans to this project, including John Klicka and the University of Washington Burke Museum, the American Museum of Natural History, the Cleveland Museum of Natural History, the Cornell University Museum of Vertebrates, the Field Museum of Natural History, the Louisiana State University Museum of Natural Science, the Midwest Museum of Natural History, the Museum of Southwest Biology, the Museum of Vertebrate Zoology, the New York State Museum, the Royal Alberta Museum, the San Diego Natural History Museum, the Smithsonian National Museum of Natural History, the University of Alaska Museum, the University of Montana Philip Wright Museum, and the University of Wyoming Museum of Vertebrates. We are very thankful to the many hands that provided help and logistical assistance collecting birds: Tim Grieves, Doug Eddy, Gregory Toreev, Matt Carling, Cole Wolf, Trey Sasser, Phred Benham, Nick Sly, Henry Pollock, Phil Unitt, Chris Witt, Andy Johnson, Blair Wolf, Eric Gulson, David Winkler, Charles Dardia, Link Smith, Pamela Yeh, Eleanor Diamant, Kevin Burns, and Point Loma Nazarene University. We are grateful to the field stations that hosted our work: UNM Sevilleta Field Station, UW-NPS Research Station, Mt. Evans Field Station, and the Southwestern Research Station. We also thank Rena Schweizer and Thom Nelson for guidance with RAD processing and pop gen analysis, and the Cheviron lab for feedback on an earlier version of this manuscript.

FUNDING
This work was supported by funds from the American Museum of Natural History Chapman Fund, the American Philosophical Society Lewis and Clark Fund, the Explorers Club, the Illinois Ornithological Society, the Nuttall-Ornithological Society, Sigma Xi, the Society for Integrative and Comparative Biology, the Society of Systematic Biologists, the University of Illinois Graduate School, the University of Illinois School of Integrative Biology, and the Wilson Ornithological Society (to M.S.); the University of Montana (startup to Z.A.C). M.S. was supported by the National Science Foundation Graduate Research Fellowship Program, P.E.O. International, and the University of Montana Graduate School Bertha Morton Fellowship.

AUTHOR CONTRIBUTIONS
M.S. and Z.A.C. conceived of the study; N.R.S. helped capture birds for acclimation studies; D.L.S. performed *in situ* measurements in AZ and SD; M.S. performed all other data collection and analyses and drafted the manuscript; N.R.S. and Z.A.C. contributed edits to the manuscript.

REFERENCES

Baird NA, Etter PD, Atwood TS, Currey MC, Shiver AL, Lewis ZA, Selker EU, Cresko WA, Johnson EA. 2008. Rapid SNP discovery and genetic mapping using sequenced RAD markers. *PLOS ONE* 3:e3376.

Barrett R, Schluter D. 2008. Adaptation from standing genetic variation. *Trends in Ecology & Evolution* 23:38–44.

Beall CM. 2007. Two routes to functional adaptation: Tibetan and Andean high-altitude natives. *Proceedings of the National Academy of Sciences* 104:8655–8660.

Benham PM, Cheviron ZA. 2020. Population history and the selective landscape shape patterns of osmoregulatory trait divergence in tidal marsh Savannah sparrows (Passerculus sandwichensis). *Evolution* 74:57–72.

Botero CA, Weissing FJ, Wright J, Rubenstein DR. 2015. Evolutionary tipping points in the capacity to adapt to environmental change. *Proc Natl Acad Sci USA* 112:184–189.

Buckley LB, Khaliq I, Swanson DL, Hof C. 2018. Does metabolism constrain bird and mammal ranges and predict shifts in response to climate change? *Ecol Evol*:ece3.4537.

Catchen JM, Amores A, Hohenlohe P, Cresko W, Postlethwait JH. 2011. *Stacks* : Building and Genotyping Loci *De Novo* From Short-Read Sequences. *G3* 1:171–182.

Cavieres G, Sabat P. 2008. Geographic variation in the response to thermal acclimation in rufous-collared sparrows: are physiological flexibility and environmental heterogeneity correlated? *Functional Ecology* 22:509–515.

Cooley D, decode_pl) PB (Author of c++, pacakge) R (Functions written for the L. 2018. googleway: Accesses Google Maps APIs to Retrieve Data and Plot Maps. Available from: https://CRAN.R-project.org/package=googleway

Crispo E. 2008. Modifying effects of phenotypic plasticity on interactions among natural selection, adaptation and gene flow. *Journal of Evolutionary Biology* 21:1460–1469.

Danecek P, Auton A, Abecasis G, Albers CA, Banks E, DePristo MA, Handsaker RE, Lunter G, Marth GT, Sherry ST, et al. 2011. The variant call format and VCFtools. *Bioinformatics* 27:2156–2158.

Davey JW, Blaxter ML. 2010. RADSeq: next-generation population genetics. *Briefings in Functional Genomics* 9:416–423.

Day T, Pritchard J, Schluter D. 1994. A comparison of two sticklebacks. *Evolution* 48:1723–1734.

Ernande B, Dieckmann U. 2004. The evolution of phenotypic plasticity in spatially structured environments: implications of intraspecific competition, plasticity costs and environmental characteristics. *Journal of Evolutionary Biology* 17:613–628.

Fangue NA, Richards JG, Schulte PM. 2009. Do mitochondrial properties explain intraspecific variation in thermal tolerance? *Journal of Experimental Biology* 212:514–522.

Forester BR, Jones MR, Joost S, Landguth EL, Lasky JR. 2016. Detecting spatial genetic signatures of local adaptation in heterogeneous landscapes. *Molecular Ecology* 25:104–120.

Forester BR, Lasky JR, Wagner HH, Urban DL. 2018. Comparing methods for detecting multilocus adaptation with multivariate genotype–environment associations. *Molecular Ecology* 27:2215–2233.

Friis G, Aleixandre P, Rodríguez-Estrella R, Navarro-Sigüenza AG, Milá B. 2016. Rapid postglacial diversification and long-term stasis within the songbird genus *Junco* : phylogeographic and phylogenomic evidence. *Mol Ecol* 25:6175–6195.

Friis G, Fandos G, Zellmer AJ, McCormack JE, Faircloth BC, Milá B. 2018. Genome-wide signals of drift and local adaptation during rapid lineage divergence in a songbird. *Mol Ecol* 27:5137–5153.

Gelman A. 2008. Scaling regression inputs by dividing by two standard deviations. *Statist. Med.* 27:2865–2873.

Ghalambor CK, McKAY JK, Carroll SP, Reznick DN. 2007. Adaptive versus non-adaptive phenotypic plasticity and the potential for contemporary adaptation in new environments. *Funct Ecology* 21:394–407.

Gianoli E, González-Teuber M. 2005. Environmental heterogeneity and population differentiation in plasticity to drought in Convolvulus Chilensis (Convolvulaceae). *Evol Ecol* 19:603–613.

Gunderson AR, Stillman JH. 2015. Plasticity in thermal tolerance has limited potential to buffer ectotherms from global warming. *Proc. R. Soc. B* 282:20150401.

Hadfield JD. 2010. MCMC methods for multi-response generalized linear mixed models: the MCMCglmm R package. *Journal of Statistical Software* 33:1–22.

Hadfield JD, Nakagawa S. 2010. General quantitative genetic methods for comparative biology: phylogenies, taxonomies and multi-trait models for continuous and categorical characters. *Journal of Evolutionary Biology* 23:494–508.

Hayes JP, O'Connor CS. 1999. Natural selection on thermogenic capacity of high-altitude deer mice. *Evolution* 53:1280–1287.

van Heerwaarden B, Lee RFH, Overgaard J, Sgrò CM. 2014. No patterns in thermal plasticity along a latitudinal gradient in Drosophila simulans from eastern Australia. *Journal of Evolutionary Biology* 27:2541–2553.

Hijmans RJ, Cameron SE, Parra JL, Jones PG, Jarvis A. 2005. Very high resolution interpolated climate surfaces for global land areas. *nternational Journal of Climatology* 25:1965–1978.

Hijmans RJ, Etten J van, Sumner M, Cheng J, Baston D, Bevan A, Bivand R, Busetto L, Canty M, Forrest D, et al. 2020. raster: Geographic Data Analysis and Modeling. Available from: https://CRAN.R-project.org/package=raster

Hijmans RJ, Williams E, Vennes C. 2019. geosphere: Spherical Trigonometry. Available from: https://CRAN.R-project.org/package=geosphere

Hufkens K, Basler D, Milliman T, Melaas E, Richardson A. 2018. An integrated phenology modelling framework in R. *Methods in Ecology and Evolution* 9:1276–1285.

Jombart T, Kamvar ZN, Collins C, Lustrik R, Beugin M-P, Knaus BJ, Solymos P, Mikryukov V, Schliep K, Maié T, et al. 2020. adegenet: Exploratory Analysis of Genetic and Genomic Data. Available from: https://CRAN.R-project.org/package=adegenet

Jones MR, Forester BR, Teufel AI, Adams RV, Anstett DN, Goodrich BA, Landguth EL, Joost S, Manel S. 2013. Integrating landscape genomics and spatially explicit approaches to detect loci under selection in clinal populations. *Evolution* 67:3455–3468.

Kawecki TJ, Ebert D. 2004. Conceptual issues in local adaptation. *Ecology Letters* 7:1225–1241.

Kearney M, Shine R, Porter WP. 2009. The potential for behavioral thermoregulation to buffer "cold-blooded" animals against climate warming. *Proc Natl Acad Sci U S A* 106:3835–3840.

Ketterson ED, Atwell JW. 2016. Snowbird: integrative biology and evolutionary Ddversity in the Junco. University of Chicago Press

Leimu R, Fischer M. 2008. A meta-analysis of local adaptation in plants. Buckling A, editor. *PLoS ONE* 3:e4010.

Lenormand T. 2002. Gene flow and the limits to natural selection. *Trends in Ecology & Evolution* 17:183–189.

Li H. 2013. Aligning sequence reads, clone sequences and assembly contigs with BWA-MEM. *ArXiv* 1303.

Lind MI, Ingvarsson PK, Johansson H, Hall D, Johansson F. 2011. Gene flow and selection on phenotypic plasticity in an island system of *Rana temporaria*. *Evolution* 65:684–697.

Lind MI, Johansson F. 2007. The degree of adaptive phenotypic plasticity is correlated with the spatial environmental heterogeneity experienced by island populations of Rana temporaria. *Journal of Evolutionary Biology* 20:1288–1297.

Lundblad CG, Conway CJ. 2020. Variation in selective regimes drives intraspecific variation in life-history traits and migratory behaviour along an elevational gradient. *Journal of Animal Ecology* 89:397–411.

Mcnab B. 2002. The physiological ecology of vertebrates: a view from energetics. In: Copeia. Vol. 2002.

Miazgowicz KL, Shocket MS, Ryan SJ, Villena OC, Hall RJ, Owen J, Adanlawo T, Balaji K, Johnson LR, Mordecai EA, et al. 2020. Age influences the thermal suitability of Plasmodium falciparum transmission in the Asian malaria vector *Anopheles stephensi*. *Proceedings of the Royal Society B: Biological Sciences* 287:20201093.

Milá B, McCormack JE, Castañeda G, Wayne RK, Smith TB. 2007. Recent postglacial range expansion drives the rapid diversification of a songbird lineage in the genus *Junco*. *Proc. R. Soc. B* 274:2653–2660.

Miller AH. 1941. Speciation in the avian genus Junco. Berkeley, California: University of California Press

Moran NA. 1992. The evolutionary maintenance of alternative phenotypes. *The American Naturalist* 139:971–989.

Naya DE, Spangenberg L, Naya H, Bozinovic F. 2012. Latitudinal patterns in rodent metabolic flexibility. *The American Naturalist* 179:E172–E179.

Nolan, Jr. V, Ketterson ED, Cristol DA, Rogers CM, Clotfelter ED, Titus RC, Schoech SJ, Snajdr E. 2002. Dark-eyed Junco (Junco hyemalis). Poole A, Gill F, editors. *Birds N. Am.* [Internet]. Available from: https://birdsna.org/Species-Account/bna/species/daejun/introduction

Nussey DH, Postma E, Gienapp P, Visser ME. 2005. Selection on heritable phenotypic plasticity in a wild bird population. *Science* 310:304–306.

Oksanen J, Blanchet FG, Friendly M, Kindt R, Legendre P, McGlinn D, Minchin PR, O'Hara RB, Simpson GL, Solymos P, et al. 2019. vegan: Community Ecology Package. Available from: https://CRAN.R-project.org/package=vegan

Overgaard J, Kristensen TN, Mitchell KA, Hoffmann AA. 2011. Thermal tolerance in widespread and tropical *Drosophila* species: does phenotypic plasticity increase with latitude? *The American Naturalist* 178:S80–S96.

Parchman TL, Gompert Z, Mudge J, Schilkey FD, Benkman CW, Buerkle CA. 2012. Genome-wide association genetics of an adaptive trait in lodgepole pine: association mapping of serotiny. *Molecular Ecology* 21:2991–3005.

Petit M, Clavijo-Baquet S, Vézina F. 2017. Increasing winter maximal metabolic rate improves intrawinter survival in small birds. *Physiological and Biochemical Zoology* 90:166–177.

Piersma T, Drent J. 2003. Phenotypic flexibility and the evolution of organismal design. *Trends in Ecology & Evolution* 18:228–233.

Piersma T, van Gils JA. 2011. The flexible phenotype: a body-centred integration of ecology, physiology, and behaviour. Oxford University Press Available from: https://www.rug.nl/research/portal/publications/the-flexible-phenotype(c8607bf1-682c-4a61-bd41-36bd37386378)/export.html

Pigliucci M. 2005. Evolution of phenotypic plasticity: where are we going now? *Trends in Ecology & Evolution* 20:481–486.

Price TD, Qvarnström A, Irwin DE. 2003. The role of phenotypic plasticity in driving genetic evolution. *Proc. R. Soc. Lond. B* 270:1433–1440.

R Core Team. 2018. R: The R project for statistical computing. *R Foundation for Statistical Computing, Vienna, Austria* [Internet]. Available from: https://www.r-project.org/

Riddell EA, Iknayan KJ, Wolf BO, Sinervo B, Beissinger SR. 2019. Cooling requirements fueled the collapse of a desert bird community from climate change. *Proc Natl Acad Sci USA* 116:21609–21615.

Riechert SE. 1993. Investigation of potential gene flow limitation of behavioral adaptation in an aridlands spider. *Behav Ecol Sociobiol* 32:355–363.

Scheiner SM. 2013. The genetics of phenotypic plasticity. XII. Temporal and spatial heterogeneity. *Ecol Evol* 3:4596–4609.

Sørensen JG, Kristensen TN, Overgaard J. 2016. Evolutionary and ecological patterns of thermal acclimation capacity in Drosophila: is it important for keeping up with climate change? *Current Opinion in Insect Science* 17:98–104.

Stager M, Cheviron ZA. 2020. Is there a role for sarcolipin in avian facultative thermogenesis in extreme cold? *Biology Letters* 16:20200078.

Stager M, Pollock HS, Benham PM, Sly ND, Brawn JD, Cheviron ZA. 2016. Disentangling environmental drivers of metabolic flexibility in birds: the importance of temperature extremes versus temperature variability. *Ecography* 39:787–795.

Stager M, Senner NR, Tobalske BW, Cheviron ZA. 2020. Body temperature maintenance acclimates in a winter-tenacious songbird. *J Exp Biol* 223:jeb221853.

Stone GN, Nee S, Felsenstein J. 2011. Controlling for non-independence in comparative analysis of patterns across populations within species. *Phil. Trans. R. Soc. B* 366:1410–1424.

Sullivan KA. 2018. Yellow-eyed Junco - Junco phaeonotus - v1.1 from Birds of North America - Birds of the World. Available from: https://birdsoftheworld.org/bow/historic/bna/yeejun/1.1/introduction

Sultan SE, Spencer HG. 2002. Metapopulation structure favors plasticity over local adaptation. *The American Naturalist* 160:271–283.

Sunday JM, Bates AE, Kearney MR, Colwell RK, Dulvy NK, Longino JT, Huey RB. 2014. Thermal-safety margins and the necessity of thermoregulatory behavior across latitude and elevation. *Proceedings of the National Academy of Sciences* 111:5610–5615.

Swanson D, Zhang Y, Liu J-S, Merkord CL, King MO. 2014. Relative roles of temperature and photoperiod as drivers of metabolic flexibility in dark-eyed juncos. *Journal of Experimental Biology* 217:866–875.

Swanson DL. 1990a. Seasonal variation in cold hardiness and peak rates of cold-induced thermogenesis in the Dark-Eyed Junco (Junco hyemalis). *The Auk* 107:6.

Swanson DL. 1990b. Seasonal variation of vascular oxygen transport in the Dark-Eyed Junco. *The Condor* 92:62–66.

Swanson DL. 2010. Seasonal metabolic variation in birds: functional and mechanistic correlates. In: Thompson CF, editor. Current Ornithology Volume 17. New York, NY: Springer New York. p. 75–129. Available from: http://link.springer.com/10.1007/978-1-4419-6421-2_3

Swanson DL, Drymalski MW, Brown JR. 1996. Sliding vs static cold exposure and the measurement of summit metabolism in birds. *Journal of Thermal Biology* 21:221–226.

Swanson DL, Thomas NE, Liknes ET, Cooper SJ. 2012. Intraspecific correlations of basal and maximal metabolic rates in birds and the aerobic capacity model for the evolution of endothermy.Halsey LG, editor. *PLoS ONE* 7:e34271.

Thornton PE, Thornton MM, Mayer BW, Wei Y, Devarakonda R, Vose RS, Cook RB. 2016. Daymet: Daily Surface Weather Data on a 1-km Grid for North America, Version 3. *ORNL DAAC* [Internet]. Available from: https://daac.ornl.gov/cgi-bin/dsviewer.pl?ds_id=1328

Tienderen PHV. 1991. Evolution of generalists and specialist in spatially heterogeneous environments. *Evolution* 45:1317.

Vezina F, Ruhs E, O'Connor E, Le Pogam A, Regimbald L, Love O, Jimenez AG. 2020. Consequences of being phenotypically mismatched with the environment: rapid muscle ultrastructural changes in cold-shocked black-capped chickadees (Poecile atricapillus). *American Journal of Physiology-Regulatory, Integrative and Comparative Physiology* 318:R274–R283.

Wang IJ, Bradburd GS. 2014. Isolation by environment. *Molecular Ecology* 23:5649–5662.

Weir BS, Cockerham CC. 1984. Estimating F-Statistics for the analysis of population structure. *Evolution* 38:1358–1370.

West-Eberhard MJ. 2003. Developmental plasticity and evolution. 1 edition. Oxford ; New York: Oxford University Press

Yeh PJ, Price TD. 2004. Adaptive phenotypic plasticity and the successful colonization of a novel environment. *The American Naturalist* 164:531–542.

Table 1. Effects of daily temperature range (T_{d_range}), morph, and their interaction on *in situ* M_{sum} while controlling for differences in M_b. Estimates vary depending on which morphotype is used as the reference (OR shown here, others shown in Table S3). AICc = 882.03, df = 281, $R^2 = 0.49$.

Variable	Beta	SD	p
Intercept	**4.97**	**0.15**	**$< 2.0 \times 10^{-16}$**
M_b	**1.43**	**0.17**	**4.38×10^{-15}**
Morph (GH)	**1.18**	**0.46**	**0.01**
Morph (PS)	**0.56**	**0.20**	**6.06×10^{-3}**
Morph (SC)	**2.14**	**0.42**	**5.52×10^{-7}**
Morph (YE)	-0.91	0.49	0.06
T_{d_range}	**2.45**	**0.27**	**$< 2.0 \times 10^{-16}$**
T_{d_range} x GH	-1.49	0.99	0.13
T_{d_range} x PS	**-2.47**	**0.56**	**1.47×10^{-5}**
T_{d_range} x SC	-0.82	0.58	0.16
T_{d_range} x YE	-1.49	0.90	0.10

Figure 1. Sampling scheme. Approximate breeding ranges of *Junco* taxa in shaded polygons, derived from geo-referenced samples listed in Miller (1941). Open black circles denote *in situ* sampling sites (detailed information in Table S1). Filled circles denote origin of population genetic samples, with size of circle indicating number of specimens used for the corresponding locale (n = 1 to 4; detailed information in Table S2). White Xs mark the five collection sites for the acclimation experiment.

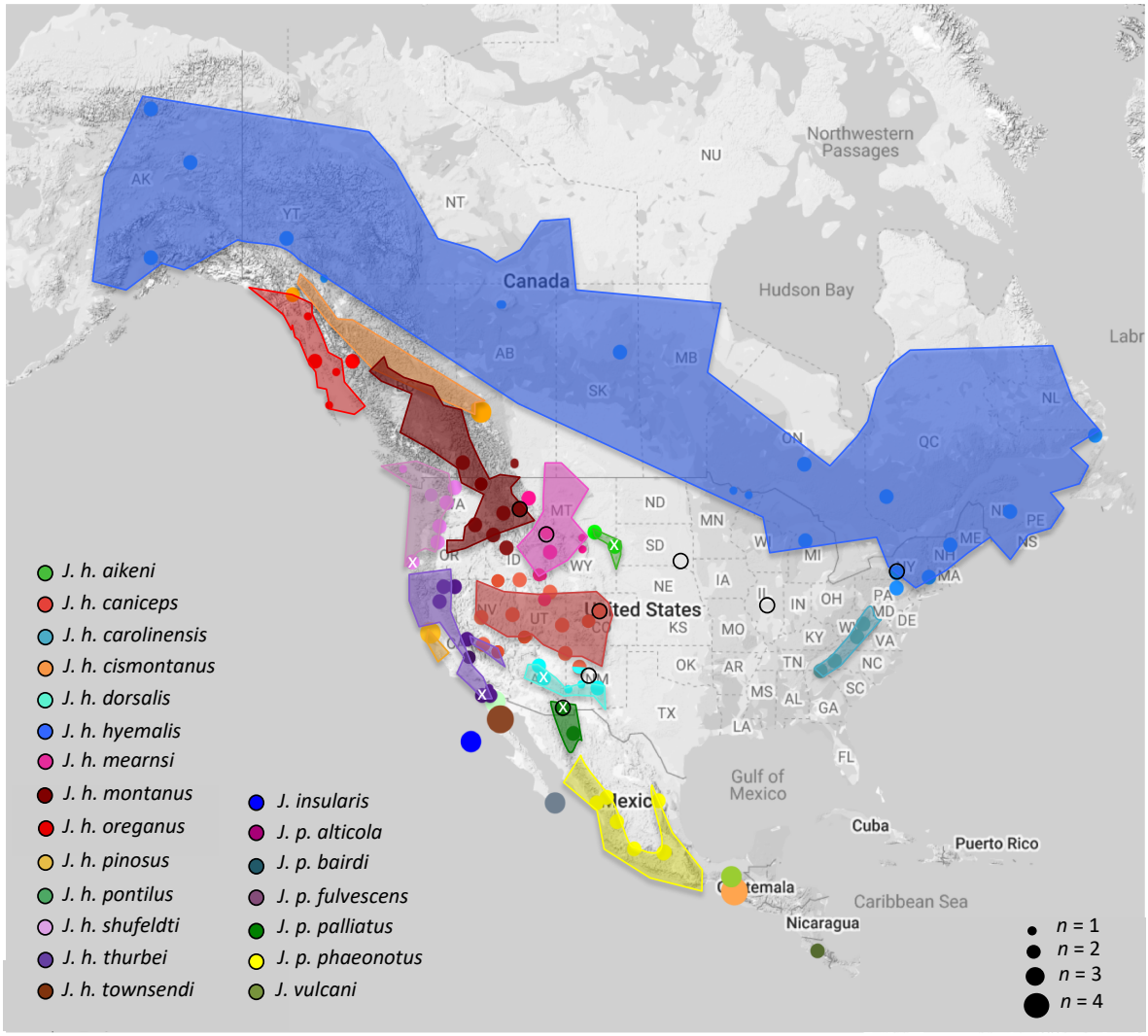

Figure 2. Population genetic structuring along 4 RDA axes in (top) unconditioned and (bottom) conditioned RDA. Arrows indicate loadings of 6 WorldClim variables. Dots represent individuals, colors denote museum-based taxon assignments.

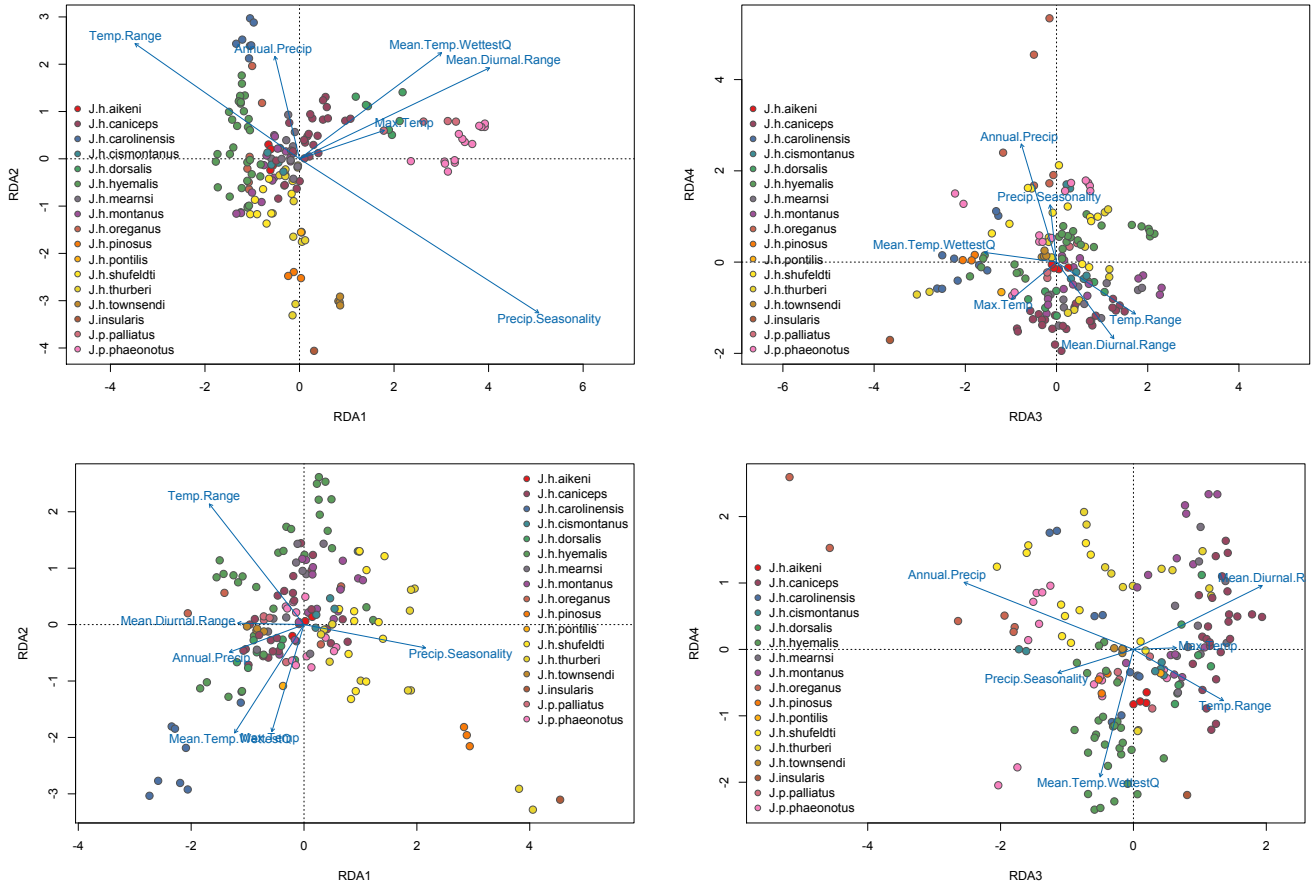

Figure 3. Change in M_{sum} (post- minus pre-acclimation) over the acclimation period for each population in order from lowest to highest native temperature range (from left to right): *J. h. thurberi* of California (CA), *J. h. shufeldti* of Oregon (OR), *J. p. palliatus* of Arizona (YE), *J. h. dorsalis* of Arizona (AZ), and *J. h. aikeni* of South Dakota (SD). Control birds in red, cold-acclimated birds in blue; $n = 94$.

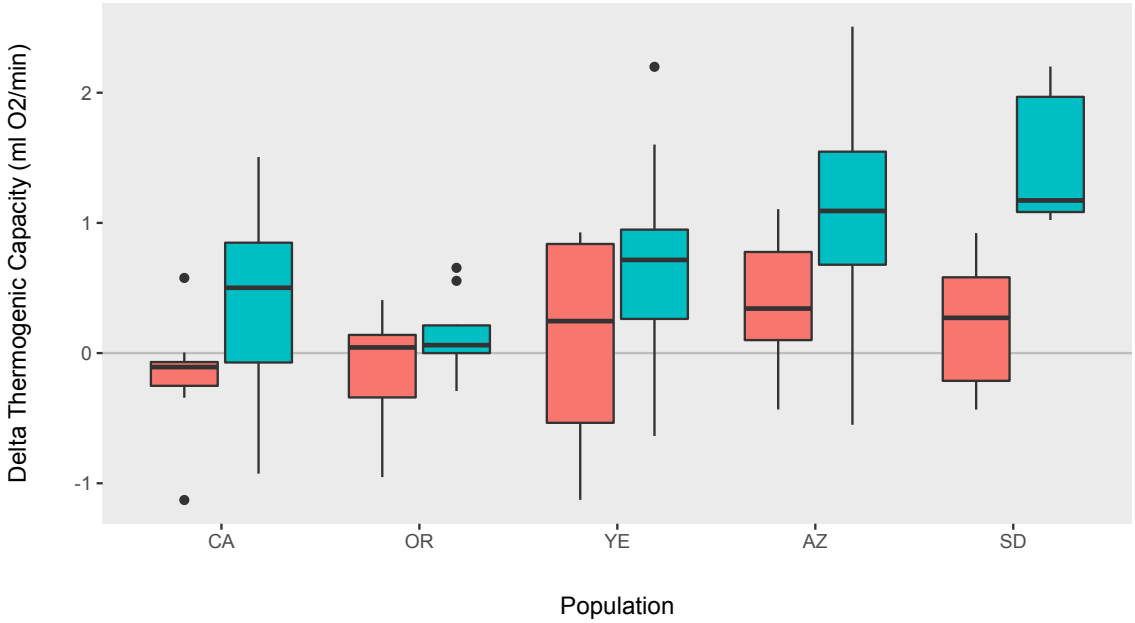

Supplemental Materials

Table S1. Information for *in situ* sampling.

Individual	State	Morphotype	Latitude	Longitude	Capture Date	Measurer
32013	AZ	YE	31.9	-109.28	3/19/13	D.L.S.
42013	AZ	YE	31.9	-109.28	3/19/13	D.L.S.
30766	AZ	YE	31.9	-109.28	3/11/15	D.L.S.
30767	AZ	YE	31.9	-109.28	3/11/15	D.L.S.
30768	AZ	YE	31.9	-109.28	3/11/15	D.L.S.
22013	AZ	YE	31.91	-109.25	3/18/13	D.L.S.
30740	AZ	YE	31.91	-109.25	3/9/15	D.L.S.
30763	AZ	YE	31.91	-109.25	3/9/15	D.L.S.
30764	AZ	YE	31.91	-109.25	3/10/15	D.L.S.
30578	AZ	YE	31.88	-109.21	3/8/15	D.L.S.
30757	AZ	YE	31.88	-109.21	3/8/15	D.L.S.
30769	AZ	YE	31.88	-109.21	3/12/15	D.L.S.
30775	AZ	YE	31.88	-109.21	3/12/15	D.L.S.
52013	AZ	YE	31.93	-109.26	3/20/13	D.L.S.
62013	AZ	YE	31.93	-109.26	3/20/13	D.L.S.
30765	AZ	YE	31.93	-109.26	3/10/15	D.L.S.
B1081	CO	GH	39.71	-105.61	8/9/15	M.S.
B1090	CO	GH	39.66	-105.6	8/11/15	M.S.
B1089	CO	GH	39.66	-105.6	8/11/15	M.S.
B1048	CO	GH	39.66	-105.6	8/1/15	M.S.
B1049	CO	GH	39.66	-105.6	8/1/15	M.S.
B1047	CO	GH	39.66	-105.6	8/1/15	M.S.
B1057	CO	GH	39.66	-105.6	8/3/15	M.S.
B1074	CO	GH	39.66	-105.6	8/6/15	M.S.
B1058	CO	GH	39.66	-105.6	8/3/15	M.S.
B1079	CO	GH	39.66	-105.6	8/7/15	M.S.
B1053	CO	GH	39.64	-105.59	8/2/15	M.S.
B1078	CO	GH	39.64	-105.59	8/7/15	M.S.
B1051	CO	GH	39.64	-105.59	8/2/15	M.S.
B1072	CO	GH	39.64	-105.59	8/5/15	M.S.
B1070	CO	GH	39.64	-105.59	8/5/15	M.S.
B1068	CO	GH	39.64	-105.59	8/5/15	M.S.
B1077	CO	GH	39.64	-105.59	8/7/15	M.S.
B1063	CO	GH	39.64	-105.59	8/4/15	M.S.
B1069	CO	GH	39.64	-105.59	8/5/15	M.S.
B1052	CO	GH	39.64	-105.59	8/2/15	M.S.
B1062	CO	GH	39.64	-105.59	8/4/15	M.S.
B1080	CO	GH	39.72	-105.51	8/8/15	M.S.
B1083	CO	GH	39.72	-105.51	8/9/15	M.S.
B1082	CO	GH	39.72	-105.51	8/9/15	M.S.
B1084	CO	GH	39.72	-105.51	8/10/15	M.S.
B1085	CO	GH	39.72	-105.51	8/10/15	M.S.
B1086	CO	GH	39.72	-105.51	8/10/15	M.S.
B1087	CO	GH	39.72	-105.51	8/10/15	M.S.
B1088	CO	GH	39.72	-105.51	8/10/15	M.S.
CUDEJU2	IL	SC	40.1	-88.2	12/7/13	M.S.
CUDEJU1	IL	SC	40.1	-88.2	12/7/13	M.S.
CUDEJU3	IL	SC	40.1	-88.2	12/8/13	M.S.
2311-51801	IL	SC	40.1	-88.2	1/9/14	M.S.

2311-51802	IL	SC	40.1	-88.2	1/9/14	M.S.
CUDEJU13	IL	SC	40.1	-88.2	12/9/13	M.S.
CUDEJU10	IL	SC	40.1	-88.2	12/9/13	M.S.
CUDEJU12	IL	SC	40.1	-88.2	12/9/13	M.S.
CUDEJU6	IL	SC	40.1	-88.2	12/9/13	M.S.
CUDEJU7	IL	SC	40.1	-88.2	12/9/13	M.S.
CUDEJU9	IL	SC	40.1	-88.2	12/9/13	M.S.
CUDEJU11	IL	SC	40.1	-88.2	12/9/13	M.S.
CUDEJU14	IL	SC	40.1	-88.2	12/9/13	M.S.
CUDEJU8	IL	SC	40.1	-88.2	12/9/13	M.S.
YRB	MT	OR	46.92	-113.45	8/1/17	M.S.
LLY	MT	OR	46.92	-113.45	7/13/16	M.S.
LLB	MT	OR	46.92	-113.45	7/13/16	M.S.
LB	MT	OR	46.92	-113.45	7/13/16	M.S.
DDL	MT	OR	46.92	-113.45	7/15/16	M.S.
RO	MT	OR	46.92	-113.45	7/16/16	M.S.
RD	MT	OR	46.92	-113.45	7/16/16	M.S.
YL	MT	OR	46.92	-113.45	7/12/16	M.S.
RK	MT	OR	46.92	-113.45	7/16/16	M.S.
GY	MT	OR	46.92	-113.45	7/14/16	M.S.
LDE	MT	OR	46.92	-113.45	7/31/17	M.S.
YW	MT	OR	46.92	-113.45	7/12/16	M.S.
YB	MT	OR	46.92	-113.45	7/12/16	M.S.
LO	MT	OR	46.92	-113.45	7/13/16	M.S.
GO	MT	OR	46.92	-113.45	7/14/16	M.S.
RLE	MT	OR	46.92	-113.45	7/29/17	M.S.
GR	MT	OR	46.92	-113.45	7/14/16	M.S.
LLO	MT	OR	46.92	-113.45	7/13/16	M.S.
RE	MT	OR	46.92	-113.45	7/16/16	M.S.
LW	MT	OR	46.92	-113.45	7/13/16	M.S.
OL	MT	OR	46.92	-113.45	7/19/16	M.S.
LDR	MT	OR	46.92	-113.45	7/31/17	M.S.
LE	MT	OR	46.92	-113.45	7/13/16	M.S.
DW	MT	OR	46.92	-113.45	7/15/16	M.S.
LD	MT	OR	46.92	-113.45	7/13/16	M.S.
GYRR	MT	OR	46.92	-113.45	7/27/17	M.S.
DD	MT	OR	46.92	-113.45	7/15/16	M.S.
RRB	MT	OR	46.92	-113.45	7/16/16	M.S.
GK	MT	OR	46.92	-113.45	7/14/16	M.S.
DO	MT	OR	46.92	-113.45	7/15/16	M.S.
OY	MT	OR	46.92	-113.45	7/19/16	M.S.
DG	MT	OR	46.92	-113.45	7/15/16	M.S.
OE	MT	OR	46.92	-113.45	7/19/16	M.S.
YO	MT	OR	46.92	-113.45	7/12/16	M.S.
RRO	MT	OR	46.92	-113.45	7/16/16	M.S.
GD	MT	OR	46.92	-113.45	7/14/16	M.S.
DL	MT	OR	46.92	-113.45	7/15/16	M.S.
LLW	MT	OR	46.92	-113.45	7/13/16	M.S.
OD	MT	OR	46.92	-113.45	7/19/16	M.S.
GE	MT	OR	46.92	-113.45	7/14/16	M.S.
DDW	MT	OR	46.92	-113.45	7/15/16	M.S.
GW	MT	OR	46.92	-113.45	7/14/16	M.S.
DY	MT	OR	46.92	-113.45	7/15/16	M.S.
DGEE	MT	OR	46.92	-113.45	8/3/17	M.S.
OG	MT	OR	46.92	-113.45	7/19/16	M.S.

DR	MT	OR	46.92	-113.45	7/15/16	M.S.
OOY	MT	OR	46.92	-113.45	7/19/16	M.S.
YY	MT	OR	46.92	-113.45	7/12/16	M.S.
DDE	MT	OR	46.92	-113.45	7/15/16	M.S.
YG	MT	OR	46.92	-113.45	7/12/16	M.S.
LR	MT	OR	46.92	-113.45	7/13/16	M.S.
RL	MT	OR	46.92	-113.45	7/16/16	M.S.
DDK	MT	OR	46.92	-113.45	7/15/16	M.S.
LDDD	MT	OR	46.92	-113.45	7/31/17	M.S.
RLY	MT	OR	46.92	-113.45	7/29/17	M.S.
DE	MT	OR	46.92	-113.45	7/15/16	M.S.
RY	MT	OR	46.92	-113.45	7/16/16	M.S.
GGL	MT	OR	46.92	-113.45	7/14/16	M.S.
RLW	MT	OR	46.92	-113.45	7/29/17	M.S.
DDR	MT	OR	46.92	-113.45	7/15/16	M.S.
LDBB	MT	OR	46.92	-113.45	7/31/17	M.S.
RB	MT	OR	46.92	-113.45	7/16/16	M.S.
RW	MT	OR	46.92	-113.45	7/16/16	M.S.
RR	MT	OR	46.92	-113.45	7/16/16	M.S.
YRG	MT	OR	46.92	-113.45	8/1/17	M.S.
RLB	MT	OR	46.92	-113.45	7/29/17	M.S.
DGR	MT	OR	46.92	-113.45	8/3/17	M.S.
GYG	MT	OR	46.92	-113.45	7/27/17	M.S.
RLD	MT	OR	46.92	-113.45	7/29/17	M.S.
YRWW	MT	OR	46.92	-113.45	8/1/17	M.S.
RLG	MT	OR	46.92	-113.45	7/29/17	M.S.
GYD	MT	OR	46.92	-113.45	7/27/17	M.S.
DGE	MT	OR	46.92	-113.45	8/3/17	M.S.
DGRR	MT	OR	46.92	-113.45	8/3/17	M.S.
GYGG	MT	OR	46.92	-113.45	7/27/17	M.S.
YRW	MT	OR	46.92	-113.45	8/1/17	M.S.
YRYY	MT	OR	46.92	-113.45	8/1/17	M.S.
LDB	MT	OR	46.92	-113.45	7/31/17	M.S.
RLYY	MT	OR	46.92	-113.45	7/29/17	M.S.
YRD	MT	OR	46.92	-113.45	8/1/17	M.S.
YRL	MT	OR	46.92	-113.45	8/1/17	M.S.
LDW	MT	OR	46.92	-113.45	7/31/17	M.S.
RLL	MT	OR	46.92	-113.45	7/29/17	M.S.
LDLL	MT	OR	46.92	-113.45	7/31/17	M.S.
LDGG	MT	OR	46.92	-113.45	7/31/17	M.S.
LDY	MT	OR	46.92	-113.45	7/31/17	M.S.
DGB	MT	OR	46.92	-113.45	8/3/17	M.S.
LDL	MT	OR	46.92	-113.45	7/31/17	M.S.
YRLL	MT	OR	46.92	-113.45	8/1/17	M.S.
DK	MT	OR	46.92	-113.45	7/15/16	M.S.
LDWW	MT	OR	46.92	-113.45	7/31/17	M.S.
RLR	MT	OR	46.92	-113.45	7/28/17	M.S.
RLDD	MT	OR	46.92	-113.45	7/29/17	M.S.
DGY	MT	OR	46.92	-113.45	8/3/17	M.S.
DGD	MT	OR	46.92	-113.45	8/3/17	M.S.
YRY	MT	OR	46.92	-113.45	8/1/17	M.S.
GYLL	MT	OR	46.92	-113.45	7/27/17	M.S.
DDYS	MT	OR	47.52	-113.67	6/19/16	M.S.
2780-95901	MT	OR	47.52	-113.67	6/15/16	M.S.
2780-95904	MT	OR	47.52	-113.67	6/17/16	M.S.

2780-95903	MT	OR	47.52	-113.67	6/17/16	M.S.
2780-95905	MT	OR	47.52	-113.67	6/17/16	M.S.
2780-95908	MT	OR	47.52	-113.67	6/20/16	M.S.
2780-95910	MT	OR	47.52	-113.67	6/20/16	M.S.
2780-95909	MT	OR	47.52	-113.67	6/20/16	M.S.
2780-95902	MT	OR	47.52	-113.67	6/15/16	M.S.
GGYS	MT	OR	47.52	-113.67	6/19/16	M.S.
2780-95912	MT	OR	47.52	-113.67	6/21/16	M.S.
2780-95911	MT	OR	47.52	-113.67	6/21/16	M.S.
NK174539	NM	PS	34.33	-106.86	12/18/13	M.S.
NK174538	NM	PS	34.33	-106.86	12/18/13	M.S.
NK174534	NM	PS	34.33	-106.86	12/18/13	M.S.
NK174541	NM	PS	34.33	-106.86	12/18/13	M.S.
NK174535	NM	PS	34.33	-106.86	12/18/13	M.S.
NK174530	NM	PS	34.33	-106.86	12/17/13	M.S.
NK174527	NM	PS	34.33	-106.86	12/16/13	M.S.
NK174540	NM	PS	34.33	-106.86	12/18/13	M.S.
NK174536	NM	PS	34.33	-106.86	12/18/13	M.S.
NK174529	NM	OR	34.33	-106.86	12/16/13	M.S.
NK174531	NM	PS	34.33	-106.86	12/17/13	M.S.
NK174537	NM	PS	34.33	-106.86	12/18/13	M.S.
NK174528	NM	PS	34.33	-106.86	12/16/13	M.S.
NK174544	NM	OR	34.33	-106.86	12/18/13	M.S.
NK174526	NM	PS	34.33	-106.86	12/16/13	M.S.
NK174533	NM	OR	34.33	-106.86	12/18/13	M.S.
NK174543	NM	OR	34.33	-106.86	12/18/13	M.S.
NK174542	NM	OR	34.33	-106.86	12/18/13	M.S.
NK174532	NM	OR	34.33	-106.86	12/17/13	M.S.
BT4165	NY	SC	42.37	-76.28	6/29/13	M.S.
BT4161	NY	SC	42.37	-76.28	6/26/13	M.S.
BT4162	NY	SC	42.37	-76.28	6/26/13	M.S.
BT4160	NY	SC	42.37	-76.28	6/26/13	M.S.
BT4159	NY	SC	42.37	-76.28	6/26/13	M.S.
BT4158	NY	SC	42.37	-76.28	6/25/13	M.S.
2W.06	SD	SC	42.81	-96.52	1/19/06	D.L.S.
3W.06	SD	SC	42.81	-96.52	2/11/06	D.L.S.
1W.07	SD	SC	42.81	-96.52	1/20/07	D.L.S.
2W.07	SD	SC	42.81	-96.52	1/20/07	D.L.S.
3W.07	SD	SC	42.81	-96.52	1/23/07	D.L.S.
4W.07	SD	SC	42.81	-96.52	1/23/07	D.L.S.
5W.07	SD	SC	42.81	-96.52	1/23/07	D.L.S.
6W.07	SD	SC	42.81	-96.52	1/30/07	D.L.S.
7W.07	SD	SC	42.81	-96.52	1/30/07	D.L.S.
8W.07	SD	SC	42.81	-96.52	1/30/07	D.L.S.
9W.07	SD	SC	42.81	-96.52	2/6/07	D.L.S.
10W.07	SD	SC	42.81	-96.52	2/6/07	D.L.S.
11W.07	SD	SC	42.81	-96.52	2/6/07	D.L.S.
12w.07	SD	SC	42.81	-96.52	2/9/07	D.L.S.
13W.07	SD	SC	42.81	-96.52	2/9/07	D.L.S.
14W.07	SD	SC	42.81	-96.52	2/9/07	D.L.S.
15W.07	SD	SC	42.81	-96.52	2/13/07	D.L.S.
17W.07	SD	SC	42.81	-96.52	2/13/07	D.L.S.
21W.07	SD	SC	42.81	-96.52	2/23/07	D.L.S.
22W.07	SD	SC	42.81	-96.52	2/23/07	D.L.S.
23W.07	SD	SC	42.81	-96.52	2/23/07	D.L.S.

24W.07	SD	SC	42.81	-96.52	2/27/07	D.L.S.
18W.07	SD	SC	42.81	-96.52	2/22/07	D.L.S.
19W.07	SD	SC	42.81	-96.52	2/22/07	D.L.S.
20W.07	SD	SC	42.81	-96.52	2/22/07	D.L.S.
1W.08	SD	SC	42.81	-96.52	1/31/08	D.L.S.
2W.08	SD	SC	42.81	-96.52	1/31/08	D.L.S.
3W.08	SD	SC	42.81	-96.52	2/6/08	D.L.S.
4W.08	SD	SC	42.81	-96.52	2/6/08	D.L.S.
5W.08	SD	SC	42.81	-96.52	2/12/08	D.L.S.
6W.08	SD	SC	42.81	-96.52	2/12/08	D.L.S.
7W.08	SD	SC	42.81	-96.52	2/15/08	D.L.S.
8W.08	SD	SC	42.81	-96.52	2/15/08	D.L.S.
DEJU4_602	WY	PS	43.94	-110.64	6/2/13	M.S.
DEJU3_602	WY	PS	43.94	-110.64	6/2/13	M.S.
DEJU3_617	WY	PS	43.94	-110.64	6/16/13	M.S.
DEJU1_616	WY	PS	43.94	-110.64	6/16/13	M.S.
DEJU1_617	WY	PS	43.94	-110.64	6/16/13	M.S.
DEJU2_617	WY	PS	43.94	-110.64	6/16/13	M.S.
B762	WY	PS	43.8	-110.25	6/9/13	M.S.
B758	WY	PS	43.8	-110.25	6/4/13	M.S.
B757	WY	PS	43.8	-110.25	6/4/13	M.S.
B1002	WY	PS	43.92	-110.46	6/1/15	M.S.
B780	WY	PS	43.92	-110.46	6/15/13	M.S.
B781	WY	PS	43.92	-110.46	6/15/13	M.S.
B1014	WY	PS	43.92	-110.46	6/6/15	M.S.
B1005	WY	PS	43.92	-110.46	6/3/15	M.S.
B767	WY	PS	43.92	-110.46	6/10/13	M.S.
B1010	WY	PS	43.92	-110.46	6/4/15	M.S.
B1003	WY	PS	43.92	-110.46	6/2/15	M.S.
B775	WY	PS	43.92	-110.46	6/12/13	M.S.
B1016	WY	PS	43.92	-110.46	6/6/15	M.S.
B763	WY	PS	43.92	-110.46	6/10/13	M.S.
B772	WY	PS	43.92	-110.46	6/11/13	M.S.
B1007	WY	PS	43.92	-110.46	6/3/15	M.S.
B1012	WY	PS	43.92	-110.46	6/5/15	M.S.
B1004	WY	PS	43.92	-110.46	6/1/15	M.S.
B1043	WY	PS	43.92	-110.46	6/15/15	M.S.
B771	WY	PS	43.92	-110.46	6/10/13	M.S.
B1011	WY	PS	43.92	-110.46	6/5/15	M.S.
B1015	WY	PS	43.92	-110.46	6/6/15	M.S.
B1042	WY	PS	43.92	-110.46	6/15/15	M.S.
B1036	WY	PS	43.92	-110.46	6/13/15	M.S.
B1022	WY	PS	43.92	-110.46	6/8/15	M.S.
B776	WY	PS	43.92	-110.46	6/12/13	M.S.
B1035	WY	PS	43.92	-110.46	6/13/15	M.S.
B1021	WY	PS	43.92	-110.46	6/8/15	M.S.
B1009	WY	PS	43.92	-110.46	6/4/15	M.S.
B1041	WY	PS	43.92	-110.46	6/15/15	M.S.
B1008	WY	PS	43.92	-110.46	6/3/15	M.S.
B1046	WY	PS	43.92	-110.46	6/16/15	M.S.
B1037	WY	PS	43.92	-110.46	6/13/15	M.S.
B1019	WY	PS	43.92	-110.46	6/7/15	M.S.
B1018	WY	PS	43.92	-110.46	6/7/15	M.S.
B769	WY	PS	43.92	-110.46	6/10/13	M.S.
B1006	WY	PS	43.92	-110.46	6/3/15	M.S.

B1013	WY	PS	43.92	-110.46	6/5/15	M.S.
B766	WY	PS	43.92	-110.46	6/10/13	M.S.
B1045	WY	PS	43.92	-110.46	6/16/15	M.S.
B1044	WY	PS	43.92	-110.46	6/16/15	M.S.
B779	WY	PS	43.92	-110.46	6/12/13	M.S.
B770	WY	PS	43.92	-110.46	6/10/13	M.S.
B778	WY	PS	43.92	-110.46	6/12/13	M.S.
B1017	WY	PS	43.92	-110.46	6/7/15	M.S.
B1025	WY	PS	43.75	-110.23	6/10/15	M.S.
B1033	WY	PS	43.75	-110.23	6/11/15	M.S.
B1034	WY	PS	43.75	-110.23	6/11/15	M.S.
B1040	WY	PS	43.75	-110.23	6/14/15	M.S.
B1039	WY	PS	43.75	-110.23	6/14/15	M.S.
B1026	WY	PS	43.75	-110.23	6/10/15	M.S.
B1029	WY	PS	43.75	-110.23	6/11/15	M.S.
B1027	WY	PS	43.75	-110.23	6/10/15	M.S.
B1038	WY	PS	43.75	-110.23	6/14/15	M.S.
B1023	WY	PS	43.75	-110.23	6/10/15	M.S.
B1031	WY	PS	43.75	-110.23	6/11/15	M.S.
B1032	WY	PS	43.75	-110.23	6/11/15	M.S.
B1028	WY	PS	43.75	-110.23	6/10/15	M.S.
B1024	WY	PS	43.75	-110.23	6/10/15	M.S.
B1030	WY	PS	43.75	-110.23	6/10/15	M.S.

Table S2. Information for population genetic samples.

Institution	Catalogue #	Date	Latitude	Longitude	Species	Subspecies
UWBM	53922	6/16/1995	67.49	-149.87	hyemalis	hyemalis
UWBM	118044	5/29/2009	23.81	-99.85	phaeonotus	phaeonotus
UWBM	104984	1/5/2003	21.88	-103.87	phaeonotus	phaeonotus
UWBM	90464	6/16/2010	45.83	-117.88	hyemalis	montanus
UWMV	B1052	//2015	39.60	-105.64	hyemalis	caniceps
AMNH	228735	5/27/1985	37.57	-80.19	hyemalis	carolinensis
UWBM	118114	5/4/2012	37.36	-118.69	hyemalis	thurberi
AMNH	229181	6/6/1990	53.00	-117.34	hyemalis	cismontanus
UWBM	106707	5/18/2004	32.85	-116.42	hyemalis	thurberi
MMNH	47897	6/20/2009	23.65	-109.98	phaeonotus	bairdi
CUMV	BT4159	6//2013	42.37	-76.27	hyemalis	hyemalis
AMNH	228797	7/6/1985	47.62	-112.64	hyemalis	mearnsi
AMNH	203757	5/21/1988	30.91	-115.45	hyemalis	townsendi
UWBM	82536	8/14/2006	23.59	-105.87	phaeonotus	phaeonotus
USNM	648103	6/2/2011	41.91	-113.51	hyemalis	caniceps
AMNH	228930	6/5/1986	47.74	-77.33	hyemalis	hyemalis
UAM	40270	5/28/2016	61.20	-149.87	hyemalis	hyemalis
MVZ	182561	7/13/2006	40.34	-121.43	hyemalis	thurberi
UWBM	105212	1/7/2004	19.05	-99.32	phaeonotus	phaeonotus
MVZ	182089	7/11/2006	37.87	-122.26	hyemalis	pinosus
UWBM	116546	5/31/2012	39.13	-117.28	hyemalis	caniceps
UWBM	112167	7/9/1993	60.20	-132.84	hyemalis	hyemalis
AMNH	228944	6/10/1986	49.78	-85.43	hyemalis	hyemalis
AMNH	229173	6/3/1990	56.40	-103.62	hyemalis	hyemalis
AMNH	229229	6/15/1990	62.09	-136.51	hyemalis	hyemalis
USNM	648671	5/31/2014	34.34	-111.14	hyemalis	dorsalis
MSB	21370	7/8/1994	35.23	-107.61	hyemalis	caniceps
AMNH	231723	6/15/1993	38.50	-109.27	hyemalis	caniceps
AMNH	232004	5/22/1996	32.40	-115.88	hyemalis	pontilis
UWBM	109189	6/18/2004	33.50	-105.78	hyemalis	dorsalis
UWBM	99275	7/7/1998	37.58	-112.60	hyemalis	caniceps
LSU	62689	7/9/2002	42.24	-111.23	hyemalis	mearnsi
AMNH	225057	7/27/1984	44.36	-70.99	hyemalis	hyemalis
UWBM	115982	5/24/2006	35.29	-111.65	hyemalis	dorsalis
AMNH	203755	5/21/1988	30.91	-115.45	hyemalis	townsendi
RAM	Z96.18.3	6/4/1996	49.85	-113.97	hyemalis	montanus
CMNH	71193	6/14/2008	41.34	-76.34	hyemalis	carolinensis
UWBM	115225	4/29/2006	19.42	-102.24	phaeonotus	phaeonotus
UWBM	100206	6/23/2005	45.10	-110.87	hyemalis	mearnsi
AMNH	228862	7/19/1985	44.31	-104.12	hyemalis	aikeni
UWBM	100458	6/15/2006	43.25	-124.12	hyemalis	shufeldti
UWMV	B766	//2013	43.87	-110.48	hyemalis	mearnsi
UWBM	69539	7/24/2001	47.73	-122.08	hyemalis	shufeldti
AMNH	228766	6/28/1985	45.13	-116.12	hyemalis	montanus
AMNH	229183	6/6/1990	53.00	-117.34	hyemalis	cismontanus
MVZ	188263	6/17/2012	15.43	-92.34	phaeonotus	alticola
FMNH	394075	9/7/1989	16.80	-92.64	phaeonotus	fulvescens
MVZ	188265	6/18/2012	15.43	-92.34	phaeonotus	alticola
MSB	40609	6/9/2013	65.37	-146.00	hyemalis	hyemalis
USNM	634217	6/5/2003	38.58	-79.64	hyemalis	carolinensis
AMNH	228867	5/9/1986	34.87	-83.81	hyemalis	carolinensis

MVZ	177471	6/23/1996	41.41	-119.88	hyemalis	thurberi
UWBM	118287	6/6/2014	48.28	-119.95	hyemalis	shufeldti
UWBM	118013	5/24/2009	29.65	-108.17	phaeonotus	palliatus
MVZ	180357	6/30/2003	37.87	-122.27	hyemalis	pinosus
UWBM	100203	6/26/2005	41.88	-115.43	hyemalis	caniceps
UAM	34179	5/12/2013	59.41	-135.93	hyemalis	cismontanus
LSU	16242		9.70	-84.09	vulcani	
UWBM	106976	6/14/2004	31.85	-109.33	phaeonotus	palliatus
AMNH	229059	6/17/1988	51.63	-56.70	hyemalis	hyemalis
UWBM	108713	7/26/2005	39.30	-114.21	hyemalis	caniceps
RAM	Z95.10.16	6/7/1995	58.93	-115.20	hyemalis	hyemalis
CMNH	72566	6/23/2011	44.71	-85.29	hyemalis	hyemalis
UAM	37203	6/23/2015	55.92	-130.03	hyemalis	oreganus
MSB	29429				hyemalis	dorsalis
CMNH	70523	5/21/2007	35.71	-82.40	hyemalis	carolinensis
CMNH	74824	6/16/2017	47.78	-90.89	hyemalis	hyemalis
UWBM	97846	5/1/1998	36.36	-115.66	hyemalis	caniceps
USNM	644223	6/13/2010	40.49	-110.97	hyemalis	mearnsi
UWBM	117971	5/18/2009	24.09	-104.93	phaeonotus	phaeonotus
MVZ	183385	7/11/2008	35.95	-118.33	hyemalis	thurberi
UWBM	118252	6/9/2014	47.33	-120.69	hyemalis	shufeldti
AMNH	225012	11/20/1983	16.73	-92.64	phaeonotus	fulvescens
USNM	644191	6/14/2010	40.96	-110.49	hyemalis	caniceps
UAM	9183	6/24/1998	55.33	-131.62	hyemalis	oreganus
AMNH	232015	6/1/1996	29.04	-118.28	insularis	
UWBM	53396	7/15/1993	38.84	-106.48	hyemalis	caniceps
MSB	41094	6/2/2013	36.25	-109.05	hyemalis	caniceps
AMNH	228775	6/30/1985	44.25	-114.75	hyemalis	montanus
AMNH	229053	6/10/1988	46.73	-65.07	hyemalis	hyemalis
UAM	6056	6/1/1992	55.86	-133.68	hyemalis	oreganus
UMPWM	20648	7//2016	46.89	-113.46	hyemalis	montanus
AMNH	231995	5/22/1996	32.40	-115.88	hyemalis	pontilis
UWBM	110508	6/19/2002	44.87	-107.33	hyemalis	mearnsi
UWBM	117647	6/6/2013	44.57	-121.58	hyemalis	shufeldti
AMNH	229268	6/4/1991	49.88	-119.07	hyemalis	montanus
UWBM	117642	5/21/2013	41.44	-121.03	hyemalis	thurberi
AMNH	228850	7/17/1985	45.31	-106.07	hyemalis	aikeni
UWBM	54065	5/18/1995	48.37	-117.19	hyemalis	montanus
UWBM	113645	5/10/2008	19.08	-99.22	phaeonotus	phaeonotus
NYSM	zo-11135	6/30/2010	42.13	-73.13	hyemalis	hyemalis
SDNHM	51646	5/17/2006	32.88	-117.23	hyemalis	thurberi
UWBM	80775	6/13/2005	45.72	-121.43	hyemalis	shufeldti
AMNH	228738	6/21/1985	46.64	-115.09	hyemalis	montanus
MMNH	47899	6/22/2009	23.65	-109.98	phaeonotus	bairdi
UWBM	118105	5/1/2012	36.95	-117.12	hyemalis	caniceps
CUMV	BT4161	6//2013	42.37	-76.27	hyemalis	hyemalis
UWBM	54098	5/17/1995	48.65	-117.24	hyemalis	montanus
AMNH	229182	6/6/1990	53.00	-117.34	hyemalis	cismontanus
AMNH	228799	7/6/1985	47.62	-112.64	hyemalis	mearnsi
AMNH	231726	6/15/1993	38.50	-109.27	hyemalis	caniceps
UWBM	115229	4/29/2006	19.42	-102.24	phaeonotus	phaeonotus
RAM	Z96.18.7	6/4/1996	49.82	-113.95	hyemalis	montanus
UAM	38138		55.92	-130.03	hyemalis	oreganus
UWBM	117839	6/6/2013	44.57	-121.58	hyemalis	shufeldti
UWBM	104986	1/5/2003	21.88	-103.87	phaeonotus	phaeonotus

AMNH	232018	6/1/1996	29.04	-118.28	insularis	
AMNH	228742	6/21/1985	46.64	-115.09	hyemalis	montanus
UWBM	105123	6/28/2003	49.50	-125.00	hyemalis	shufeldti
AMNH	228768	6/28/1985	45.13	-116.12	hyemalis	montanus
UWMV	B778	//2013	43.87	-110.48	hyemalis	mearnsi
RAM	Z07.1.11	5/2/2003	53.32	-117.87	hyemalis	cismontanus
AMNH	231996	5/22/1996	32.40	-115.88	hyemalis	pontilis
MVZ	181965	7/25/2005	37.87	-122.26	hyemalis	pinosus
UWBM	118015	5/24/2009	29.65	-108.17	phaeonotus	palliatus
FMNH	394076	9/9/1989	16.80	-92.64	phaeonotus	fulvescens
UWBM	109191	6/18/2004	33.50	-105.78	hyemalis	dorsalis
MSB	47704	6/21/2010	44.05	-107.29	hyemalis	mearnsi
UWBM	118047	5/30/2009	23.81	-99.85	phaeonotus	phaeonotus
NYSM	zo-11136	6/30/2010	42.13	-73.13	hyemalis	hyemalis
UWBM	90516	6/16/2010	45.83	-117.88	hyemalis	montanus
AMNH	228736	5/27/1985	37.57	-80.19	hyemalis	carolinensis
UWBM	99276	7/7/1998	37.65	-112.80	hyemalis	caniceps
UAM	11202	6/14/1999	53.37	-132.30	hyemalis	oreganus
RAM	Z95.10.79	6/10/1995	58.93	-115.43	hyemalis	hyemalis
UWBM	54015	6/15/1995	67.49	-149.87	hyemalis	hyemalis
AMNH	228931	6/5/1986	47.74	-77.33	hyemalis	hyemalis
CMNH	72451	6/16/2011	48.06	-92.37	hyemalis	hyemalis
SDNHM	52933	7/24/2009	32.88	-117.24	hyemalis	thurberi
UWBM	108745	7/26/2005	39.30	-114.21	hyemalis	caniceps
CMNH	70525	5/21/2007	35.71	-82.40	hyemalis	carolinensis
AMNH	228868	5/9/1986	34.87	-83.81	hyemalis	carolinensis
MVZ	183387	7/14/2008	35.83	-118.30	hyemalis	thurberi
MVZ	188267	6/18/2012	15.43	-92.34	phaeonotus	alticola
MSB	40611	6/9/2013	65.37	-146.04	hyemalis	hyemalis
USNM	644274	6/14/2010	40.96	-110.49	hyemalis	caniceps
LSU	62701	7/9/2002	42.23	-111.56	hyemalis	mearnsi
UWBM	113649	5/10/2008	19.08	-99.22	phaeonotus	phaeonotus
AMNH	229060	6/17/1988	51.63	-56.70	hyemalis	hyemalis
UMPWM	20649	7//2016	46.89	-113.46	hyemalis	montanus
UWBM	114942	6/14/2004	31.78	-109.30	phaeonotus	palliatus
AMNH	229057	6/10/1988	46.73	-65.07	hyemalis	hyemalis
AMNH	228946	6/10/1986	49.78	-85.43	hyemalis	hyemalis
UWBM	106720	6/4/2004	36.33	-115.63	hyemalis	caniceps
AMNH	228865	7/19/1985	44.31	-104.12	hyemalis	aikeni
USNM	648104	6/2/2011	41.91	-113.51	hyemalis	caniceps
MVZ	182562	7/13/2006	40.34	-121.43	hyemalis	thurberi
UWBM	53404	7/15/1993	38.84	-106.41	hyemalis	caniceps
UWBM	100500	6/15/2006	43.25	-124.12	hyemalis	shufeldti
AMNH	228776	6/30/1985	44.25	-114.75	hyemalis	montanus
AMNH	229281	6/4/1991	49.88	-119.07	hyemalis	montanus
UAM	7489	7/14/1996	55.86	-133.68	hyemalis	oreganus
UWBM	107113	6/26/2005	41.78	-115.70	hyemalis	caniceps
MMNH	47898	6/21/2009	23.65	-109.98	phaeonotus	bairdi
CMNH	72869	6/21/2011	44.69	-85.31	hyemalis	hyemalis
UWBM	118339	6/9/2014	47.33	-120.69	hyemalis	shufeldti
FMNH	394074	9/7/1989	16.80	-92.64	phaeonotus	fulvescens
UAM	40225	5/12/2013	59.41	-135.93	hyemalis	cismontanus
UAM	40271	5/28/2016	61.20	-149.87	hyemalis	hyemalis
MSB	41095	6/1/2013	36.25	-109.05	hyemalis	caniceps
AMNH	225059	7/27/1984	44.36	-70.99	hyemalis	hyemalis

USNM	634220	6/6/2003	38.58	-79.64	hyemalis	carolinensis
UWBM	116031	5/24/2006	35.28	-111.64	hyemalis	dorsalis
AMNH	229230	6/15/1990	62.09	-136.51	hyemalis	hyemalis
AMNH	224997	11/9/1983	30.91	-115.45	hyemalis	townsendi
MSB	26870				hyemalis	dorsalis
MVZ	188264	6/17/2012	15.43	-92.34	phaeonotus	alticola
UWBM	117690	5/21/2013	41.44	-121.03	hyemalis	thurberi
UWBM	106712	5/18/2004	32.85	-116.42	hyemalis	thurberi
AMNH	232020	6/1/1996	29.04	-118.28	insularis	
AMNH	203756	5/21/1988	30.91	-115.45	hyemalis	townsendi
UWBM	81678	6/13/2005	45.72	-121.43	hyemalis	shufeldti
UWBM	100250	6/24/2005	45.28	-110.53	hyemalis	mearnsi
USNM	644266	6/13/2010	40.44	-111.08	hyemalis	mearnsi
CMNH	71373	6/14/2008	41.34	-76.34	hyemalis	carolinensis
UWBM	82650	8/14/2006	23.59	-105.87	phaeonotus	phaeonotus
SDNHM	53914	6/26/2013	33.54	-116.48	hyemalis	thurberi
UWMV	B1072	//2015	39.60	-105.64	hyemalis	caniceps
UWBM	118115	5/4/2012	37.36	-118.69	hyemalis	thurberi
UWBM	118106	5/1/2012	36.95	-117.12	hyemalis	caniceps
AMNH	228851	7/17/1985	45.31	-106.07	hyemalis	aikeni
UWBM	117973	5/18/2009	24.09	-104.93	phaeonotus	phaeonotus
UWBM	105213	1/7/2004	19.05	-99.32	phaeonotus	phaeonotus
MSB	21371	7/8/1994	35.23	-107.61	hyemalis	caniceps
AMNH	229176	6/3/1990	56.40	-103.62	hyemalis	hyemalis
UWBM	116571	5/30/2012	39.13	-117.28	hyemalis	caniceps
UWBM	87111	7/21/2007	58.27	-134.39	hyemalis	oreganus
LSU	16243		9.70	-84.09	vulcani	
MVZ	177474	6/23/1996	41.41	-119.88	hyemalis	thurberi
UWBM	87116	6/21/2007	47.80	-122.13	hyemalis	shufeldti
UWBM	118331	6/6/2014	48.28	-119.95	hyemalis	shufeldti
USNM	648752	5/31/2014	34.34	-111.14	hyemalis	dorsalis

Table S3. Effects of environmental variables on *in situ* M_{sum}. Weather variables are mean value for the 7 days preceding capture. All continuous variables were standardized; n = 292 individuals.

Variable	K	R^2	AICc	ΔAIC
$t_{d\_range} + M_b + Morph$	3	0.46	894.87	0
$prcp + M_b + Morph$	3	0.44	906.33	11.46
$t_{max} + M_b + Morph$	3	0.36	942.85	47.98
$t_{min} + M_b + Morph$	3	0.33	956.09	61.22
$elev + M_b + Morph$	3	0.33	956.46	61.59
$wvp + M_b + Morph$	3	0.33	956.55	61.68
$M_b + Morph$ (null)	2	0.33	956.56	61.69
$dayl + M_b + Morph$	3	0.33	958.08	63.21

Table S4. Effects of daily temperature range (T_{d_range}), morph, and their interaction on *in situ* M_{sum} while controlling for differences in M_b. Estimates vary depending on which morphotype is used as the reference (OR shown in Table1). AICc = 882.03, *n* = 292 individuals, df = 281, R^2 = 0.49.

PS as reference:

Variable	Beta	SD	p
Intercept	**5.53**	**0.14**	**< 2.0 x 10^{-16}**
M_b	**1.43**	**0.17**	**4.38 x 10^{-15}**
Morph (SC)	**1.58**	**0.40**	**1.15 x 10^{-4}**
Morph (YE)	**-1.48**	**0.48**	**2.49 x 10^{-3}**
Morph (GH)	0.62	0.46	0.18
Morph (OR)	**-0.56**	**0.20**	**6.07 x 10^{-3}**
T_{d_range}	-0.02	0.49	0.97
T_{d_range} x SC	**1.65**	**0.71**	**0.02**
T_{d_range} x YE	0.98	0.98	0.32
T_{d_range} x GH	0.98	1.07	0.36
T_{d_range} x OR	**2.47**	**0.56**	**1.47 x 10^{-5}**

GH as reference:

Variable	Beta	SD	p
Intercept	**6.15**	**0.43**	**< 2.0 x 10^{-16}**
M_b	**1.43**	**0.17**	**4.38 x 10^{-15}**
Morph (PS)	-0.62	0.46	0.18
Morph (SC)	0.96	0.56	0.09
Morph (YE)	**-2.09**	**0.63**	**9.72 x 10^{-4}**
Morph (OR)	**-1.18**	**0.46**	**0.01**
T_{d_range}	0.96	0.94	0.31
T_{d_range} x PS	-0.98	1.07	0.36
T_{d_range} x SC	0.67	1.07	0.53
T_{d_range} x YE	0.00	1.28	1.00
T_{d_range} x OR	1.49	0.98	0.13

YE as reference:

Variable	Beta	SD	p
Intercept	**4.06**	**0.46**	**< 2.0 x 10^{-16}**
M_b	**1.43**	**0.17**	**4.38 x 10^{-15}**
Morph (GH)	**2.09**	**0.63**	**9.7 x 10^{-4}**
Morph (OR)	0.91	0.49	0.06
Morph (PS)	**1.47**	**0.48**	**2.49 x 10^{-3}**
Morph (SC)	**3.05**	**0.58**	**2.84 x 10^{-7}**
T_{d_range}	0.96	0.85	0.26
T_{d_range} x GH	-0.00	1.28	1.00
T_{d_range} x OR	1.49	0.90	0.10
T_{d_range} x PS	-0.98	0.98	0.32
T_{d_range} x SC	0.67	1.00	0.50

SC as reference:

Variable	Beta	SD	p
Intercept	**7.11**	**0.37**	**< 2.0 x 10^{-16}**
M_b	**1.43**	**0.17**	**4.38 x 10^{-15}**
Morph (GH)	-0.96	0.56	0.09
Morph (OR)	**-2.14**	**0.42**	**5.52 x 10^{-7}**
Morph (PS)	**-1.58**	**0.40**	**1.15 x 10^{-4}**
Morph (YE)	**-3.05**	**0.58**	**2.84 x 10^{-7}**
T_{d_range}	**1.63**	**0.51**	**1.63 x 10^{-3}**
T_{d_range} x GH	-0.67	1.07	0.53
T_{d_range} x OR	0.82	0.58	0.16
T_{d_range} x PS	**-1.65**	**0.71**	**0.02**
T_{d_range} x YE	-0.67	1.00	0.50

Table S5. Biplot scores for constraining variables in (a) RDA and (b) partial RDA.

(a)

	RDA1	RDA2	RDA3	RDA4	RDA5	RDA6
Mean.Diurnal.Range	0.54843	0.30061	0.38751	-0.51932	-0.04403	-0.432513
Max.Temp	0.24483	0.09411	-0.30458	-0.25235	-0.24632	-0.845033
Temp.Range	-0.47468	0.38066	0.53332	-0.35184	-0.46263	-0.086740
Mean.Temp.WettestQ	0.40998	0.35079	-0.48905	0.06597	-0.64290	0.228068
Annual.Precip	-0.07106	0.33847	-0.23844	0.80106	0.42421	0.043553
Precip.Seasonality	0.69048	-0.50899	-0.04359	0.38808	-0.33414	0.002988

(b)

	RDA1	RDA2	RDA3	RDA4	RDA5	RDA6
Mean.Diurnal.Range	-0.2764	0.006157	0.6281	0.314405	0.4754	-0.017983
Max.Temp	-0.1342	-0.457997	0.2086	0.007904	0.6153	-0.562337
Temp.Range	-0.3948	0.516296	0.4389	-0.252257	0.3531	0.022666
Mean.Temp.WettestQ	-0.2892	-0.463663	-0.1625	-0.628075	0.2319	0.325699
Annual.Precip	-0.3107	-0.118057	-0.8262	0.330436	-0.2874	-0.009349
Precip.Seasonality	0.5067	-0.099768	-0.3679	-0.115856	0.3708	0.220625

Table S6. Genetic variation explained by climatic variable from variance partitioning on RDA.

Climatic Variable	**Df**	**Variance**	**F**	***p***
Mean Diurnal Temperature Range	1	295.5	1.4854	0.001
Maximum Temperature	1	212.9	1.0706	0.012
Temperature Range	1	339.5	1.7067	0.001
Mean Temperature of Wettest Quarter	1	258.7	1.3004	0.001
Annual Precipitation	1	243.6	1.2250	0.001
Precipitation Seasonality	1	240.2	1.2077	0.001
Residual	157	31227.6		

Table S7. Pairwise estimates of Weir and Cockerham weighted F_{ST}. This includes: all 4 *J. h. aikeni* samples, all 7 *J. h. dorsalis* samples, all 4 *J. p. palliatus* samples, 4 *J. h. shufeldti* samples from OR, and 5 *J. h. thurberi* from southern CA.

	J. h. aikeni	*J. h. dorsalis*	*J. h. palliatus*	*J. h. shufeldti*	*J. h. thurberi*
J. h. aikeni		0.031	0.046	0.017	0.039
J. h. dorsalis	0.031		0.013	0.020	0.038
J. h. palliatus	0.046	0.013		0.035	0.053
J. h. shufeldti	0.017	0.020	0.035		0.020
J. h. thurberi	0.039	0.038	0.053	0.020	

Table S8. Linear effects of cold treatment on phenotypic traits before acclimation.

Trait	*n*	Intercept			Cold Treatment			R^2
		β	SE	p	β	SE	p	
M_b	95	20.42	0.32	$< 2 \times 10^{-16}$	0.06	0.46	0.89	0.02
M_{sum}	95	6.87	0.12	$< 2 \times 10^{-16}$	0.21	0.17	0.21	0.01

Figure S1. The five populations — four *J. hyemalis* and one sister group *J. phaeonotus*—used in the acclimation study span ~20°C in annual temperature range. Colors indicates T_{range} in °C from low (pink) to high (green) from WorldClim dataset.

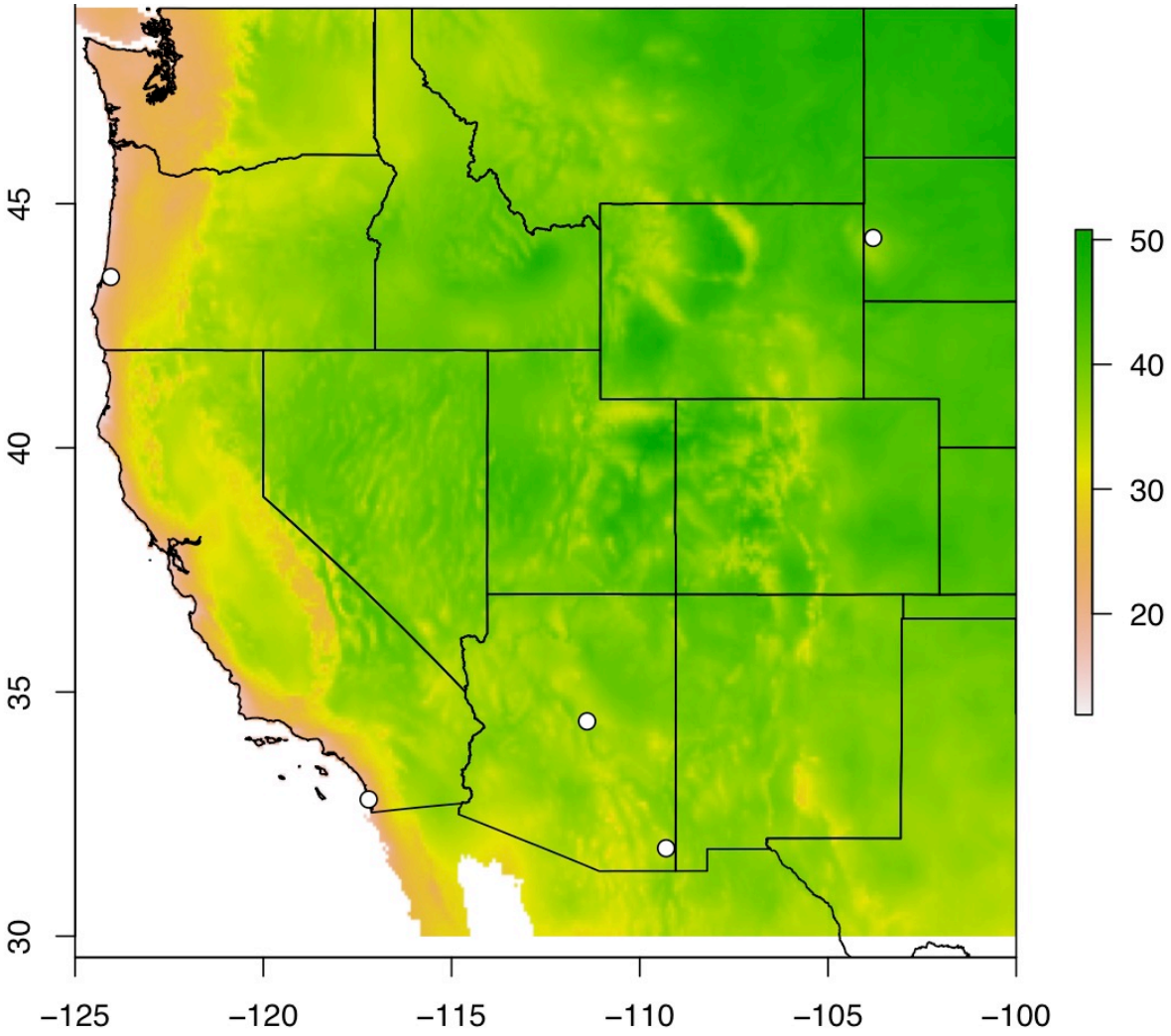

Figure S2. Visualizing population genetic variation with PCA for the subset dataset (n = 164).

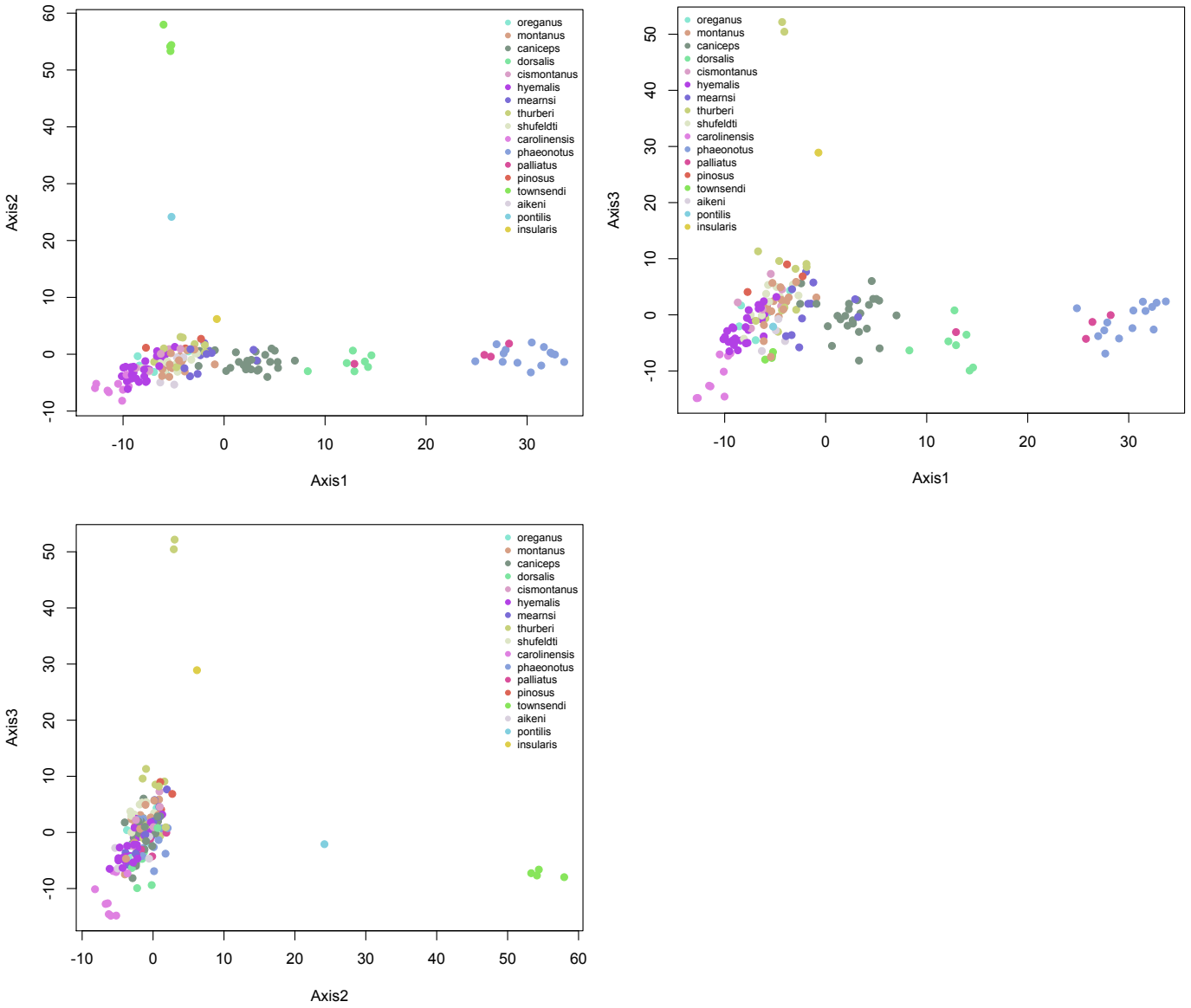

Figure S3. Change in mass over the acclimation period for each population in order from lowest to highest native temperature range (from left to right): *J. h. thurberi* of California (CA), *J. h. shufeldti* of Oregon (OR), *J. p. palliatus* of Arizona (YE), *J. h. dorsalis* of Arizona (AZ), and *J. h. aikeni* of South Dakota (SD). Control birds in red, cold-acclimated birds in blue; $n = 94$.

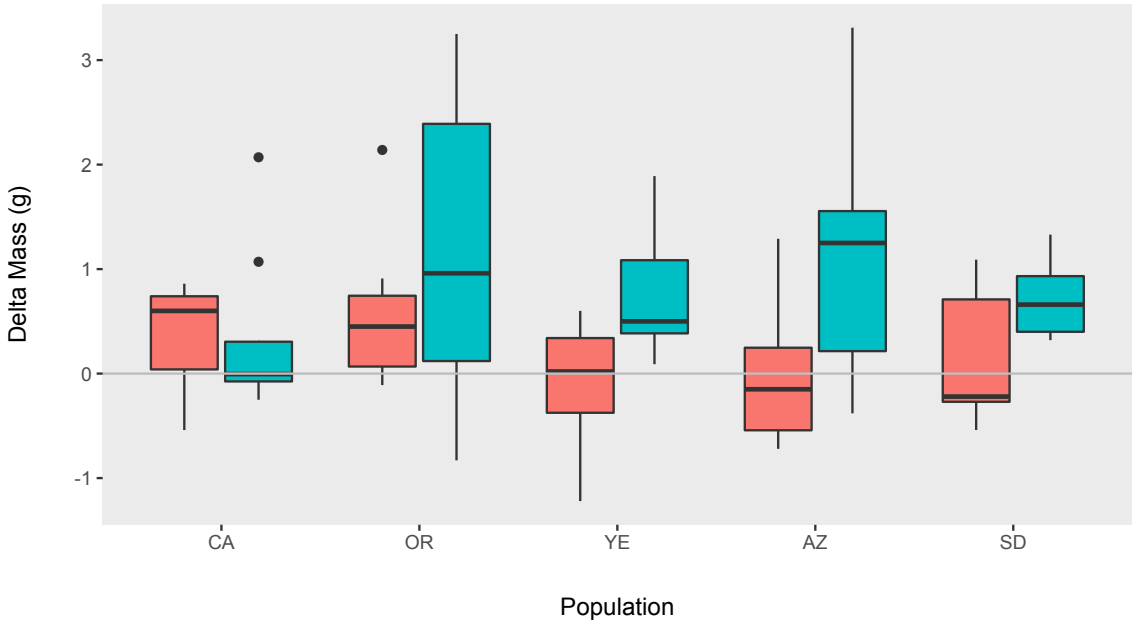

A mechanistic framework for understanding developmental plasticity and phenotypic flexibility

Maria Stager, Jonathan P. Velotta, Zachary A. Cheviron, and Nathan R. Senner

Abstract

Phenotypic plasticity plays a central role in eco-evolutionary theory, but it has long been recognized that the term actually encompasses two processes — developmental plasticity and phenotypic flexibility. These processes are rarely differentiated and are often thought to exist on either side of a continuum. However, the last decade has brought much nuance to this discussion. As we show here, developmental plasticity and phenotypic flexibility actually represent two separate evolutionary outcomes that are regulated by different underlying mechanisms and result in distinct evolutionary trajectories. We thus advocate for a mechanistic approach to elucidating the differences between these two processes and outline how treating them separately has the potential to broaden our understanding of eco-evolutionary dynamics in natural systems. Specifically, we outline how traits tend to either be developmentally plastic or phenotypically flexible as a result of the costs and benefits of repeated trait alteration. We then use this cost-benefit framework to illustrate how developmentally plastic and phenotypically flexible traits vary in their likelihood to become mismatched with the environment and will therefore experience selection differentially. This, in turn, influences their evolutionary consequences, such as population stability and the rate of trait evolution. This framework highlights directions for future theoretical and empirical work that can help determine the importance of developmental plasticity and phenotypic flexibility in eco-evolutionary dynamics.

Introduction

Phenotypic plasticity is the process by which a single genotype expresses multiple trait values in response to changes in the environment (West-Eberhard 2005). As a result of this environmental responsiveness, plasticity is frequently viewed as an adaptive process that can allow individuals to match their phenotype to their environment (Via and Lande 1985). Nonetheless, depending on the environmental context, plasticity can also be neutral or even maladaptive (Van Kleunen and Fischer 2005). This context-dependency, in turn, determines the influence of plasticity on a population's evolutionary dynamics (Ghalambor et al. 2007). For instance, when plasticity is adaptive, it can shield genetic variation from selection and slow evolutionary change (Crispo 2008) or, alternatively, facilitate the persistence of populations in the face of environmental change, enabling local adaptation to occur (Price et al. 2003). On the other hand, when maladaptive, plasticity is hypothesized to increase the rate of evolutionary change by increasing the strength of selection on plastic traits (Ghalambor et al. 2015; Fischer et al. 2016). Given this contingency, there is still much to be learned about when and how plasticity might impact the rate and direction of evolution (Hendry 2016).

One aspect of plasticity that is critical to eco-evolutionary theory but underappreciated, is the fact that the term 'phenotypic plasticity' is frequently used to encompass two separate processes — 'developmental plasticity' and 'phenotypic flexibility' (Piersma and Drent 2003). Developmental plasticity refers to situations in which an individual's environment induces an irreversible, environmentally-specific phenotype (e.g., the jaw morphology of the cichlid fish, *Astatoreochromis alluaudi*; Greenwood 1965), and thus variation is observed *among individuals*. Although the name 'developmental' suggests early-life, these changes do not necessarily occur as a neonate or juvenile (Peng et al. 2020). In contrast, phenotypic flexibility refers to situations in which an individual can reversibly

and repeatedly alter its phenotype in response to environmental conditions throughout its life (e.g., pectoralis muscle size in migratory birds; Piersma et al. 1999), and thus variation is observed *within an individual*. Although it has long been recognized that the expression of some traits is flexible and that of others is developmentally plastic (Stearns 1989), the distinction among them is often overlooked in the literature. A Web of Science search at the time of writing revealed more than 16,000 articles about 'phenotypic plasticity' with 3,396 articles containing 'developmental plasticity', while in contrast only 543 included 'phenotypic flexibility.' This not only illustrates the disproportionate attention paid to developmental plasticity, but also the persistent disregard for distinguishing between the two processes. Moreover, the idea that the two processes may arise as a result of separate, but potentially interacting, processes remains a topic of debate (Woods 2014; Beaman et al. 2016; Burggren 2020). To complicate matters even further, when phenotypic flexibility is discussed, it may be referred to as either 'reversible plasticity' (Alpert and Simms 2002; Gabriel et al. 2005), 'activational plasticity' (Snell-Rood 2013), or 'reversible acclimation' (Beaman et al. 2016). This complex nest of terms has led to frequent confusion and stifled our ability to fully explore the importance of either process.

Here we take a mechanistic approach to understanding the differences between developmental plasticity and phenotypic flexibility (hereafter, plasticity and flexibility). To do this, we first contrast the environmental conditions under which these two processes evolve. We then consider the costs of generating and maintaining plasticity and flexibility, as well as the ways in which selection may act differentially on these two processes. Finally, we review the kinds of traits that tend to be plastic versus flexible and summarize recent research on the genetic basis of each process. Our review highlights that plastic traits differ from flexible traits in a number of key respects, especially their likelihood of becoming mismatched with prevailing environmental conditions. Because these differences can alter the outcomes of selection, we develop predictions about how these two processes should affect the rate and trajectory of evolutionary change. In combination, our framework will help elucidate the role that plasticity and flexibility play in the evolutionary process and identify the degree to which each may enable populations to respond to future environmental change.

The Evolution of Plastic and Flexible Traits

Environmental Variability and Predictability

The spatial and temporal scale of environmental variation and the predictability of environmental change are central to theory regarding the likelihood that canalized (a phenotype exhibits a fixed trait value), plastic, or flexible traits evolve in a particular environment (Schlichting and Pigliucci 1998; Gabriel et al. 2005). It is important to note that, although spatial and temporal variability are often used interchangeably in this paradigm, there are conditions in which they are not the same. For instance, depending on the scale, some organisms may be capable of avoiding spatial variation, while few organisms can avoid temporal variation indefinitely (Camacho et al. 2020). However, here we combine these terms and refer to them simply as 'environmental variation.'

In general, canalized traits are hypothesized to evolve at either extremely high or extremely low levels of environmental variation and predictability (Baythavong 2011; Murren et al. 2015). For instance, in constant, predictable environments, there is likely to be a single phenotypic optimum, with either directional selection driving phenotypic expression toward that optimum or stabilizing selection maintaining that optimum once it has been achieved (Smith and Fretwell 1974). Extremely high levels of environmental variation coupled with low predictability, however, can also lead to the evolution of canalized traits through either conservative or diversified bet hedging (Sasaki and Ellner 1995). Conservative bet hedging evolves when environmental variability is so high that multiple phenotypic

optima exist over the course of an individual's life *and* the rate of environmental change is too rapid or unpredictable to allow the repeated matching of a trait's expression to the environment (see section on 'costs and constraints' below; (Kingsolver et al. 2001)). Thus, in situations of extreme variability, it is optimal to constitutively express the trait value with the highest mean fitness across all environments. Diversified bet hedging, on the other hand, evolves when there is less environmental variation, but predictability remains low and it is therefore optimal for an individual's phenotype to be determined in a probabilistic manner, irrespective of their developmental environment (Einum and Fleming 2004).

Given sufficient genetic variation, plasticity and flexibility evolve somewhere in between extremely low and extremely high levels of environmental variability when predictability is high. In such cases, plasticity tends to evolve when the environment varies across generations, but an individual is unlikely to encounter an environment that differs from that in which it develops (Schlichting and Pigliucci 1998). Flexibility evolves when an individual is likely to experience multiple environments over the course of its life, favoring the ability to alter a phenotype repeatedly (Gabriel et al. 2005). Empirical studies generally support these predictions and, additionally, show that the degree of plasticity and flexibility closely follow gradients in environmental heterogeneity (Gianoli and González-Teuber 2005; Lind and Johansson 2007; Chapter 4).

Costs and Constraints

Two categories of costs and constraints can influence the evolution of plastic and flexible traits — environmentally specific costs (e.g., 'phenotype' costs) and genotypically specific ones (e.g., 'plasticity' costs; Childs et al. 2010; Hallsson and Björklund 2012). Phenotype costs arise when energy must be allocated toward producing, altering, or reversing a phenotype and away from other activities under particular environmental conditions (Botero et al. 2015). Plasticity costs, instead, are attributed to the maintenance of the regulatory, physiological, and developmental machinery needed to produce plastic or flexible traits (McNamara et al. 2016).

Support for the existence of these hypothesized costs and constraints are mixed. Plasticity costs, for instance, are frequently invoked to help explain why more traits are not ubiquitously plastic or why plasticity is lost in constant environments (Van Buskirk and Steiner 2009). Recent empirical research, however, has failed to find evidence for such costs (Masel 2007; Maughan et al. 2007; Latta et al. 2012). Instead, these studies indicate that plasticity tends to be lost in constant environments *via* the relaxed selection and mutation accumulation; as plasticity is no longer under selection, otherwise deleterious mutations can accumulate and blunt ancestral plastic responses in a manner consistent with neutral processes (Masel 2007; Maughan et al. 2007; Latta et al. 2012). Thus, rather than selection acting *against* plasticity in constant environments, loss of plasticity appears to be due to relaxed selection on its maintenance (Leiby and Marx 2014). Nonetheless, other physiological systems must be maintained in order for trait values to be matched with the prevailing environmental conditions (Dore et al. 2018). For example, sensory systems that can assess environmental cues are necessary for the production of environmentally responsive traits (Rouse and Bretman 2016). Alteration of sensory systems may come with pleiotropic costs, as these systems exist both as a part of and separate from those directly involved in producing plastic and/or flexible traits (Sumner-Rooney 2018). Selection can thus act on sensory traits in ways that alter the ability of an organism to produce these phenotypic responses, irrespective of how selection acts on the plastic and/or flexible traits themselves (Niven and Laughlin 2008). Efforts to identify the costs associated with the maintenance of plastic and flexible traits cannot, therefore, solely focus on the genetic machinery needed to

produce them, but must also consider the maintenance of the broader physiological systems of which they are component parts (Dore et al. 2018).

In contrast, existence of phenotype costs has received increasing theoretical and empirical support in recent years (Botero et al. 2015; Siljestam and Östman 2017; Barbosa et al. 2018; but see Magris et al. 2018). These studies suggest that the more energetically costly a trait is to produce, the higher the fitness payoff must be to justify subsequently altering the value of that trait (Bauchinger and McWilliams 2009). Pleiotropic constraints related to altering the trait value may exist, as well (Berger et al. 2014), with entire trait networks needing to be simultaneously altered in order to reverse a single trait in some cases (Naya et al. 2007; but see Chapter 3). Additionally, some traits can take longer to alter or produce than others, leading to significant time lags between the onset of environmental change and an individual's ability to appropriately match their phenotype to that environment (Kaji and Palmer 2017). Thus a cost gradient may exist whereby canalized traits are the most costly or complex to produce or change, plastic traits less so, and flexible traits least of all (Houslay et al. 2017). Accordingly, when the phenotypic cost of a trait is doubled, the predicted trait space in a given environment significantly shifts toward plasticity and away from flexibility (Figure 1; Botero et al. 2015). The question that must be asked when trying to determine whether plasticity or flexibility is likely to evolve in a particular environment is therefore: Can the phenotypic cost of altering a trait's value be sustained by an individual before the environment changes again (Dowd and Denny 2020)?

In this light, some traits are unlikely to evolve flexibility — irrespective of the amount of environmental variation present, the predictability of that variation, or the amount of genetic variation exhibited within a population. However, predictability and environmental variability also mediate the influence of these costs and constraints (Haaland et al. 2019; Botero et al. 2015). As a result, as environments become more variable or less predictable, only those traits with the largest fitness-to-cost ratio are likely to evolve plasticity or flexibility (Siljestam and Östman 2017).

How Does Selection Act on Plastic and Flexible Traits?

The fact that plastic traits are only produced a single time during an individual's life, while flexible traits are repeatedly produced or altered, dictates three things: **(1)** The reaction norm for a plastic trait is an emergent property of selection on alternative trait values across generations within a population, as no single individual ever expresses multiple forms of the induced trait during its lifetime (Via and Lande 1985; De Jong 2005). In contrast, the reaction norm for a flexible trait can emerge from selection on multiple trait values within an individual, as each individual may express all possible forms of a trait over the course of its life (Gabriel et al. 2005). **(2)** As a result, plastic traits are more likely to shield genetic variation from selection in a given generation, because no one individual (or generation) necessarily exposes all variation to direct selection (Gomez-Mestre and Jovani 2013). **(3)** Additionally, the ability of an individual to express a flexible trait may be contingent upon their energetic state and the costs of having previously produced that trait in a different environment (e.g., reversible state effects; *sensu* Senner et al. 2015), while an individual's ability to produce a plastic trait may be constrained by costs carried over from previous generations (e.g., parental effects; Bonduriansky and Day 2009). Despite having the appropriate genotype, individuals may thus be unable to produce the optimal trait value in a given environment as a result of constraints imposed over different timescales depending on whether the trait is plastic (Dong et al. 2018) or flexible (Hennin et al. 2018).

These differences are evident when comparing how selection acts on two hypothetical species — one is semelparous and multi-voltine, while the other is long-lived and iteroparous. In this scenario, the multi-voltine species produces a new generation each

season, with each generation matching its phenotype to the prevailing environmental conditions through the induction of plastic traits — e.g., one generation exhibits trait values tailored to cooler conditions in spring, the next generation trait values optimal for warmer conditions in summer, and, a third generation, trait values for cooler conditions in fall (e.g., Bonduriansky and Day 2009). Genetic variation related to warm conditions may thus be shielded from selection during the spring and fall and *vice versa* for trait values related to cool conditions during the summer (Vellichirammal et al. 2016). Furthermore, the reaction norms of these plastic traits only evolve in response to selection on each generation in succession, as those generations respond to first cool, then warm, and then cool conditions again (Suzuki 2006). In the iteroparous species, on the other hand, an individual that possesses flexibility has the potential to repeatedly match its phenotype to the environment as the seasons change. As a result, if an individual fails to properly match its phenotype to the environment during one season, or is forced to produce a trait value when it is energetically compromised, these costs may limit its ability to properly match its phenotype to the environment in subsequent seasons (Lameris et al. 2017). Selection can then act on a flexible trait both directly within a single season — e.g., *via* a mortality event or reduction in reproductive output resulting directly from the phenotype — or cumulatively across seasons — e.g., *via* constraints resulting from reversible state effects initiated in previous seasons (Senner et al. 2015). As the term reversible state effect implies, however, these costs need not cascade throughout an individual's life, but can be dissipated at any point in time (Senner et al. 2014). Both plastic and flexible traits can thus buffer genetic variation from selection, but do so in different manners: For plastic traits, buffering occurs on a generational timescale, with some parts of the genome being entirely shielded from selection within a generation, while for flexible traits, buffering occurs within an individual, over multiple events, seasons, or years during the course of its life.

Which Types of Traits Tend to be Flexible?

Because plasticity and flexibility differ in the environmental conditions in which they evolve, the costs of their production, and the ways in which selection acts on them, it would follow that they also differ in the types of traits they are associated with. A rough dichotomy appears to exist whereby traits that are more energetically expensive to produce — e.g., morphological traits (Liao et al. 2010) — or traits that tend to be parts of syndromes and therefore linked with many other traits — e.g., an individual's life-history strategy (Kendall et al. 2015; Lackey et al. 2019) — tend to be plastic, while those that are less expensive to produce — e.g., physiological (Battley et al. 2000; Stager et al. 2020) or behavioral traits (O'Mara et al. 2019) — are generally flexible. Furthermore, among flexible traits, there also appears to be a gradient of environmental responsiveness, with more expensive traits being less flexible, while less expensive traits are more flexible (Bauchinger and McWilliams 2009; Chapter 3)

Take small teleost fishes for example. Teleosts have been the subjects of numerous studies investigating plasticity and flexibility and have therefore contributed greatly to our understanding of which trait classes are most likely to be plastic or flexible. For instance, cichlids are renowned for their morphological plasticity, such as the jaw morphology of *Astatoreochromis alluaudi*, which is determined by diet-based developmental plasticity (Greenwood 1965). This plasticity is underlain by changes in gene expression during specific developmental windows (Schneider et al. 2014) and, in turn, is thought to have to played an important role in the dramatic adaptive radiation of cichlids in Lake Malawi (Schneider and Meyer 2017). While many morphological traits appear to be plastic in fishes, this pattern is not universal. Threespine stickleback (*Gasterosteus aculeatus*), for example, can reversibly

alter their morphology — including mouth shape and body size — in response to changes in diet until at least four months into development (Wund et al. 2012).

In contrast, physiological traits tend to be flexible. Euryhaline fish, such as mummichog (*Fundulus heteroclitus*), have markedly flexible responses to changes in environmental salinity (Figure 2). Mummichog begin changing their gill and intestinal physiology within hours of being exposed to a new salinity (Scott et al. 2008). In the transition from fresh- to saltwater, mummichog make rapid alterations to their drinking rate (Scott et al. 2006), the expression and trafficking of ion transport proteins (Marshall et al. 1999), and activation of sodium-potassium pumps at the gill (Flemmer et al. 2010), all of which aid homeostasis in saltwater. There are some circumstances, however, under which aspects of a species' physiology may instead be plastic. For instance, in zebrafish (*Danio rerio*), exposure to warm temperatures during development can lead to plastic changes in an individual's metabolic physiology. Importantly, these metabolic traits remain flexible, but an individual's early-life experiences winnow the degree of flexibility in these traits later in life (Scott and Johnston 2012).

The interaction between plasticity and flexibility is not uncommon and is particularly evident when examining life-history strategies and their subordinate traits. For example, a long series of studies has shown that the presence of predators can lead Trinidadian guppies (*Poecilia reticulata*) to exhibit developmental plasticity in their life-history strategy and personality, leading individuals in the presence of predators to exhibit faster growth, furtive feeding behavior, an earlier age at reproduction, and shorter lifespans (Handelsman et al. 2013). As with the effects of temperature on zebrafish metabolic physiology (Scott and Johnston 2012), however, these divergent life-history strategies do not preclude flexibility in the expression of individual traits, but rather determine the degree of flexibility in those traits (Foster et al. 2015).

While we have outlined rough delineations between those types of traits that tend to be either plastic or flexible, as the teleost fish examples suggest, exceptions do exist (Burggren 2020). These exceptions are informative, however, as they likely reflect the relative fitness benefits of repeatedly altering a trait in relation to its energetic cost (Lázaro et al. 2019). They also can provide powerful opportunities to explore differences in the regulation of plasticity and flexibility within the same traits.

The Regulation of Plastic and Flexible Traits

Determining how plasticity and flexibility are regulated and encoded at the genetic level has long proven difficult. This line of research has made leaps and bounds over the last decade, and recent work has begun to piece these mechanisms together. This work suggests that the two processes may fundamentally differ in their underlying genetic architecture, epigenetic regulation, and patterns of gene expression.

Genetic architecture refers to the landscape of genetic contributions to a given phenotype. It is impossible to conclusively assess all of the ways in which the genetic architecture of plastic and flexible traits might differ at this time, because no complex trait has had its entire genetic architecture mapped (Timpson et al. 2018). Nonetheless, a pattern is beginning to emerge whereby the architecture of flexible traits appears to involve more loci than that of plastic traits (Shao et al. 2008; Kooke et al. 2015; Bresadola et al. 2019). Regardless of the process, pervasive epistatic interactions among genes influencing complex phenotypes is the rule, making it difficult to fully map the effects of specific alleles and indicating that the architecture of most traits may span much of the genome (Taylor and Ehrenreich 2015).

Physical changes to the genome can also regulate gene activity, a process known as epigenetic change. Currently, three types of epigenetic modifications are thought to

contribute to the regulation of gene expression: modifications to the structure of a chromosome (i.e., chromosome folding), modifications to histones, and direct DNA methylation (Zhang and Meaney 2010). These three types of modifications differ in their physical stability and thus the energy required to alter them. Functionally this means that some modifications — like DNA methylation — can fade after a relatively short period of time (e.g., generally hours to days; Sani et al. 2013), while others — like histone modification — can last an individual's entire lifetime or even be passed on to subsequent generations (Klosin et al. 2017). For instance, histone modification and chromatin remodeling have been implicated in the developmental plasticity of social castes in honey bees (Dickman et al. 2013; Wojciechowski et al. 2018) and ants (Simola et al. 2016). On the other hand, DNA methylation can be reversible and thus may be an appropriate mechanism for rapid responses to environmental stimuli (Kohli and Zhang 2013). These distinctions suggest how the regulation of plastic and flexible traits may differ, with potentially longer-lasting alterations affecting the expression of plastic traits, and more transient alterations affecting flexible ones.

Recent transcriptomic work demonstrates a distinction in the regulation of gene expression underlying the two processes. Gene expression can be regulated along two axes: whether or not a gene is being expressed and, if it is being expressed, to what degree (Whitehead and Crawford 2006). Because flexible traits are reversible throughout an individual's life, the expression of the genes encoding flexible traits can vary dramatically, and reversibly, over time (van Bussel et al. 2019). In contrast, the expression of genes related to plastic traits often follow one of three patterns. These genes can (1) be expressed solely during the developmental window during which the phenotype for which they encode is determined (Schneider et al. 2014), (2) set their level of expression during that developmental window and thereafter keep it constant (Lam et al. 2015), or (3) potentially vary over time but have no further impact on the phenotype (Green et al. 2017). In these latter two scenarios, the expression profiles of plastic traits may resemble those of canalized traits for much of an individual's life. These transcriptomic mechanisms are the most clear-cut differences between the two processes and provide a basis for further explorations of other regulatory mechanisms.

Additionally, it is likely that these three mechanisms are operating in concert. For example, Duncan et al. (2020) recently demonstrated that genes that plastically respond to an environmental cue colocalize in clusters across the honeybee genome marked by histone modifications that, in turn, coordinate widespread changes in gene expression. Similarly, despite its impermanence, DNA methylation is also a key player in genomic imprinting and transgenerational plasticity (reviewed in Bell and Hellmann 2019) such that responses to short-term environmental cues by the parent can result in altered phenotypes for subsequent offspring when the histones of these methylated genes are subsequently modified (Skinner et al. 2018). Ultimately, though, more work needs to be done to identify how plasticity and flexibility are regulated, as understanding these three mechanisms is among the frontiers in biology (Laland et al. 2015; Lämke and Bäurle 2017).

The Evolutionary Impacts of Plasticity and Flexibility

The role that phenotypic plasticity plays in the evolutionary process has been predicted under a number of different environmental scenarios (Via and Lande 1985; Chevin and Lande 2011; Ghalambor et al. 2015). Nonetheless, few predictions exist, as of yet, that explicitly differentiate between the roles of plasticity and flexibility (Botero et al. 2015). Two critical questions thus emerge from the fundamental differences we have outlined between these two processes: First, do plastic and flexible traits evolve at different rates? And, second, how do plastic and flexible traits affect the eco-evolutionary dynamics of populations? To begin

filling these gaps, we present a series of predictions about how selection on each process should influence the evolutionary trajectories of populations. We then outline priorities to focus future work in order to test these predictions.

The most salient difference between the two processes is their likelihood to become mismatched with the environment. A plastic trait has only a single opportunity to match its value with its environment, meaning that as environments become more variable, plastic traits are more likely to become mismatched with environmental conditions (Sheriff et al. 2010), experience frequent and/or strong selection, and, therefore, evolve rapidly (Ghalambor et al. 2015). In contrast, because an individual can alter a flexible trait multiple times, potentially reducing the frequency or strength of selection on that trait (Espeland and Rice 2012; Nwaogu et al. 2019), flexible traits should evolve more slowly (Garland and Ives 2000; Jones et al. 2013). At the population level, however, these same differences suggest that — given the same trait — a flexible version of the phenotype should buffer a population more thoroughly from environmental variation than a plastic version of that phenotype (Davidowitz et al. 2012). Populations with more flexibility, in general, may also be more stable (Senner et al. 2017; McFarlane et al. 2018) and evolve longer life spans and slower life-history strategies (Ratikainen and Kokko 2019). Projections of future environmental change predict that many ecosystems will become more variable (Prein et al. 2017). We would therefore expect to see a trend toward the evolution of more flexible traits across populations (Nussey et al. 2005), accompanied by frequent extinctions among small populations characterized by plasticity when newly variable environments exert strong selection (Senner et al. 2018). Alternatively, if conditions become too variable or unpredictable, bet-hedging strategies may become more common (Crowley et al. 2016).

Another frequent prediction is that continued global change will lead to novel or 'non-analog' environments (Williams et al. 2007). In such circumstances, we predict that plastic and flexible traits are equally likely to become mismatched with the new environmental conditions, as neither is predisposed to tracking environmental conditions outside their evolved reaction norms. Instead, potential differences in genetic variation, architecture, and regulation that influence trait evolvability will play a larger role in a population's response to novel environments (Velotta and Cheviron 2018; Draghi 2019). The outcome of future studies on the genetics of plasticity and flexibility will therefore determine whether past predictions (suggesting that novel environments will exert strong selection pressures on traits and lead to frequent extinctions) are robust to treating plastic and flexible traits separately (Ghalambor et al. 2015).

Testing these predictions will require a concerted effort to undertake studies that cross traditional boundaries among disciplines. For instance, studies are needed to identify how phenotype costs are manifested, especially for flexible traits. Current models only assess costs in plastic traits where there is a one-time cost to trait production (Skelly 1992; Rolandi and Schilman 2018; Innes-Gold et al. 2019). However, in flexible traits, we also need to take into account the cost of trait reversion. Importantly, the costs of altering flexible traits may further differ depending on the direction in which a trait is being changed (e.g., from trait value A to B as opposed to B to A), but this hypothesis lacks either empirical or theoretical support. Accurately quantifying the phenotype costs of plastic and flexible traits will go a long way toward helping confirm predictions about the environments in which flexibility and plasticity should be favored.

Similarly, we need to deepen our understanding of how demographic processes may influence the ways in which selection acts on plastic and flexible traits. Gene flow among populations with dissimilar selection regimes is predicted to increase plasticity/flexibility in order to aid offspring that experience a dissimilar environment from their parents (Sultan and Spencer 2002; Stone et al. 2011). Additional historical demographic processes can shape

adaptive outcomes, as well (Benham and Cheviron 2020). Few empirical studies have taken such processes into account (but see Lind et al. 2011; Chapter 4) and thus more empirical studies are needed to link demographic processes with variation in plasticity and flexibility across a species' range and help place contemporary selection regimes in an evolutionary context.

Finally, few studies have actually measured selection on either flexibility or plasticity (Nussey et al. 2005). Without appropriate selection coefficients, it is difficult to identify the degree to which either process may lend stability to populations in the face of environmental change. As a result, there remains debate about whether plasticity will be sufficient to buffer populations against climate change (Gill et al. 2014; Gunderson et al. 2017). More long-term field studies focused on selection on plastic and flexible traits are needed as environments begin to change more rapidly (Senner et al. 2020).

Conclusion

Although much remains to be learned about plasticity and flexibility, clear differences exist between the two processes. These differences suggest that plastic and flexible traits may not only evolve under different circumstances, but also are likely to influence eco-evolutionary dynamics in distinct ways, affecting how populations are able to respond to environmental change. We thus advocate that future efforts should consider phenotypic flexibility and developmental plasticity to be separate processes, each worthy of interest in their own right. Only in this way can we begin to more fully elucidate how evolution should be expected to proceed across populations and environmental contexts.

References

Alpert, P., and E. L. Simms. 2002. The relative advantages of plasticity and fixity in different environments: when is it good for a plant to adjust? Evolutionary Ecology 16:285–297.

Barbosa, F., D. Rebar, and M. D. Greenfield. 2018. When do trade-offs occur? The roles of energy constraints and trait flexibility in bushcricket populations. Journal of Evolutionary Biology 31:287–301.

Battley, P. F., T. Piersma, M. W. Dietz, S. Tang, A. Dekinga, and K. Hulsman. 2000. Empirical evidence for differential organ reductions during trans–oceanic bird flight. Proceedings of the Royal Society of London. Series B: Biological Sciences 267:191–195.

Bauchinger, U., and S. McWilliams. 2009. Carbon turnover in tissues of a passerine bird: allometry, isotopic clocks, and phenotypic flexibility in organ size. Physiological and Biochemical Zoology 82:787–797.

Baythavong, B. S. 2011. Linking the spatial scale of environmental variation and the evolution of phenotypic plasticity: selection favors adaptive plasticity in fine-grained environments. The American Naturalist 178:75–87.

Beaman, J. E., C. R. White, and F. Seebacher. 2016. Evolution of plasticity: mechanistic link between development and reversible acclimation. Trends in Ecology & Evolution 31:237–249.

Bell, A. M., and J. K. Hellmann. 2019. An Integrative framework for understanding the mechanisms and multigenerational consequences of transgenerational plasticity. Annual Review of Ecology, Evolution, and Systematics 50:97–118.

Benham, P. M., and Z. A. Cheviron. 2020. Population history and the selective landscape shape patterns of osmoregulatory trait divergence in tidal marsh Savannah sparrows (Passerculus sandwichensis). Evolution 74:57–72.

Berger, D., R. J. Walters, and W. U. Blanckenhorn. 2014. Experimental evolution for generalists and specialists reveals multivariate genetic constraints on thermal reaction norms. Journal of Evolutionary Biology 27:1975–1989.

Bonduriansky, R., and T. Day. 2009. Nongenetic inheritance and its evolutionary implications. Annual Review of Ecology, Evolution, and Systematics 40:103–125.

Botero, C. A., F. J. Weissing, J. Wright, and D. R. Rubenstein. 2015. Evolutionary tipping points in the capacity to adapt to environmental change. Proceedings of the National Academy of Sciences 112:184–189.

Bresadola, L., C. Caseys, S. Castiglione, C. A. Buerkle, D. Wegmann, and C. Lexer. 2019. Admixture mapping in interspecific *Populus* hybrids identifies classes of genomic architectures for phytochemical, morphological and growth traits. New Phytologist 223:2076–2089.

Burggren, W. W. 2020. phenotypic switching resulting from developmental plasticity: fixed or reversible? Frontiers in Physiology 10:1634.

Camacho, C., A. Sanabria-Fernández, A. Baños-Villalba, and P. Edelaar. 2020. Experimental evidence that matching habitat choice drives local adaptation in a wild population. Proceedings of the Royal Society B: Biological Sciences 287:20200721.

Chevin, L.-M., and R. Lande. 2011. Adaptation to marginal habitats by evolution of increased phenotypic plasticity: evolving plasticity in marginal populations. Journal of Evolutionary Biology 24:1462–1476.

Childs, D. Z., C. J. E. Metcalf, and M. Rees. 2010. Evolutionary bet-hedging in the real world: empirical evidence and challenges revealed by plants. Proceedings of the Royal Society B: Biological Sciences 277:3055–3064.

Crispo, E. 2008. Modifying effects of phenotypic plasticity on interactions among natural selection, adaptation and gene flow. Journal of Evolutionary Biology 21:1460–1469.

Crowley, P. H., S. M. Ehlman, E. Korn, and A. Sih. 2016. Dealing with stochastic environmental variation in space and time: bet hedging by generalist, specialist, and diversified strategies. Theoretical Ecology 9:149–161.

Davidowitz, G., H. F. Nijhout, and D. A. Roff. 2012. Predicting the response to simultaneous selection: genetic architecture and physiological constraints. Evolution 66:2916–2928.

De Jong, G. 2005. Evolution of phenotypic plasticity: patterns of plasticity and the emergence of ecotypes. New Phytologist 166:101–118.

Dickman, M. J., R. Kucharski, R. Maleszka, and P. J. Hurd. 2013. Extensive histone post-translational modification in honey bees. Insect Biochemistry and Molecular Biology 43:125–137.

Dong, B.-C., M. van Kleunen, and F.-H. Yu. 2018. Context-dependent parental effects on clonal offspring performance. Frontiers in Plant Science 9:1824.

Dore, A. A., L. McDowall, J. Rouse, A. Bretman, M. J. G. Gage, and T. Chapman. 2018. The role of complex cues in social and reproductive plasticity. Behavioral Ecology and Sociobiology 72:124.

Dowd, W. W., and M. W. Denny. n.d. A series of unfortunate events: characterizing the contingent nature of physiological extremes using long-term environmental records 9.

Draghi, J. 2019. Phenotypic variability can promote the evolution of adaptive plasticity by reducing the stringency of natural selection. Journal of Evolutionary Biology 32:1274–1289.

Duncan, E. J., M. P. Leask, and P. K. Dearden. 2020. Genome architecture facilitates phenotypic plasticity in the honeybee (*Apis mellifera*). Molecular Biology and Evolution 37:1964–1978.

Einum, S., and I. A. Fleming. 2004. Environmental unpredictability and offspring size: conservative versus diversified bet-hedging. Evolutionary Ecology Research 6:443–455.

Espeland, E. K., and K. J. Rice. 2012. Within- and trans-generational plasticity affects the opportunity for selection in barbed goatgrass (*Aegilops triuncialis*). American Journal of Botany 99:2058–2062.

Evans, D. H., P. M. Piermarini, and K. P. Choe. 2005. The multifunctional fish gill: dominant site of gas exchange, osmoregulation, acid-base regulation, and excretion of nitrogenous waste. Physiological Reviews 85:97–177.

Fischer, E. K., C. K. Ghalambor, and K. L. Hoke. 2016. Can a network approach resolve how adaptive vs nonadaptive plasticity impacts evolutionary trajectories? Integrative and Comparative Biology 56:877–888.

Flemmer, A. W., M. Y. Monette, M. Djurisic, B. Dowd, R. Darman, I. Gimenez, and B. Forbush. 2010. Phosphorylation state of the Na+-K+-Cl- cotransporter (NKCC1) in the gills of Atlantic killifish (*Fundulus heteroclitus*) during acclimation to water of varying salinity. Journal of Experimental Biology 213:1558–1566.

Foster, S. A., M. A. Wund, M. A. Graham, R. L. Earley, R. Gardiner, T. Kearns, and J. A. Baker. 2015. Iterative development and the scope for plasticity: contrasts among trait categories in an adaptive radiation. Heredity 115:335–348.

Gabriel, W., B. Luttbeg, A. Sih, and R. Tollrian. 2005. Environmental tolerance, heterogeneity, and the evolution of reversible plastic responses. The American Naturalist 166:339–353.

Garland, T., and A. R. Ives. 2000. Using the past to predict the present: confidence intervals for regression equations in phylogenetic comparative methods. The American Naturalist 155:346–364.

Ghalambor, C. K., K. L. Hoke, E. W. Ruell, E. K. Fischer, D. N. Reznick, and K. A. Hughes. 2015. Non-adaptive plasticity potentiates rapid adaptive evolution of gene expression in nature. Nature 525:372–375.

Ghalambor, C. K., J. K. McKAY, S. P. Carroll, and D. N. Reznick. 2007. Adaptive versus non-adaptive phenotypic plasticity and the potential for contemporary adaptation in new environments. Functional Ecology 21:394–407.

Gianoli, E., and M. González-Teuber. 2005. Environmental heterogeneity and population differentiation in plasticity to drought in *Convolvulus Chilensis* (Convolvulaceae). Evolutionary Ecology 19:603–613.

Gill, J. A., J. A. Alves, W. J. Sutherland, G. F. Appleton, P. M. Potts, and T. G. Gunnarsson. 2014. Why is timing of bird migration advancing when individuals are not? Proceedings of the Royal Society B: Biological Sciences 281:20132161.

Gomez-Mestre, I., and R. Jovani. 2013. A heuristic model on the role of plasticity in adaptive evolution: plasticity increases adaptation, population viability and genetic variation. Proceedings of the Royal Society B: Biological Sciences 280:20131869.

Green, R. M., J. L. Fish, N. M. Young, F. J. Smith, B. Roberts, K. Dolan, I. Choi, et al. 2017. Developmental nonlinearity drives phenotypic robustness. Nature Communications 8:1970.

Greenwood, P. H. 1965. Environmental effects on the pharyngeal mill of a cichlid fish, *Astatoreochromis alluaudi*, and their taxonomic implications. Proceedings of the Linnean Society of London 176:1–10.

Gunderson, A. R., M. E. Dillon, and J. H. Stillman. 2017. Estimating the benefits of plasticity in ectotherm heat tolerance under natural thermal variability. (S. C. Trullas, ed.)Functional Ecology 31:1529–1539.

Haaland, T. R., J. Wright, and I. I. Ratikainen. n.d. Bet-hedging across generations can affect the evolution of variance-sensitive strategies within generations 10.

Hallsson, L. R., and M. Björklund. 2012. Selection in a fluctuating environment leads to decreased genetic variation and facilitates the evolution of phenotypic plasticity: Evolutionary response in a fluctuating environment. Journal of Evolutionary Biology 25:1275–1290.

Handelsman, C. A., E. D. Broder, C. M. Dalton, E. W. Ruell, C. A. Myrick, D. N. Reznick, and C. K. Ghalambor. 2013. Predator-induced phenotypic plasticity in metabolism and rate of growth: rapid adaptation to a novel environment. Integrative and Comparative Biology 53:975–988.

Hendry, A. P. 2016. Key questions on the role of phenotypic plasticity in eco-evolutionary dynamics. Journal of Heredity 107:25–41.

Hennin, H. L., C. J. Dey, J. Bêty, H. G. Gilchrist, P. Legagneux, T. D. Williams, and O. P. Love. 2018. Higher rates of prebreeding condition gain positively impacts clutch size: A mechanistic test of the condition-dependent individual optimization model. (S. Portugal, ed.) Functional Ecology 32:2019–2028.

Houslay, T. M., K. F. Houslay, J. Rapkin, J. Hunt, and L. F. Bussière. 2017. Mating opportunities and energetic constraints drive variation in age-dependent sexual signalling. (C. Miller, ed.)Functional Ecology 31:728–741.

Innes-Gold, A. A., N. Y. Zuczek, and J. C. Touchon. 2019. Right phenotype, wrong place: predator-induced plasticity is costly in a mismatched environment. Proceedings of the Royal Society B: Biological Sciences 286:20192347.

Jones, N. T., B. C. Husband, and A. S. MacDougall. 2013. Reproductive system of a mixed-mating plant responds to climate perturbation by increased selfing. Proceedings of the Royal Society B: Biological Sciences 280:20131336.

Kaji, T., and A. R. Palmer. 2017. How reversible is development? Contrast between developmentally plastic gain and loss of segments in barnacle feeding legs. Evolution 71:756–765.

Kendall, N. W., J. R. McMillan, M. R. Sloat, T. W. Buehrens, T. P. Quinn, G. R. Pess, K. V. Kuzishchin, et al. 2015. Anadromy and residency in steelhead and rainbow trout

(*Oncorhynchus mykiss*): a review of the processes and patterns. (M. Bradford, ed.) Canadian Journal of Fisheries and Aquatic Sciences 72:319–342.

Kingsolver, J. G., H. E. Hoekstra, J. M. Hoekstra, D. Berrigan, S. N. Vignieri, C. E. Hill, A. Hoang, et al. 2001. The strength of phenotypic selection in natural populations. The American Naturalist 157:245–261.

Klosin, A., E. Casas, C. Hidalgo-Carcedo, T. Vavouri, and B. Lehner. 2017. Transgenerational transmission of environmental information in *C. elegans*. Science 356:320–323.

Kohli, R. M., and Y. Zhang. 2013. TET enzymes, TDG and the dynamics of DNA demethylation. Nature 502:472–479.

Kooke, R., F. Johannes, R. Wardenaar, F. Becker, M. Etcheverry, V. Colot, D. Vreugdenhil, et al. 2015. Epigenetic basis of morphological variation and phenotypic plasticity in *Arabidopsis thaliana*. The Plant Cell 27:337–348.

Lackey, A. C. R., M. P. Moore, J. Doyle, N. Gerlanc, A. Hagan, M. Geile, C. Eden, et al. 2019. Lifetime fitness, sex-specific life history, and the maintenance of a polyphenism. The American Naturalist 194:230–245.

Laland, K. N., T. Uller, M. W. Feldman, K. Sterelny, G. B. Müller, A. Moczek, E. Jablonka, et al. 2015. The extended evolutionary synthesis: its structure, assumptions and predictions. Proceedings of the Royal Society B: Biological Sciences 282:20151019.

Lam, D. D., F. S. J. de Souza, S. Nasif, M. Yamashita, R. López-Leal, V. Otero-Corchon, K. Meece, et al. 2015. Partially redundant enhancers cooperatively maintain mammalian Pomc expression above a critical functional threshold. (G. S. Barsh, ed.)PLOS Genetics 11:e1004935.

Lameris, T. K., I. Scholten, S. Bauer, M. M. P. Cobben, B. J. Ens, and B. A. Nolet. 2017. Potential for an Arctic-breeding migratory bird to adjust spring migration phenology to Arctic amplification. Global Change Biology 23:4058–4067.

Lämke, J., and I. Bäurle. 2017. Epigenetic and chromatin-based mechanisms in environmental stress adaptation and stress memory in plants. Genome Biology 18:124.

Latta, L. C., L. J. Weider, J. K. Colbourne, and M. E. Pfrender. 2012. The evolution of salinity tolerance in Daphnia: a functional genomics approach. Ecology Letters 15:794–802.

Lázaro, J., M. Hertel, M. Muturi, and D. K. N. Dechmann. 2019. Seasonal reversible size changes in the braincase and mass of common shrews are flexibly modified by environmental conditions. Scientific Reports 9:2489.

Leiby, N., and C. J. Marx. 2014. Metabolic erosion primarily through mutation accumulation, and not tradeoffs, drives limited evolution of substrate specificity in *Escherichia coli*. (N. A. Moran, ed.)PLoS Biology 12:e1001789.

Liao, B.-Y., M.-P. Weng, and J. Zhang. 2010. Contrasting genetic paths to morphological and physiological evolution. Proceedings of the National Academy of Sciences 107:7353–7358.

Lind, M. I., P. K. Ingvarsson, H. Johansson, D. Hall, and F. Johansson. 2011. Gene flow and selection on phenotypic plasticity in an island system of *Rana temporaria*. Evolution 65:684–697.

Lind, M. I., and F. Johansson. 2007. The degree of adaptive phenotypic plasticity is correlated with the spatial environmental heterogeneity experienced by island populations of *Rana temporaria*. Journal of Evolutionary Biology 20:1288–1297.

Magris, M., G. Chimetto, S. Rizzi, and A. Pilastro. 2018. Quick-change artists: male guppies pay no cost to repeatedly adjust their sexual strategies. Behavioral Ecology 29:1113–1123.

Marshall, W. S., T. R. Emberley, T. D. Singer, S. E. Bryson, and S. D. McCormick. 1999. Time course of salinity adaptation in a strongly euryhaline estuarine teleost, *Fundulus heteroclitus*: a multivariable approach. Journal of Experimental Biology 202:1534–1544.

Masel, J. 2007. The Loss of Adaptive Plasticity during long periods of environmental stasis. The American Naturalist 169:38–46.

Maughan, H., J. Masel, C. W. Birky, and W. L. Nicholson. 2007. The roles of mutation accumulation and selection in loss of sporulation in experimental populations of *Bacillus subtilis*. Genetics 177:937–948.

McFarlane, S. E., M. Ålund, P. M. Sirkiä, and A. Qvarnström. 2018. Difference in plasticity of resting metabolic rate - the proximate explanation to different niche breadth in sympatric *Ficedula* flycatchers. Ecology and Evolution 8:4575–4586.

McNamara, J. M., S. R. X. Dall, P. Hammerstein, and O. Leimar. 2016. Detection vs. selection: integration of genetic, epigenetic and environmental cues in fluctuating environments. (T. Coulson, ed.)Ecology Letters 19:1267–1276.

Murren, C. J., J. R. Auld, H. Callahan, C. K. Ghalambor, C. A. Handelsman, M. A. Heskel, J. G. Kingsolver, et al. 2015. Constraints on the evolution of phenotypic plasticity: limits and costs of phenotype and plasticity. Heredity 115:293–301.

Naya, D. E., C. Veloso, J. L. P. Muñoz, and F. Bozinovic. 2007. Some vaguely explored (but not trivial) costs of tail autotomy in lizards. Comparative Biochemistry and Physiology Part A: Molecular & Integrative Physiology 146:189–193.

Niven, J. E., and S. B. Laughlin. 2008. Energy limitation as a selective pressure on the evolution of sensory systems. Journal of Experimental Biology 211:1792–1804.

Nussey, D. H., E. Postma, P. Gienapp, and M. E. Visser. 2005. Selection on heritable phenotypic plasticity in a wild bird population. Science 310:304–306.

Nwaogu, C. J., B. I. Tieleman, and W. Cresswell. 2019. Weak breeding seasonality of a songbird in a seasonally arid tropical environment arises from individual flexibility and strongly seasonal moult. Ibis 161:533–545.

O'Mara, M. T., M. Wikelski, B. Kranstauber, and D. K. N. Dechmann. 2019. First three-dimensional tracks of bat migration reveal large amounts of individual behavioral flexibility. Ecology 100:e02762.

Peng, C., Q. Wang, H. Shi, J. Chen, S. Li, H. Zhao, H. Lin, et al. 2020. Natural sex change in mature protogynous orange-spotted grouper (*Epinephelus coioides*): gonadal restructuring, sex hormone shifts and gene profiles. Journal of Fish Biology jfb.14434.

Piersma, T., and J. Drent. 2003. Phenotypic flexibility and the evolution of organismal design. Trends in Ecology & Evolution 18:228–233.

Piersma, T., G. A. Gudmundsson, and K. Lilliendahl. 1999. Rapid changes in the size of different functional organ and muscle groups during refueling in a long-distance migrating shorebird. Physiological and Biochemical Zoology 72:405–415.

Prein, A. F., R. M. Rasmussen, K. Ikeda, C. Liu, M. P. Clark, and G. J. Holland. 2017. The future intensification of hourly precipitation extremes. Nature Climate Change 7:48–52.

Price, T. D., A. Qvarnström, and D. E. Irwin. 2003. The role of phenotypic plasticity in driving genetic evolution. Proceedings of the Royal Society of London. Series B: Biological Sciences 270:1433–1440.

Ratikainen, I. I., and H. Kokko. 2019. The coevolution of lifespan and reversible plasticity. Nature Communications 10:538.

Rolandi, C., and P. E. Schilman. 2018. The costs of living in a thermal fluctuating environment for the tropical haematophagous bug, Rhodnius prolixus. Journal of Thermal Biology 74:92–99.

Rouse, J., and A. Bretman. 2016. Exposure time to rivals and sensory cues affect how quickly males respond to changes in sperm competition threat. Animal Behaviour 122:1–8.

Sani, E., P. Herzyk, G. Perrella, V. Colot, and A. Amtmann. 2013. Hyperosmotic priming of Arabidopsis seedlings establishes a long-term somatic memory accompanied by specific changes of the epigenome. Genome Biology 14:R59.

Sasaki, A., and S. Ellner. 1995. The evolutionarily stable phenotype distribution in a random environment. Evolution 49:337–350.

Schlichting, C. D., and M. Pigliucci. 1998. Phenotypic evolution: a reaction norm perspective.

Schneider, R. F., Y. Li, A. Meyer, and H. M. Gunter. 2014. Regulatory gene networks that shape the development of adaptive phenotypic plasticity in a cichlid fish. Molecular Ecology 23:4511–4526.

Schneider, R. F., and A. Meyer. 2017. How plasticity, genetic assimilation and cryptic genetic variation may contribute to adaptive radiations. Molecular Ecology 26:330–350.

Scott, G. R., D. W. Baker, P. M. Schulte, and C. M. Wood. 2008. Physiological and molecular mechanisms of osmoregulatory plasticity in killifish after seawater transfer. Journal of Experimental Biology 211:2450–2459.

Scott, G. R., and I. A. Johnston. 2012. Temperature during embryonic development has persistent effects on thermal acclimation capacity in zebrafish. Proceedings of the National Academy of Sciences 109:14247–14252.

Scott, G. R., P. M. Schulte, and C. M. Wood. 2006. Plasticity of osmoregulatory function in the killifish intestine: drinking rates, salt and water transport, and gene expression after freshwater transfer. Journal of Experimental Biology 209:4040–4050.

Senner, N. R., J. R. Conklin, and T. Piersma. 2015. An ontogenetic perspective on individual differences. Proceedings of the Royal Society B: Biological Sciences 282:20151050.

Senner, N. R., W. M. Hochachka, J. W. Fox, and V. Afanasyev. 2014. An exception to the rule: carry-over effects do not accumulate in a long-distance migratory bird. (H.-U. Peter, ed.)PLoS ONE 9:e86588.

Senner, N. R., Y. E. Morbey, and B. K. Sandercock. 2020. Editorial: Flexibility in the Migration Strategies of Animals. Frontiers in Ecology and Evolution 8:111.

Senner, N. R., M. Stager, and Z. A. Cheviron. 2018. Spatial and temporal heterogeneity in climate change limits species' dispersal capabilities and adaptive potential. Ecography 41:1428–1440.

Senner, N. R., M. Stager, and B. K. Sandercock. 2017. Ecological mismatches are moderated by local conditions for two populations of a long-distance migratory bird. Oikos 126:61–72.

Shao, H., L. C. Burrage, D. S. Sinasac, A. E. Hill, S. R. Ernest, W. O'Brien, H.-W. Courtland, et al. 2008. Genetic architecture of complex traits: Large phenotypic effects and pervasive epistasis. Proceedings of the National Academy of Sciences 105:19910–19914.

Sheriff, M. J., C. J. Krebs, and R. Boonstra. 2010. The ghosts of predators past: population cycles and the role of maternal programming under fluctuating predation risk. Ecology 91:12.

Siljestam, M., and Ö. Östman. 2017. The combined effects of temporal autocorrelation and the costs of plasticity on the evolution of plasticity. Journal of Evolutionary Biology 30:1361–1371.

Simola, D. F., R. J. Graham, C. M. Brady, B. L. Enzmann, C. Desplan, A. Ray, L. J. Zwiebel, et al. 2016. Epigenetic (re)programming of caste-specific behavior in the ant Camponotus floridanus. Science 351.

Skelly, D. K. 1992. Field evidence for a cost of behavioral antipredator response in a larval amphibian. Ecology 73:704–708.

Skinner, M. K., M. Ben Maamar, I. Sadler-Riggleman, D. Beck, E. Nilsson, M. McBirney, R. Klukovich, et al. 2018. Alterations in sperm DNA methylation, non-coding RNA and histone

retention associate with DDT-induced epigenetic transgenerational inheritance of disease. Epigenetics & Chromatin 11:8.

Smith, C. C., and S. D. Fretwell. 1974. The optimal balance between size and number of offspring. The American Naturalist 108:499–506.

Snell-Rood, E. C. 2013. An overview of the evolutionary causes and consequences of behavioural plasticity. Animal Behaviour 85:1004–1011.

Stager, M., N. R. Senner, B. W. Tobalske, and Z. A. Cheviron. 2020. Body temperature maintenance acclimates in a winter-tenacious songbird. The Journal of Experimental Biology 223:jeb221853.

Stearns, S. C. 1989. The evolutionary significance of phenotypic plasticity. BioScience 39:436–445.

Stone, G. N., S. Nee, and J. Felsenstein. 2011. Controlling for non-independence in comparative analysis of patterns across populations within species. Philosophical Transactions of the Royal Society B: Biological Sciences 366:1410–1424.

Sultan, S. E., and H. G. Spencer. 2002. Metapopulation structure favors plasticity over local adaptation. The American Naturalist 160:271–283.

Sumner-Rooney, L. 2018. The kingdom of the blind: disentangling fundamental drivers in the evolution of eye loss. Integrative and Comparative Biology 58:372–385.

Suzuki, Y. 2006. Evolution of a polyphenism by genetic accommodation. Science 311:650–652.

Taylor, M. B., and I. M. Ehrenreich. 2015. Higher-order genetic interactions and their contribution to complex traits. Trends in Genetics 31:34–40.

Timpson, N. J., C. M. T. Greenwood, N. Soranzo, D. J. Lawson, and J. B. Richards. 2018. Genetic architecture: the shape of the genetic contribution to human traits and disease. Nature Reviews Genetics 19:110–124.

Van Buskirk, J., and U. K. Steiner. 2009. The fitness costs of developmental canalization and plasticity. Journal of Evolutionary Biology 22:852–860.

van Bussel, I. P. G., P. Fazelzadeh, G. S. Frost, M. Rundle, and L. A. Afman. 2019. Measuring phenotypic flexibility by transcriptome time-course analyses during challenge tests before and after energy restriction. The FASEB Journal 33:10280–10290.

Van Kleunen, M., and M. Fischer. 2005. Constraints on the evolution of adaptive phenotypic plasticity in plants: Research review. New Phytologist 166:49–60.

Vellichirammal, N. N., N. Madayiputhiya, and J. A. Brisson. 2016. The genomewide transcriptional response underlying the pea aphid wing polyphenism. Molecular Ecology 25:4146–4160.

Velotta, J. P., and Z. A. Cheviron. 2018. Remodeling ancestral phenotypic plasticity in local adaptation: a new framework to explore the role of genetic compensation in the evolution of homeostasis. Integrative and Comparative Biology 58:1098–1110.

Via, S., and R. Lande. 1985. Genotype-environment interaction and the evolution of phenotypic plasticity. Evolution 39:505–522.

West-Eberhard, M. J. 2005. Developmental plasticity and the origin of species differences. Proceedings of the National Academy of Sciences 102:6543–6549.

Whitehead, A., and D. L. Crawford. 2006. Neutral and adaptive variation in gene expression. Proceedings of the National Academy of Sciences 103:5425–5430.

Williams, J. W., S. T. Jackson, and J. E. Kutzbach. 2007. Projected distributions of novel and disappearing climates by 2100 AD. Proceedings of the National Academy of Sciences 104:5738–5742.

Wojciechowski, M., R. Lowe, J. Maleszka, D. Conn, R. Maleszka, and P. J. Hurd. 2018. Phenotypically distinct female castes in honey bees are defined by alternative chromatin states during larval development. Genome Research 28:1532–1542.

Woods, H. A. 2014. Mosaic physiology from developmental noise: within-organism physiological diversity as an alternative to phenotypic plasticity and phenotypic flexibility. Journal of Experimental Biology 217:35–45.

Wund, M. A., S. Valena, S. Wood, and J. A. Baker. 2012. Ancestral plasticity and allometry in threespine stickleback reveal phenotypes associated with derived, freshwater ecotypes. Biological Journal of the Linnean Society 105:573–583.

Zhang, T.-Y., and M. J. Meaney. 2010. Epigenetics and the environmental regulation of the genome and its function. Annual Review of Psychology 61:439–466.

Figure 1. Characterization of the evolution of flexible (light green) or plastic (green) vs. canalized (grey) phenotypes under different levels of environmental predictability, variation, and phenotype cost. Modified from Botero et al. (2015), who modeled adaptation to environmental variation using individual-based evolutionary simulations. In their model, Botero et al. (2015) assess the evolutionary response of a theoretical trait under different environmental conditions. Figure represents a summary of 100 simulated reaction norms produced across levels of environmental predictability (P) and the timescale of environmental variation log(R) that evolve after the model ran for 50,000 generations. R, the relative timescale of environmental variation, represents the number of generations experienced per simulated environmental cycle (*e.g.,* temperature change). Environmental predictability, P, is a proportion ranging from 0 (no cue proceeds an upcoming environmental change) to 1 (a cue always predicts an environmental change). (**A**) Phenotypic flexibility and plasticity are more likely to evolve when environmental predictability is high. As R becomes larger, the benefit of environmental matching no longer surpasses the costs of phenotypic adjustment, and individuals exhibit phenotypic plasticity exclusively during development. At very long timescales, genetic variation is more likely to produce a single canalized trait that matches the slow change in the environment (adaptive tracking). (**B**) As the cost of phenotype production increases (K_d), evolution is more likely to favor trait canalization (*i.e.*, bet hedging strategies) at higher levels of environmental variability. As the cost of reversing a phenotype after development increases (K_a), the evolution of plasticity over flexibility becomes more likely. Dotted lines represent values from (**A**), and arrows point to shifts as values of K_a and K_d were doubled in the Botero et al. (2015) model.

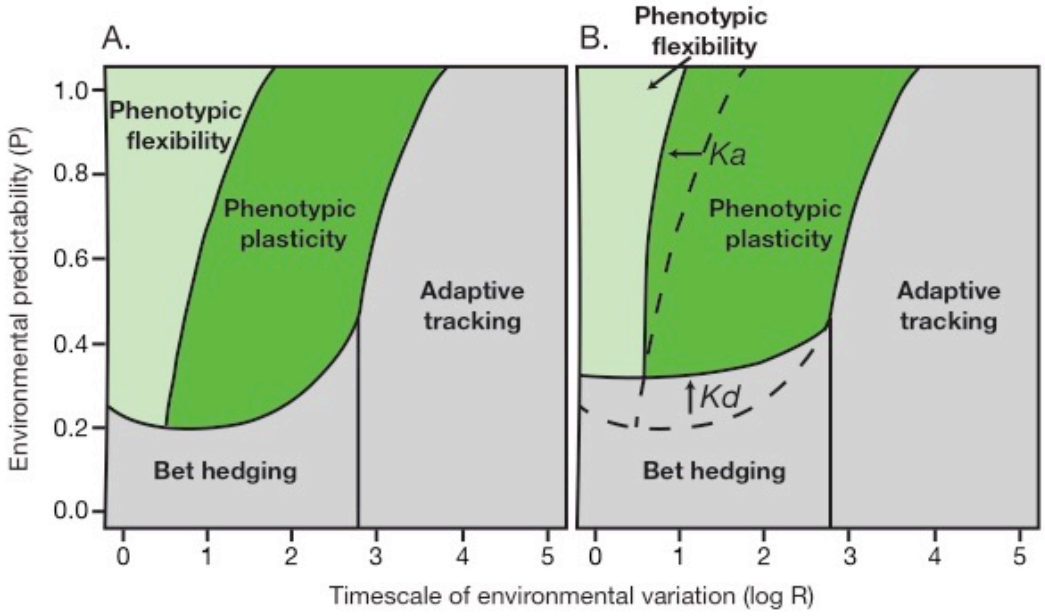

Figure 2. Flexible remodeling of gill and gut physiology of euryhaline fishes in response to changes in salinity. In order to maintain osmotic homeostasis, euryhaline fish alter their rate of drinking, production of urine, and the expression, localization, and activation of gill and gut ion transport proteins. Adapted from (Evans et al. 2005). Fish artwork by Emily C. Moore.